THE UNIVERSITY OF QUEENSLAND

AUSTRALIA

Variations in electrosensory system morphology in teleost and elasmobranch fishes

Arnault Roger Gaston Gauthier

Bachelor of Sciences (Honours)

A thesis submitted for the degree of Doctor of Philosophy at

The University of Queensland in 2018

School of Biomedical Sciences

Abstract

The sense of electroreception is the ability to detect weak electric fields in the surrounding environment. This sense has evolved independently several times in vertebrates, and, in elasmobranchs is associated with the ampullae of Lorenzini, and in catfishes (Siluridae) with teleost ampullary organs. This thesis investigates how the lifestyle, diet, and environment of an elasmobranch impact the distribution and morphology of their electrosensory system, as well as whether the ampullary organs of silurids could be phenotypically plastic. I first studied three species of sympatric benthic rays, *Neotrygon trigonoides*, *Maculabatis toshi*¸ and *Hemitrygon fluviorum*. Despite all three species possessing markedly different diets the structure of their electrosensory system is nearly identical; however, I describe previously unreported features of their ampullae of Lorenzini. Some of the ventral ampullary canals were of a peculiar quasi-sinusoidal shape, and the supportive cells of the sensory epithelium extended out heavily into the ampullary lumen and were apically nucleated. I then investigated the electrosensory system of a bentho-pelagic eagle ray, *Aetobatus ocellatus*, the ultrastructure of which is identical to the previously studied benthic rays. However, the distribution of their electrosensory system was quite peculiar for a batoid, with a complete absence of ampullary pores on their pectoral fins, and only few of them distributed over their body. This species exhibits a high concentration of ampullary pores on the snout, which I hypothesize is used to locate prey. Quasi-sinusoidal ampullary canals were also observed on both the ventral and dorsal surface of the body of this ray, suggesting that the function of this peculiar shape, if any, is unlikely to be related to prey location. The third chapter compares the ampullary organs of two species of benthic sharks, *Chiloscyllium punctatum* and *Hemiscyllium ocellatum*. The sensory epithelium of both species appears to be relatively flattened compared to other elasmobranchs but is otherwise similar in structure to those of previously studied sharks. Interestingly, despite their phylogenetic proximity, similar environments, and diets, some of the ampullary canals of *H. ocellatum* were quasi-sinusoidal, similar to those observed in batoids, yet the canals of *C. punctatum* are all linear. The ten species of galean sharks studied, *Prionace glauca*, *Carcharhinus cautus*, *Carcharhinus limbatus*, *Carcharhinus tilstoni*, *Carcharhinus longimanus*, *Carcharhinus falciformis*, *Galeocerdo cuvier*, *Hemigaleus australiensis*, *Carcharhinus brevipinna*, and *Isurus oxyrinchus*, include coastal, oceanic, bentho-pelagic, and pelagic species. While they differ in their diets they do have a general preference for teleosts, and are all more or less heavily reliant on non-electrical senses, such as vision in *I. oxyrinchus*, or olfaction in *G. cuvier*. The ultrastructure of their ampullae of Lorenzini differs little among these ten sharks.

Larger species of shark and larger individuals within a species tend to possess more numerous sensory chambers, and larger ampullary pores. Thus, size of the animal is seemingly more influential than its environment, lifestyle, or diet. However, clear differences were observed in the distribution and quantity of their ampullary pores, with members of the genus *Carcharhinus* displaying very similar distribution patterns and counts, despite coming from different environments and lifestyles, whereas other species, such as *I. oxyrinchus*, exhibit a markedly different distribution of ampullary pores that seem to fit in well with its highly visual nature and high-speed foraging strategy. The teleost ampullary organs of the salmontail catfish, *Neoarius graeffei*, differ in morphology depending on the environment of origin of the fish. Freshwater ampullae tend to be very short and stay within the limit of the epidermis, with few receptor cells per ampulla, while marine animals possess much longer ampullae with more numerous receptor cells. I investigated the potential phenotypic plasticity of the electrosensory system of this species. I collected juvenile *N. graeffei* from the Brisbane river and raised them in different environments (freshwater, estuarine, and marine) for six months and then investigated the morphology of ampullary organs at the end of this period. There was no evidence of change in the animals kept for six months from the control animals, or variations between each treatment, suggesting that these sensory organs do not undergo phenotypic plasticity if juvenile catfish move between environments that differ in salinity.

Declaration by author

This thesis is composed of my original work, and contains no material previously published or written by another person except where due reference has been made in the text. I have clearly stated the contribution by others to jointly-authored works that I have included in my thesis.

I have clearly stated the contribution of others to my thesis as a whole, including statistical assistance, survey design, data analysis, significant technical procedures, professional editorial advice, financial support and any other original research work used or reported in my thesis. The content of my thesis is the result of work I have carried out since the commencement of my higher degree by research candidature and does not include a substantial part of work that has been submitted to qualify for the award of any other degree or diploma in any university or other tertiary institution. I have clearly stated which parts of my thesis, if any, have been submitted to qualify for another award.

I acknowledge that an electronic copy of my thesis must be lodged with the University Library and, subject to the policy and procedures of The University of Queensland, the thesis be made available for research and study in accordance with the Copyright Act 1968 unless a period of embargo has been approved by the Dean of the Graduate School.

I acknowledge that copyright of all material contained in my thesis resides with the copyright holder(s) of that material. Where appropriate I have obtained copyright permission from the copyright holder to reproduce material in this thesis and have sought permission from co-authors for any jointly authored works included in the thesis.

Publications included in this thesis

Chapter 2

Gauthier, A.R.G., Whitehead, D.L., Tibbetts, I.R., Cribb, B.W., Bennett, M.B. (2018). Morphological comparison of the ampullae of Lorenzini of three sympatric benthic rays. *Journal of Fish Biology* **92**, 504-514. DOI:10.1111/jfb.13531.

Contributor	Statement of contribution
Arnault Gauthier	Designed experiment: 70% Collected data: 75% Analysed data: 100% Wrote the paper: 80%
Darryl Whitehead	Designed experiment: 30% Collected data: 15% Wrote and edited the paper: 4%
Ian Tibbetts	Wrote and edited the paper: 4%
Bronwen Cribb	Collected data: 10% Wrote and edited the paper: 4%
Mike Bennett	Wrote and edited the paper: 4%

Chapter 4

Gauthier, A.R.G., Whitehead, D.L., Tibbetts, I.R., Bennett, M.B. (2018). Comparative morphology of the electrosensory system of the epaulette shark, *Hemiscyllium ocellatum*¸ and the brown-banded bamboo shark, *Chiloscyllium punctatum*. *Journal of Fish Biology* **94**, 313-319. DOI:10.1111/jfb.13893

Contributor	Statement of contribution
Arnault Gauthier	Designed experiment: 100% Collected data: 90% Analysed data: 90% Wrote the paper: 85%
Darryl Whitehead	Wrote and edited the paper: 3%
Ian Tibbets	Wrote and edited the paper: 3%
Mike Bennett	Collected data: 10% Analysed data: 10% Wrote and edited the paper: 9%

Other publications during candidature

Peer reviewed publications

Ola, A., Gauthier, A.R.G., Xiong, Y., Lovelock, C.E. (2019). The roots of blue carbon: responses of mangrove stilt roots to variation in soil bulk density. *Biology Letters* **15**, 20180866.

Whiteley, S.L., Weisbecker, V., Georges, A., Gauthier, A.R.G., Whitehead, D.L., Holleley, C.E. (2018). Developmental asynchrony and antagonism of sex determination pathways in a lizard with temperature-induced sex reversal. *Scientific Reports* **8**, 1-9.

Whitehead, D.L., Gauthier, A.R.G., Cameron, R.M., Perutz, M, Tibbetts, I.R. (2015). Ultrastructure of the ampullary organs of *Plicofollis argyropleuron* (Siluriformes: Ariidae). *Journal of Morphology* **276(12)**, 1405-11. DOI:10.1002/jmor.20428.

Yong, R.Q-Y., Cutmore, S.C., Jones, M.K., Gauthier, A.R.G., Cribb, T.H. (2017). A complex of the blood fluke genus *Psettarium* (Digenea: Aporocotylidae) infecting tetraodontiform fishes of east Queensland waters. *Parasitology international*, **67(3)**, 321-340. DOI:10.1016/j.parint.2017.12.003.

Conference abstracts

Gauthier, A.R.G., Whitehead, D.L., Bennett, M.B., Tibbetts, I.R. Phenotypic plasticity of the teleost ampullary organs of *Neoarius graeffei*. AMSA Student Conference 2016 (North Stradbroke Island, Australia).

Gauthier, A.R.G., Whitehead, D.L., Tibbetts, I.R., Cribb, B.W., Bennett, M.B. Morphology of the electrosensory system of three sympatric dasyatids from Moreton Bay. Oceania Chondrichthyan Society 2016 (Hobart, Australia).

Gauthier, A.R.G., Whitehead, D.L., Tibbetts, I.R., Bennett, M.B. The electrosensory system of elasmobranchs from Moreton Bay. Moreton Bay & Quandamooka Catchment Forum 2016 (Brisbane, Australia).

Gauthier, A.R.G., Whitehead, D.L., Tibbetts, I.R., Bennett, M.B. Variations in the morphology of the electrosensory system of elasmobranchs. Oceania Chondrichthyan Society 2018 (North Stradbroke Island, Australia).

Gauthier, A.R.G., Whitehead, D.L., Tibbetts, I.R., Bennett, M.B. Variations in the electrosensory system of Australian elasmobranchs. Sharks International 2018 (Joao Pessoa, Brazil).

Gauthier, A.R.G., Whitehead, D.L., Tibbetts, I.R., Bennett, M.B. Variations in the morphology of the electrosensory system of Australian elasmobranchs. Electric fish meeting, satellite meeting to the International Congress of Neuroethology 2018 (Brisbane, Australia).

Contributions by others to the thesis

Chapter 1

This introductory review on electroreception in elasmobranch and teleost fishes is my own work. Contributions were made by Mike Bennett, Ian Tibbetts, and Darryl Whitehead who provided critical reviews and edits on earlier versions of the chapter.

Chapter 2

This chapter was published in the *Journal of Fish Biology* in 2018. Darryl Whitehead and Bronwen Cribb provided training in electron microscopy and some of the images were retained for the publication. All co-authors provided critical revisions to the manuscript before submission.

Chapter 3

This chapter is my own work. Contributions were made by Mike Bennett, Ian Tibbetts, and Darryl Whitehead who provided critical reviews and edits on earlier versions of the chapter.

Chapter 4

This chapter was submitted to the *Journal of Fish Biology* and is currently under review. All the work is my own apart from the short section on the diet of *Chiloscyllium punctatum*¸the data was collected and analysed by Mike Bennett. All co-authors provided critical revisions to the manuscript before submission.

Chapter 5

This chapter is my own work. Taylor Maggiacomo created the shark outlines that I used to report the distribution of the ampullary pores. Contributions were made by Mike Bennett, Ian Tibbetts, and Darryl Whitehead who provided critical reviews and edits on earlier versions of the chapter.

Chapter 6

This chapter is my own work. James Dobson assisted in the sectioning of some of the tissues. Contributions were made by Mike Bennett, Ian Tibbetts, and Darryl Whitehead who provided critical reviews and edits on earlier versions of the chapter.

Chapter 7

This general discussion is my own work. Contributions were made by Mike Bennett, Ian Tibbetts, and Darryl Whitehead who provided critical reviews and edits on earlier versions of the chapter.

Statement of parts of the thesis submitted to qualify for the award of another degree

No works submitted towards another degree have been included in this thesis.

Research Involving Human or Animal Subjects

Animal Ethics Approval: SBMS/406/14 by the University of Queensland's Animal Ethics Committee.

Acknowledgements

Over the duration of my PhD, I have met and interacted with an amazing amount of people, at the university, during field work, or at conferences, all of whom have helped shaped this thesis into what it is today. This section is an attempt to acknowledge some of you, but I will have to keep it brief or the length of this document might very well double from the thanks I owe you all.

I am going to start with my parents, Nicole and Jacques. I would not be here today without your support and confidence in my ability to get through this. I specifically sent a draft of this thesis to my sister, Aude, aka “Merdeuse” (Yep, I just did that), to review, so I could include her in this section. I was never going to hear the end of it otherwise.

This entire project would not have been possible without the help of my advisory team, Prof. Michael Bennett, A/Prof. Ian Tibbets, and Dr. Darryl Whitehead. Thank you for the research opportunity, the time you spent helping me out, sorting through my multitude of weird ideas, looking over my drafts, and so on. Additionally, thank you to A. Prof. Jennifer Ovenden and Dr. Uli Siebeck for providing me with critical reviews of my work and guidance during the milestone process.

Next on the list are all of the Bennett & Tibbets lab members. Here’s to all our terrible times together, great times, shenanigans etc. Special shout out to Amelia Armstrong, Sam Williams, Dani Davenport, Deb Bowden, Jamie Wyatt, Christine Dudgeon, Kate Burgess, and Asia Haines for all our office talks, coffee breaks, stats talks, and everything else. To the SBMS Histology Team, Erica “MuMu” Mu, Heather “Heath” Middleton, and James “Still-not-calling-you-Jamie” Dobson for our work adventures, Red Room lunches and other fun times. While I am lucky enough to call all the previously mentioned people friends, there are quite a few others I feel should be included, especially Emma, Dylan, Tahsha, Taylor, Lisa, aka “Minion”, and many more. To our occasional coffees, weird conversations, board game nights, trips, and all the time we spent together.

I spent a significant amount of time in the field during this project, most of which was based at the Moreton Bay Research Station (MBRS). Special thank you to all the staff that worked there during my time, especially to Kevin & Kathy Townsend, Martin Wynne, and Morgan Chance. But let’s not forget everyone else: Kathryn, Jennie, Liz, Sheridan, Cam, Matt, Craig,

Pablo, and Scott. You have all had a major impact on my time spent at the station and I cannot thank you enough for all the help you have provided me. In the same vein, two people to whom I owe many lifetimes of thanks are John Page and Dave Thomson, for your invaluable help in acquiring samples from Moreton Bay. Your knowledge of the area is incredible, and I cannot thank you enough for sharing some of it with me. Speaking of field work in Moreton Bay, most of my time at MBRS was spent in conjunction with members of the Cribb lab, A/Prof. Tom Cribb, Dr. Scott Cutmore, Russel “Rusty” Yong, Dan Huston, Storm Martin, and Nicholas Wee among others, thank you for your help and company. It was a genuine pleasure to share all of this time in the field with you and I hope we may find ourselves in similar situations again in the future!

I was also lucky enough to spend a little bit of time at the Heron Island Research Station. A huge thank you to all the staff of the Heron Island Research Station, especially Abbie “Crabbie” Taylor, and Sam “Max” Morrison for your assistance and fun times.

I was graciously invited to game fishing competitions in New South Wales thanks to Dr. Julian Pepperell and the New South Wales Game Fishing Association. I admit, like many scientists, I was initially biased again game fishing events, but this experience allowed me to meet some incredible people, most of whom are highly concerned about the environment and have a large interest in scientific research, including what I was doing with the sharks they provided me with. A huge thank you to Joshua Aldridge who collected some samples at the competitions I could not attend, and to Nick Otway from the Department of Primary Industry for his assistance.

The facilities of UQ’s Centre for Microscopy and Microanalysis were my home for many days, nights, and week-ends, trying, sometimes (read: almost always) in vain, to get the electron microscopy part of my project to work. A huge thank you to Robyn, Rick, Kim, Graeme, Ron, Kathryn, and Eunice for your help and preventing my break downs. I swear I will not set your mood flipchart to “Postal” any more.

Drs. Kara Yopak, Barbara Wueringer, and Charlie Huveneers, we may have only met a few times during conferences, but you have all set aside some time to have a chat and provided me with invaluable advice for my current and future work so thank you.

I think that should cover most of the named people I have to thank, but I also want to include a special mention to the “behind the scene people” at the university who make sure we have clean offices to go back to, deliveries done on time, (mostly) safe environments to work in and finances in order.

Financial support

This research was supported in parts by a grant obtained from the Moreton Bay Research Station in partnership with Sibelco.

Keywords

Electroreception, elasmobranch, silurid, histology, electron microscopy, sensory biology, shark, ray, catfish

Australian and New Zealand Standard Research Classifications (ANZSRC)

ANZSRC code: 060205 Marine and Estuarine Ecology (incl. Marine Ichthyology), 50%
ANZSRC code: 060807 Animal Structure and Function, 50%

Fields of Research (FoR) Classification

FoR code: 0602, Ecology, 50%
FoR code: 0608, Zoology, 50%

TABLE OF CONTENTS

LIST OF FIGURES

LIST OF TABLES

LIST OF ABBREVIATIONS

AC: Ampullary canal

AD: Alveolar division

AL: Ampullary lumen

ALV: Alveoli

ANOVA: Analysis of variance

AP: Ampulla proper

BM: Basement membrane

C: Centrum

CE: Cuboidal epithelial cells

CF: Collagen fibres

cm: Centimetre

CoE: Columnar epithelial cells

D: Desmosome

E: Epidermis

EOD: Electric organ discharge

Ex: Exocytosis

FE: Flattened epithelial cells

Fig.: Figure

F_o: Frequency of occurrence

h: Hour

IRI: Index of relative importance

K: Kinocilium

Kg: Kilogram

kV: Kilovolt

KS: Keradan sulfate

LM: Light microscopy

L_T: Total length

M: Mitochondria

MT: Microtubules

M_B: Body mass

min: Minute

mm: Millimetre

N: Nucleus

NBF: Neutral buffered formalin

Ne: Nerve

nm: Nanometre

NSW: New South Wales

NT: Neural terminal

N_c: Numerical composition

P: Ampullary pore

ppt: Parts per thousand

PB: Presynaptic bodies

PS: Placoid scales

QLD: Queensland

RC: Receptor cells

RF: Rootlet fibres

S: Seconds

SC: Supportive cells

SCh: Sensory chamber

SEM: Scanning electron microscopy

SW: Wall of the sensory chamber

TEM: Transmission electron microscopy

TJ: Tight junction

UHQ: Deionised water

Vac: Vacuum

V_c: Volumetric composition

W: Watts

W_D: Disc width

µm: Micrometre

Chapter I

Introduction

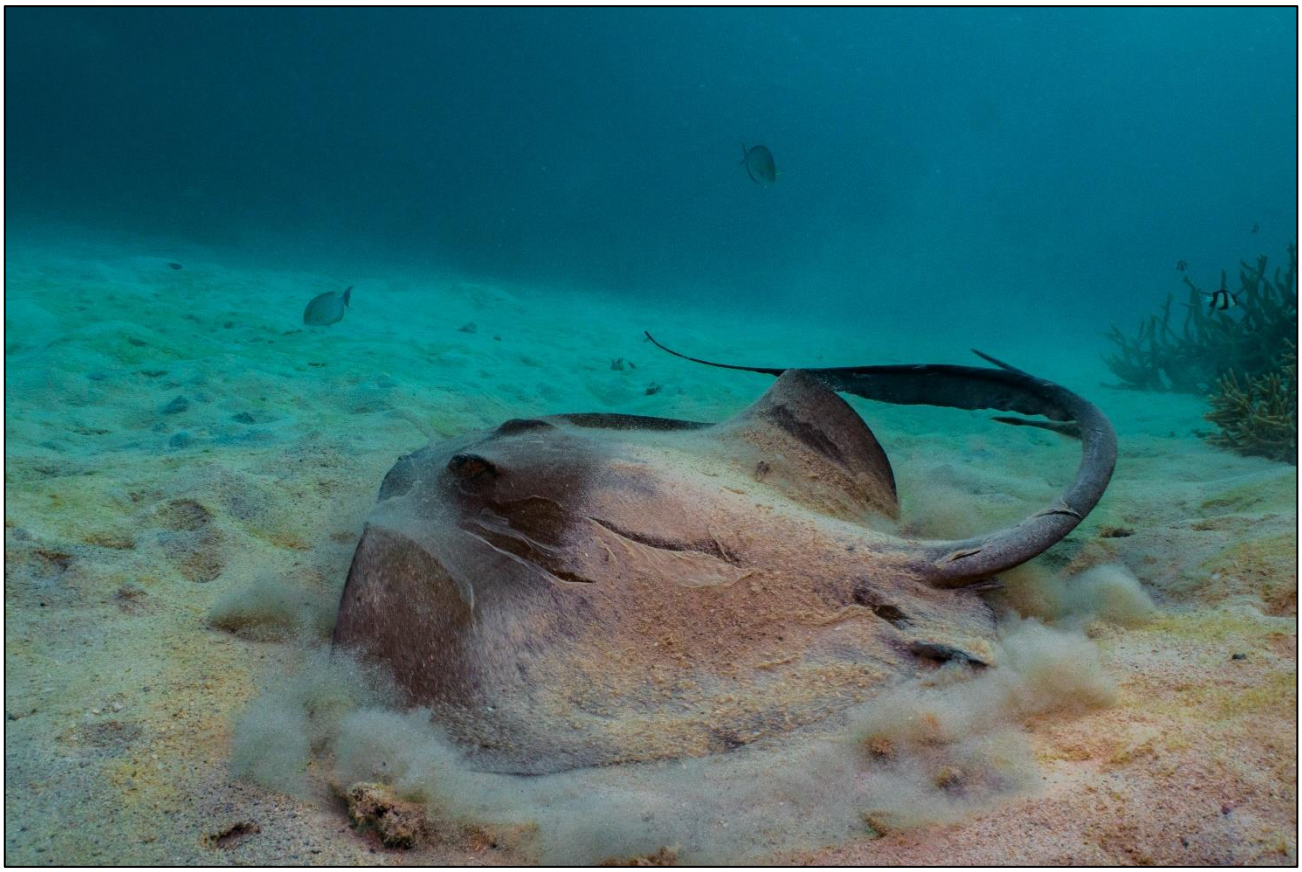

I) Sensory Systems of Fishes

Fishes have access to a wide range of senses, including vision, olfaction, audition, mechanosensory and even electroreception. The relative importance of each of these senses varies among species, and the environment each species inhabits can create a strong selective pressure that can result in structural variations in the associated sensory organs.

A) Vision

Fish eyes comprise, basically, the cornea, lens and retina (Evans, 2004). However, the shape and size of the eye, as well as the type and distribution of photoreceptor cells in the retina, are dependent on the behaviour, phylogeny, and habitat of the fish (Evans, 2004). Light can vary in wavelength, scatter, and intensity, all of which can be affected by the environment and create a strong selective pressure for the eyes to adapt (Warrant *et al*., 2003; Evans, 2004). There are two types of photoreceptors in the retina, the rod and cone cells, both linked to the brain by ganglion cells (Sillman & Dahlin, 2004). All teleost and most elasmobranch fishes have these two types of receptors (duplex retina), although their relative proportions are correlated to both their environmental conditions and behaviour (Sillman & Dahlin, 2004; Collin *et al*., 2015).

Deep sea fishes inhabit environments with little available light, particularly in the depths of the bathypelagic zone where the only light present is produced by bioluminescent organisms (Wagner *et al*., 1998; Collin *et al*., 2015). Most species living in the mesopelagic zone either have large eyes with a high density of rod cells, or tubular eyes, which allow an increase in size of the lens without increasing the size of the eye (Wagner *et al*., 1998; Warrant *et al*., 2003). A higher density of rod cells converging to a single ganglion cell increases the sensitivity of the retina to light, allowing the species frequenting these environments to see despite the low light levels (Wagner *et al*., 1998; Evans, 2004). These two eye structures are not expressed in species of the bathypelagic zone where most organisms have small, regressed eyes (Wagner *et al*., 1998; Warrant *et al*., 2003). On the other hand, shallow water species live in much brighter environments and tend to possess smaller eyes than their deep-sea counterparts. These smaller eyes have a much higher relative proportion of cone cells, each connected to a single ganglion cell, which improves their visual acuity (Evans, 2004).

The relative proportion of photoreceptor types may play a key role in the behaviour of a species. For example, while the lemon shark, *Negaprion brevirostris*, and white shark, *Carcharhodon carcharias*, both forage in shallow waters, the former is nocturnal and the latter diurnal (Sillman & Dahlin, 2004). Their retinal structures reflect this behavioural difference with 92%:8% ratio of rod to cone cells in the *N. brevirostris* retina, for good low-light level vision, versus 80%:20% ratio in *C. carcharias* with the higher visual acuity provided by the more numerous cone cells (Gruber *et al*., 1975; Gruber & Cohen, 1985; Sillman & Dahlin, 2004).

In teleosts, variations in environmental conditions can result in temporary or permanent structural changes to the eyes (Evans, 2004). Temporary variations include daily retinomotor movements, where the position of the photoreceptor cells shift according to the ambient light conditions so that only cone cells are exposed during the day to improve acuity, while at night, both cone and rod cells are exposed to accommodate the lower light levels (Burnside *et al*., 1983; Evans, 2004). Seasonal variations also occur in teleosts, where the relative proportion of vitamin A_1 and A_2 based visual pigments change to accommodate the wavelength of ambient light that differs between summer and winter time (Loew & Dartnall, 1976). An example of a permanent change in eye structure would be the metamorphosis that the eyes of deep-sea species with an epipelagic larval stage go through, to accommodate to a permanent change from a bright to a dark environment (Evans & Fernald, 1990).

Every species of teleost is theorized to have colour vision (Marshall & Vorobyev, 2003; Hart *et al*., 2004; Theiss *et al*., 2007; Van-Eyk *et al*., 2011), while selachimorphs are thought to have monochromatic vision (Collin *et al.*, 2015). However, at least one species of batoid, the giant shovelnose ray, *Glaucostegus typus*, is able to discriminate objects behaviourally on the basis of colour rather than brightness and contrast (Van-Eyk *et al*., 2011).

B) Audition

Sound propagates at speeds of around 1500m.s^{-1} in water (depending on salinity and temperature), making audition a powerful tool to detect other living organisms, or the source of anthropogenic disturbances (Yan, 2004). In fishes, sound can be perceived through their lateral lines as well as their inner ear. The latter consists of three semicircular canals, and three otolithic organs, the utriculus, which is primarily a part of the vestibular system, as well

as the laguna, and the sacculus, part of the auditory system (Popper, 2002; Yan, 2004; Collin *et al*., 2015; Vasconcelos *et al*., 2016). There are significant interspecific variations in the auditory system of fishes, including the position of the inner ear, the size and shape of the otoliths and associated otolithic organs (Fay & Popper, 1975; Platt & Popper, 1981; Popper, 2002; Vasconcelos *et al*., 2016). While the composition of the inner ear is similar between teleosts and chondrichthyans, there are some structural difference between them, such as sharks and rays possessing an enlarged sensory macula neglecta when compared to teleosts (Corwin, 1981). Some variations can be observed in the diameter and curvature of the semicircular canals, which may be a consequence of a functional difference in vestibular control (Jones & Spells, 1963; Howland & Masci, 1973; Evangelista *et al*., 2010; Collin *et al*., 2015). While elasmobranchs can only rely on their lateral line and inner ear, some teleost fishes have gas-filled structures (swim bladders) that can be used to extend their auditory sensitivity and more accurately pinpoint the origin of a sound (Yan, 2004; Ladich & Schulz-Mirbach, 2016.). Teleost fishes use sounds in a range of behaviours, including aggression, to mark their territories, or even for courtship and mating; whereas elasmobranchs are generally considered to be unable to produce sound (Popper *et al*., 2003; Collin *et al*., 2015; Vasconcelos *et al*., 2016).

C) Olfaction

Olfactory organs show considerable morphological variations depending on systematic groups and ecological habitats (Schluessel *et al*., 2008; Yopak *et al*., 2015). These variations include the size, shape, and position of the nares, as well as the number, surface area and secondary folds of the lamellae in the olfactory rosette (Yopak *et al*., 2015). The olfactory system of teleosts consists of three olfactory receptor neuron types that are widely dispersed over the sensory epithelium, and are identifiable by their morphology as either ciliated, microvilous or crypt neurons. (Thommesen, 1983; Hansen *et al*., 1997). In contrast, elasmobranchs do not have ciliated neurons, and crypt neurons were only identified in three species (Ferrando *et al*., 2006). In addition to these interspecific morphological variations, the olfactory system of teleosts also undergoes seasonal variations. The number of crypt neuron cells in the crucian carp, *Carassius carassius*, increases during the reproductive season, presumably in correlation with the mating period and the need to more accurately detect sex pheromones (Hamdani *et al*., 2008).

D) Lateral line

The mechano-sensory lateral line occurs in every species of fish and some amphibians (Coombs *et al*., 1988; Collin *et al*., 2015). This sensory system allows an organism to detect water movements, prey and predators, and assist with navigation (Dijkgraaf, 1963; Kalmijn, 1989; Montgomery & Skipworth, 1997; Montgomery *et al*., 1997; Kasumyan, 2003; Hueter *et al*., 2004; Collin *et al*., 2015). The sensory organs associated with the lateral line are neuromasts that are composed of cilia embedded in a gelatinous capsule (Janssen *et al*., 1987; Janssen, 2004, Bleckmman & Zelick, 2009). The two main types of neuromasts are the superficial neuromast, scattered on the epidermis of a fish, or the canal neuromast, occurring between pore openings inside the lateral line canal (Janssen, 2004; Bleckmann & Zelick, 2009). Superficial neuromasts are typically smaller, contain fewer hair cells, and possess a smaller cupula and sensory epithelium (Münz & Claas, 1983; Coombs *et al*., 1988; Kalmijn, 1989). Interspecific variations occur in the size and shape of the cupula, as well as type, shape and width of the canal afferent neuromast responses (Coombs *et al*., 1988; Denton & Gray, 1988, 1989; van Netten & Kroese, 1989; Coombs & Braun, 2003). The number of neuromasts is also highly variable where some species have fewer than 100 neuromasts in total, and others over a thousand (Puzdrowski, 1989; Coombs & Montgomery, 1999). The number of hair cells per neuromast increases with growth of the animal (Janssen *et al*., 1987; Janssen, 2004). In addition to these neuromasts found in the lateral line, elasmobranchs exhibit a large number of superficial neuromasts, the small pit organs, that also appear to be mechano-sensory in nature and intrinsically linked to the canal neuromasts of the lateral line (Peach & Marshall, 2000).

II) Electroreception

Electroreception can be classified either as “active” or “passive” (Montgomery, 1991; Bleckmann & Hofmann, 1999; von der Emde & Bell, 2003). Fishes with active electroreception are capable of producing a bioelectric signal (an electric organ discharge (EOD)) through the use of specialised electric organs, and can perceive the return signal through specialised tuberous electroreceptor organs attuned to the frequency of the signals emitted (Lissmann, 1958; Bastian, 1986; Kramer, 1996; New, 1997; von der Emde & Bell, 2003; von der Emde, 2006). Theoretically, these signals are used for both intra-specific communication, as well as object electrolocation (Dye & Meyer, 1986). On the other hand, passive electroreception refers to the ability of an organism to detect both biotic and abiotic

electric fields originating from an external source (Bodznick *et al*., 2003; Collin & Whitehead, 2004). For such an ability to be recognised as a sense, Bullock (1982) proposed that three requirements need to be fulfilled: there needs to be a naturally occurring stimulus in the organism's environment, a functional and beneficial use for the sense, and finally a biological sensory organ capable of detecting these stimuli.

A) Weak electric fields

Weak electric fields can originate from biotic and abiotic sources (Kalmijn, 1988). Every living organism produces weak electric fields that can either be in the form of weak electric pulses, from nerve and muscle action potentials, or DC bioelectric fields produced by respiratory or fin movements (Kalmijn, 1988). The strength of these bioelectric fields varies from species to species, but generally, crustaceans create bioelectric potentials of up to 50 µV, gastropods of up to 100 µV, and teleosts of up to 500 µV (Kalmijn, 1972; 1974). While the sensitivity of electroreceptive organisms varies interspecifically, bioelectric fields of 5 $nV.cm^{-1}$ can elicit a behavioural response in the Atlantic stingray, *Dasyatis sabina*, and many species can detect electric fields of less than 1 $nV.cm^{-1}$ (Kajiura & Holland, 2002; Kajiura, 2003; Jordan *et al*., 2009; 2011; McGowan & Kajiura, 2009; Bedore & Kajiura, 2013). Abiotic sources include environmental electric fields such as the electric fields created by large-scale ocean currents, or by the Earth's geomagnetic field (Kalmijn, 1988).

B) Functional and beneficial use of passive electroreception

Recognised functions of electroreception include the detection of weak electric fields, the ability to detect uniform electric fields, as well as intra-specific communication (Kalmijn, 1971, 1974; Tricas *et al*., 1995; Colin & Whitehead, 2004).

Point source localisation

The detection of foreign electric fields coupled with the ability to detect their point(s) of origin allow an organism to detect otherwise hidden prey and predators (Kalmijn, 1971; 1978; Collin & Whitehead, 2004; Jørgensen, 2005). In laboratory conditions, sharks can detect living prey hidden under sand or a layer of agar, or materials that allow electrical signals produced by the prey to spread to the external environment. However, prey cannot be detected when under a polyethylene film that is impervious to electric currents (Kalmijn, 1971). In an experiment that used electrodes to simulate the electric field produced by living

prey, sharks reacted to the electrodes, thus demonstrating their capacity to detect living organisms independent of the senses of olfaction, vision, hearing, and their ability to detect vibrations and changes in pressure (Kalmijn, 1971). However, *D. sabina*, was unable to discriminate between prey items of different species based solely on the electric fields they emit (Blonder & Alevizon, 1988).

The sensitivity of the ampullae of Lorenzini was tested in three species of eastern Pacific rays, *Urobatis halleri*, *Myliobatis californica*, and *Pteroplatytrygon violacea* (Jordan *et al*., 2009). All three rays were exposed to different strengths of electrical signals created using a dipole and responded differently depending on the strength of the field emitted, suggesting that they may be able to discriminate between prey of different sizes (Jordan *et al*., 2009). The rays also responded differently based on their position from the electrode, highlighting the links between electroreception and foraging behaviour (Jordan *et al*., 2009).

A study investigating the range of different senses used by sharks during foraging highlighted the importance of electroreception in the final moments of the attack (Gardiner *et al*., 2014). The successful strikes of sharks against live prey decreased dramatically after application of an insulating gel on their electrosensory pores, depriving them of their sense of electroreception. This study also confirmed the short-range nature (~50 cm) of the use of electroreception for foraging and that the relative importance of electroreception varies interspecifically (Gardiner *et al*., 2014).

Navigation

The ability to detect uniform electric fields is theorised to permit fishes to navigate and orientate themselves during migration (Kalmijn, 1974; Bodznick *et al*., 2003; Filer *et al*., 2008). Passive electronavigation refers to the use of electric fields created by horizontal movements of water (streams) through the vertical component of the Earth's geo-magnetic field, which theoretically allows migrating elasmobranchs to maintain a constant heading (Kalmijn, 1997; Bodznick *et al*., 2003). Active electronavigation, on the other hand, is used when an organism generates its own electric field while swimming and use it as a reference when crossing the vertical component of the Earth's geo-magnetic field (Kalmijn, 1997; Bodznick *et al*., 2003).

Intra-specific communication

The use of electroreception for intra-specific communication occurs in the round stingray, *Urolophus halleri*, with evidence that male stingrays can recognize the presence of buried females of the same species based solely on their bioelectric fields (Tricas *et al*., 1995). Males were similarly attracted to a plastic model of a stingray with an artificial bioelectric field mimicking those of female rays (Tricas *et al*., 1995). Sexual dimorphism in the electroceptor system of *Scyliorhinus canicula* was also attributed to its use in mating. The ampullary organs of male *S. canicula* possess more sensory chambers than the females, which the authors attributed to a need for increased sensitivity during mating season to detect the bioelectric fields generated by females ready to mate (Crooks & Warring, 2013).

C) Biological sensory organs: ampullary organs

Stephano Lorenzini first described the ampullary organs in elasmobranchs in 1678 after noticing the presence of pores on their skin. Later, this elasmobranch form of the sensory organ would retain his name to differentiate them from the morphologically different teleost ampullary organs. The first recorded observation of fish responding to electric fields was witnessed in 1917 through observation of the reactions of blinded catfish to the galvanic field surrounding metallic poles (Parker & van Heusen, 1917). Since the 20th century, electroreception has been defined as the ability of some organisms to detect biotic and abiotic low frequency electric fields in their environment through use of specific sensory units (Lissman, 1958; Lissman & Machin, 1963; Dijkgraaf, 1964; Zupanc & Bullock, 2005).

Passive electroreception in both teleosts and elasmobranchs requires the use of ampullary organs. The ampullary organs, known as ampullae of Lorenzini in Chondrichthyans, and as teleost ampullary organs in teleosts, were initially proposed to be mechanoreceptors or thermoreceptors (Sand, 1938; Murray, 1957; 1960). The confirmation of an electroreceptive ability of these sensory organs and the function of prey detection of the ampullae of Lorenzini was properly defined by Kalmijn (1971).

Despite having evolved independently, the ampullae of Lorenzini and teleost ampullary organs possess major morphological similarities. Both types of ampullary organs consist of an invaginating somatic pore in the epidermis of the electroreceptive organism (Fig. 1.1; Jørgensen, 2005). This pore leads to an ampullary canal filled with a highly conductive mucopolysaccharide gel (Doyle, 1967; Murray, 1974; Josberger *et al*., 2016). The wall of the

ampullary canal is composed of epithelial cells that can be squamous, cuboidal or columnar depending on the species and environment (Herrick, 1901; Mullinger, 1964; Wachtel & Szamier, 1969; Obara & Sugawara, 1984; Whitehead *et al*., 1999; 2000; Gauthier *et al*., 2015). Tight junctions are present between canal wall cells to maximize electrical passage through the mucopolysaccharide gel, while underlying desmosomes bind adjacent cells (Waltman, 1966; Obara & Sugawara, 1984; Kramer, 1996; Whitehead *et al*., 1999; 2000; 2002a; 2002b; 2009; 2015a; Gauthier *et al*., 2015). The ampullary canal may have a collagen sheath enveloping it to provide structural support (Zakon, 1986; Jørgensen, 2005). The distal end of the ampullary canal swells into a rounded bulb, the ampulla proper (Fig. 1.1).

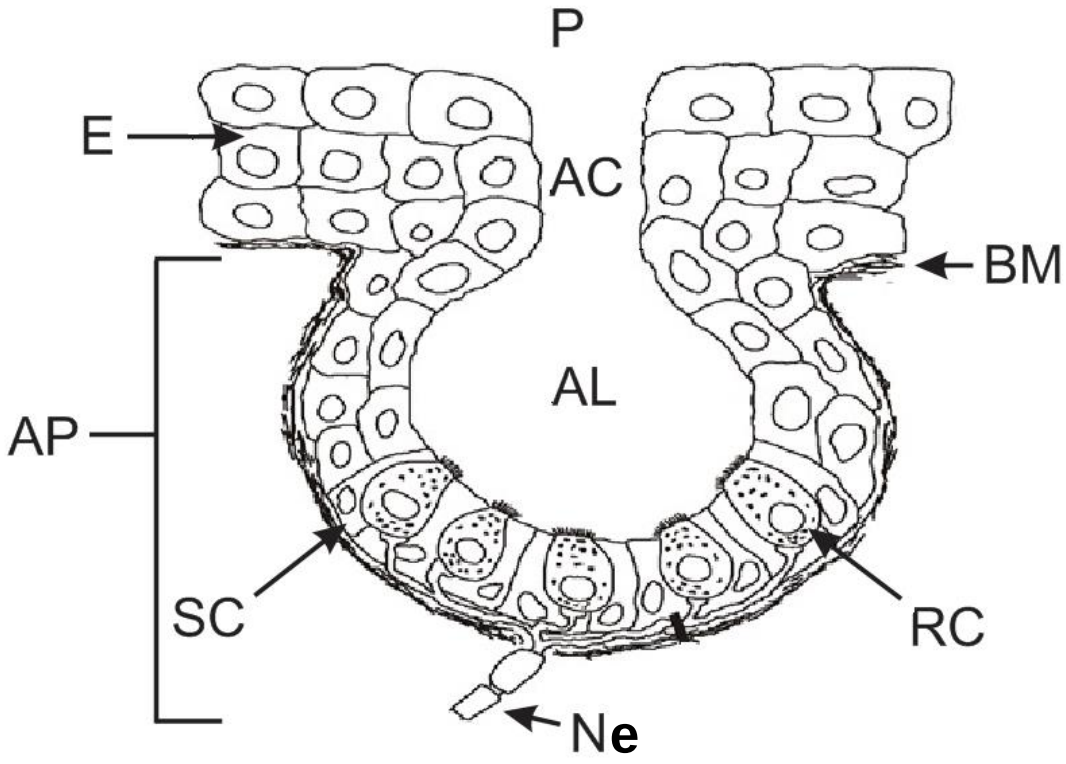

Figure 1.1. Schematic diagram of a typical ampullary organ showing a pore (P) within the epidermis (E) leading to the ampullary canal (AC). The canal opens up into the ampulla proper (AP) that is lined with supportive cells (SC) and receptor cells (RC) external to the basement membrane (BM), the apices of which are exposed to the ampullary lumen (AL). The receptor cells are connected to the central nervous system through a nerve (Ne). *Adapted from Collin & Whitehead*, *2004.*

A recent study into the composition of the mucopolysaccharide in *Sphyrna tiburo*, *Raja rhina*, and *Raja binoculata* revealed the presence of the polyglycan keratan sulfate (KS). The polyglycan KS is theorised to be responsible for the high conductivity of the jelly thanks to the protons donated by the KS acid groups (Josberger *et al*., 2016). These findings contradict those of Brown *et al*. (2005) that implied that the ampullary gel would be a poor electrical conductor between the ampullary pore and the ampulla proper.

In teleosts, the ampulla proper is composed of a single sensory chamber, lined by both receptor and supportive cells, encasing the ampullary lumen (Zakon, 1986; Jørgensen, 2005). The receptor cells are pear-shaped or elongate and their apices are exposed to the ampullary lumen. The exposed apex contains multiple microvilli (Herrick, 1901; Mullinger, 1964; Wachtel & Szamier, 1969; Kramer, 1996; Whitehead *et al*., 1999; 2000; 2003; 2015b; Raschi & Gerry, 2003; Gauthier *et al*., 2015). In Chondrichthyes, there are several types of ampullae: simple, assembled, lobular, finger-shaped, and alveolar, many of which are composed of several sensory chambers, and are aggregated in ampullary clusters (Jørgensen, 2005). Supportive and receptor cells line each of these sensory chambers, and the exposed apices of the receptor cells each possess a single kinocilium as well as some microvilli (Jørgensen, 2005). In both teleosts and elasmobranchs, unmyelinated neural terminals are located at the base of each receptor cell, and individual neurons connect each receptor cell to the central nervous system (Fig. 1.1; Bretschneider & Peters, 1992). A potential difference between the apex of the receptor cells, exposed to the ampullary lumen and in contact with the mucopolysaccharide gel, and the basal area of the receptor cell, which shares a common potential reference with all ampullae located within the same cluster, results in an inversion of the cell polarity and the generation of an action potential (Bullock, 1982; Lu & Fishman, 1994; Bodznick & Montgomery, 2005; Hopkins, 2014). This action potential creates a nerve impulse that travels through the anterior lateral line nerve towards the anterior lateral line lobe of the brain, triggering a behavioural response in the animal (Norris, 1929; Bullock, 1982; Hopkins, 2014). The length and orientation of the ampullary canals also appear to be a more important factor than the position of the ampullary pores in the creation of this potential difference (Brown *et al*., 2005).

In summary, the ability to detect weak electric fields fits the definition of a sense as described by Bullock (1982). The electric fields produced by living organisms in the ocean or, in theory, by the Earth's geo-magnetic field constitute the required natural stimuli (Collin & Whitehead, 2004; Collin *et al*., 2015). Electroreception allows for the detection of prey and predators,

orientation during navigation, communication, and is associated with several forms of sensory organs such as the ampullary organs present in many species of fish (Collin & Whitehead, 2004; Collin *et al*., 2015).

III) Taxonomy

Electroreception has emerged independently several times throughout evolution in several groups of the Animal Kingdom (Collin & Whitehead, 2004). Electroreception first evolved in Devonian fishes and some primitive chordates (Thomson, 1977). Extant Petromyzontiformes (lampreys) can detect electric fields through end bud organs (Collin & Whitehead, 2004). Many other fishes such as elasmobranchs (sharks, skates, and rays), holocephalans (chimeras), Ceratodontiformes and Lepidosireniformes (lungfishes), Coelacanthiformes (coelacanths), Polypteriformes (bichirs), and Acipenseriformes (sturgeons) are electroreceptive; however, they detect electric fields by using various forms of ampullary organs (Collin & Whitehead, 2004). The presence of an electrosensory system is confirmed in three orders of Teleost fishes: Osteoglossiformes (elephantfishes), Gymnotiformes (knifefishes), and Siluriformes (catfishes), although many other orders of fishes are yet to be studied in detail for electroreception (Collin & Whitehead, 2004; Albert & Crampton, 2005; Zupanc & Bullock, 2005). While electroreception is mainly found in fishes, the sense also occurs in the Amphibia (Urodela (salamanders), Gymnophiona (caecilians) and Anura (frogs)), and within the Mammalia (Cetacea (dolphins) and Monotremata (monotremes); Collin & Whitehead, 2004; Albert & Crampton, 2005; Zupanc & Bullock, 2005; Czech-Damal *et al*., 2012). To date, only one species of cetacean, the Indian freshwater dolphin (*Sotalia guianensis*), has been identified as electroreceptive, along with two species of monotremes that have been studied extensively: the platypus (*Ornithorhynchus anatinus*) and the short-beaked echidna (*Tachyglossus aculeatus*) (Scheich *et al*., 1986; Gregory *et al*., 1988; Andres *et al*., 1991; Manger & Pettigrew, 1996). These monotremes utilise cutaneous glands innervated by sensory components of the trigeminal nerve instead of ampullary organs to achieve electroreception (Gregory *et al*., 1988; Andres *et al*., 1991; Manger & Pettigrew, 1996).

IV) The electrosensory system of elasmobranchs

The presence of ampullae of Lorenzini in sharks and rays has been known for centuries, but it was not until 1971 that they were shown to be electroreceptors (Kalmijn, 1971). Since

then, many studies examined their sensitivity, showing that they are predominantly used for close range prey detection, but also for navigation and communication (Kalmijn, 1966, 1974, 1988). The ampullae of Lorenzini of many species can detect an electrical signal as weak as 1 $nV.cm^{-1}$ and are theorised to detect even weaker electric fields (Jordan *et al*., 2009).

The ampullae of Lorenzini derive from the lateral line system and appear soon after it develops during ontogeny (Kempster *et al*., 2013). By stage 32 of development, the embryos of the brown-banded bamboo shark, *Chiloscyllium punctatum*, halt their respiratory movements within the egg case when exposed to an external electric field (Kempster *et al*., 2013). This behaviour is associated with a predator avoidance strategy, to avoid being detected by potentially electroreceptive animals that could detect the electric fields generated by the skeletal muscles (Kempster *et al*., 2013).

Ampullary organs are restricted to the cranial regions of most species of sharks, with the exception of the dorso-ventrally flattened angel sharks, genus *Squatina*, while they are more widespread on the flattened bodies of rays (Chu & Wen, 1979; Schäfer *et al*., 2012). However, variations in the distribution and morphology of ampullary organs have been attributed to several factors (Kempster *et al*., 2012). The differences in lifestyle between benthic and pelagic sharks appears to be one such contributing factor (Jordan, 2008; Kempster *et al*., 2012). Benthic batoids typically possess a much higher concentration of ampullary pores on their ventral surface, thought to facilitate feeding given their dorsally positioned eyes (Kempster *et al*., 2012; Camilieri-Asch *et al*., 2013). However, the pelagic stingray, *Pteroplatytrygon violacea*, possesses a similar distribution of ampullary pores on the ventral surface as other dasyatids, but with only a third of the number of pores reported in benthic species (Jordan, 2008; Camilieri-Asch *et al*., 2013). In sharks, the ornate wobbegong, *Orectolobus ornatus*, has a much higher concentration of ampullary pores on the dorsal side of the head compared to pelagic sharks (Theiss *et al*., 2011; Kempster *et al*., 2012). This arrangement provides increased sensitivity in detecting potential prey swimming over the head of *O. ornatus*¸ which can be seized if the prey comes within reach (Theiss *et al*., 2011; Kempster *et al*., 2012).

Environmental salinity and, as a direct consequence, environmental conductivity, is another factor that influences the distribution of ampullary pores (Bullock, 1982). Morphological differences between freshwater and marine electrosensory systems relate to the difference in conductivity between environments of different salinities, the resistance of the fishes' skin

and the need to create a potential difference between the internal isopotential coelomic fluid of the fish and the external environment (Kalmijn, 1973; 1974). In the highly conductive marine environment, fishes have a low skin resistance. As such, electroreceptive fishes living in this environment possess long ampullary canals ending in a cluster composed of several ampullae that share a same potential reference, forming a functional unit (Bullock, 1973; Kalmijn, 1974; Kramer, 1996; Whitehead, 2002a). The long ampullary canals are necessary for the detection of uniform electric fields, but not for point-source detection (Bullock, 1973; Kalmijn, 1974; 1978). Freshwater fish, on the other hand, live in a less conductive environment, and possess a high skin resistance (Bullock, 1973; Kalmijn, 1974; Kramer, 1996; Whitehead, 2002a). As such, a potential difference, large enough to be detected can be created across the thickness of the skin (Bullock, 1973; Kalmijn, 1974; Kramer, 1996; Whitehead, 2002a).

Marine elasmobranchs tend to have ampullary organs with very long canals, sometimes reaching 20cm in length, which aggregate in clusters of ampullae in specific regions of the head (Chu & Wen, 1979). On the other hand, the ampullae of Lorenzini observed in the freshwater ray, *Potamotrygon motoro (= Potamotrygon circularis*), differed from all other ampullary organs previously documented in sharks (Szabo *et al*., 1972). *Potamotrygon circularis* possesses very short ampullary organs, termed micro-ampullae, spread over its body and are not aggregated in clusters (Szabo *et al*., 1972). Due to the low diversity of freshwater elasmobranch, no other reports on their ampullae are available, however electrosensory characteristics are expected to be consistent across this group. The ampullary organs found in freshwater specimens of the euryhaline bullshark, *Carcharhinus leucas*¸ also displayed morphological differences when compared to marine elasmobranchs (Whitehead *et al*., 2015a). The four-leaf clover shape of the ampullary canal, and the slight protrusion of the supportive cells into the ampullary lumen documented in those specimens had never been seen before, and their functions cannot yet be confirmed (Whitehead *et al*., 2015a). This peculiar shape of the ampullary canal has since then been observed in the fossilized remains of *Carcharias amonensis* (Vulo & Guinot, 2015).

Variations in the morphology of the electrosensory system of sharks are well-documented. However, the fine structure of ampullary organs of many species is still unknown, and links between the ultrastructure of ampullae of Lorenzini and factors such as diet and lifestyle are yet to be established.

V) The electrosensory system of teleosts

Many actinopterygian fishes possess an electrosensory system, most using a form of ampullary organ to detect electric fields (Collin and Whitehead, 2004). In particular, morphological data are available for the ampullary organs of Acipenseriformes, Polypteriniformes, Dipnoi and Coelacanthiformes (Jørgensen, 2005). Among the 40 orders of the Teleostei, few are known to possess an electrosensory system, but many orders have yet to be surveyed (Jørgensen, 2005). Extensive work has been realised on the ampullary organs of Gymnotiformes, as well as those of Siluriformes (Jørgensen, 2005).

Studies of the morphology of the teleost ampullary organs of many species of catfish have focused on freshwater species. However, the ampullary organs of siluroids from estuarine and marine environments differ significantly from their freshwater counterparts. The morphology of the electrosensory system of several freshwater catfish, such as *Neoarius graeffei*, *Ameiurus nebulosus*, *Plotosus tandanus* and *Kryptopterus bicirrhus* has been studied (Herrick, 1901; Wachtel & Szamier, 1969; Jørgensen, 1992; Whitehead *et al*., 2000; 2003). In these four species, the length of the ampullary canals ranged from 60 micrometres (µm) to 500 µm and the ampulla proper was lined with 8-60 receptor cells (Herrick, 1901; Wachtel & Szamier, 1969; Whitehead *et al*., 2000; 2003). There was no evidence of a supporting collagen sheath enveloping the ampullary organs thus differentiating these freshwater fishes from those found in marine environments (Herrick, 1901; Wachtel & Szamier, 1969; Whitehead *et al*., 2000; 2003).

Few estuarine silurids have been studied, the most recent being *Plicofollis argyropleuron* (Whitehead *et al*., 2015b). The ampullary canals located on the head of this species are the longest recorded for any siluriform, with canal lengths of up to 480 mm and converging in specific clusters of ampullary organs similar to the clusters observed in elasmobranchs (Whitehead *et al*., 2015b). However, the ampullary organs present on the trunk of *P. argyropleuron* were of a completely different type, being similar to the micro-ampullae found in freshwater silurids in shape, length, and quantity of receptor cells (Whitehead *et al*., 2015b). Specimens of *Neoarius graeffei* living in the estuarine reaches of the Brisbane River have ampullary canals that are longer than their freshwater counterparts, at up to 1.9 mm long, and possess more receptor cells (Whitehead *et al*., 1999; 2000; Gauthier *et al*., 2015).

The ampullary canals present on the head of marine *Plotosus lineatus* (= *P. anguillaris*) range from 10 to 30 mm in length, and their ampullae proper occur in distinctive clusters (Friedrich-Freksa, 1930; Lekander, 1949; Bauer & Denizot, 1972; Obara, 1976). Each ampulla proper is composed of 250 to 750 receptor cells (Friedrich-Freksa, 1930; Lekander, 1949; Bauer & Denizot, 1972; Obara, 1976). Marine *Neoarius graeffei* possess significantly longer ampullary organs then those found in freshwater and estuarine specimens, with more numerous receptor cells reaching a length of 600 µm with more than a 100 receptor cells per ampulla (Gauthier *et al*., 2015).

The morphology of teleost ampullary organs depends on the environmental conditions from which a fish originates, particularly the environmental salinity. However, it is still unclear whether the morphology of the ampullary organs of a fish is determined by the environmental salinity of their birthplace and is independent of changes in environmental salinity, or if they are able to adapt to changes in environmental conditions, such as changes in salinity. Species like *P. argyropleuron* also raise the question about salinity being the only factor affecting the morphology of ampullary organs given that they possess longer ampullary canals and more receptor cells than the marine species studied to date, despite their estuarine nature.

Environmental factors thus affect the morphology of the ampullary organs of both elasmobranchs and teleosts (Whitehead, 2002a; Jørgensen, 2005; Kempster *et al*., 2012; Gauthier *et al*., 2015). To better understand the variations in the morphology of ampullary organ displayed in elasmobranchs and teleosts as well as their possible causes, thorough research of known modulations is needed.

VI) Conclusion

Electroreception appears several times through evolution and is present in many species of fish allowing them to locate prey and predators, navigate and communicate (Collin and Whitehead, 2004). The ampullary organs of teleosts and elasmobranchs display remarkable morphological similarities; however, several environmental and biological factors appear to affect their morphology and distribution (Jørgensen, 2005; Kempster *et al*., 2012; Gauthier *et al*., 2015). The morphological differences exhibited by the ampullary organs of freshwater and marine teleosts also appear in elasmobranchs (Szabo *et al*., 1972; Jørgensen, 2005; Gauthier *et al*., 2015). Other factors such as the differences in uses of electroreception between benthic and pelagic Chondrichthyes also appear to affect the distribution of

ampullary organs, but whether these differences in distribution extend to morphological variation is unknown.

VII) Aims and significance of the project

This literature review highlighted the significant variations in the morphology of the ampullary organs found in elasmobranchs and teleosts, as well as identified potential factors affecting these sensory organs.

I hypothesize that the lifestyle, habitat, and diet of a species may affect the distribution, gross morphology, and ultrastructure of their ampullae of Lorenzini. The first part of this thesis investigates these claims in 16 species of elasmobranchs to identify if any morphological variations observed in their electrosensory system could be attributed to those factors:

- Chapter II of this thesis compares the ultrastructure of the ampullae of Lorenzini in three species of sympatric rays that inhabit Moreton Bay, Queensland, Australia. These three species, the blue-spotted maskray, *Neotrygon trigonoides*, the estuary stingray, *Hemitrygon fluviorum*¸ and the brown whipray, *Maculabatis toshi*, have an overlapping niche in Moreton Bay, but show considerable dietary differences in terms of the preferred prey extracted from their shared environment. The principal aim of this chapter is to investigate the potential links between these rays' dietary intake and the morphology of their ampullary organs.

- Chapter III represents the first investigation into the distribution, gross morphology, and ultrastructure of the electro-sensory system of the bentho-pelagic eagle ray *Aetobatus ocellatus*. This species of batoid primarily lives in the water column but forages on benthic prey. This chapter will compare the distribution and morphology of ampullary organs in *A. ocellatus* with the three benthic species studied in the previous chapter in order to ascertain whether their bentho-pelagic nature has any observable effects on their electrosensory system.

- Chapter IV compares the electrosensory system of two demersal sharks, the epaulette shark, *Hemiscyllium ocellatum*, and the brown-banded bamboo shark, *Chiloscyllium punctatum*. These two closely related species of carpet sharks live in

similar environments, and feed on similar type of prey. An investigation into their electrosensory system will allow for a comparison with benthic batoids, as well as bentho-pelagic and pelagic sharks.

- Chapter V regroups an analysis on the distribution, gross morphology, and ultrastructure of the electrosensory system of ten bentho-pelagic and pelagic species of sharks, *Carcharhinus brevipinna*, *Carcharhinus Cautus*, *Carcharhinus falciformis*, *Carcharhinus limbatus*, *Carcharhinus longimanus*, *Carcharhinus tilstoni*, *Galeocerdo cuvier*, *Hemigaleus australiensis*, *Isurus oxyrinchus*, and *Prionace glauca.* A range of different lifestyles and habitats are represented in these species, providing an ideal set up to compare the effect of these factors on their electrosensory systems.

Secondarily, I hypothesize that the teleost ampullary organs of the salmontail catfish, *Neoarius graeffei*, are capable of adapting morphologically to new environments during migrations:

- Chapter VI compares the morphology of the teleost ampullary organs of wild caught *Neoarius graeffei* to those of specimens raised in environments of different salinities for six months. These results will provide a better understanding of how the electrosensory system of a euryhaline species is affected by migrations through different environments.

Chapter II

Morphological comparison of the ampullae of Lorenzini of three sympatric benthic rays.

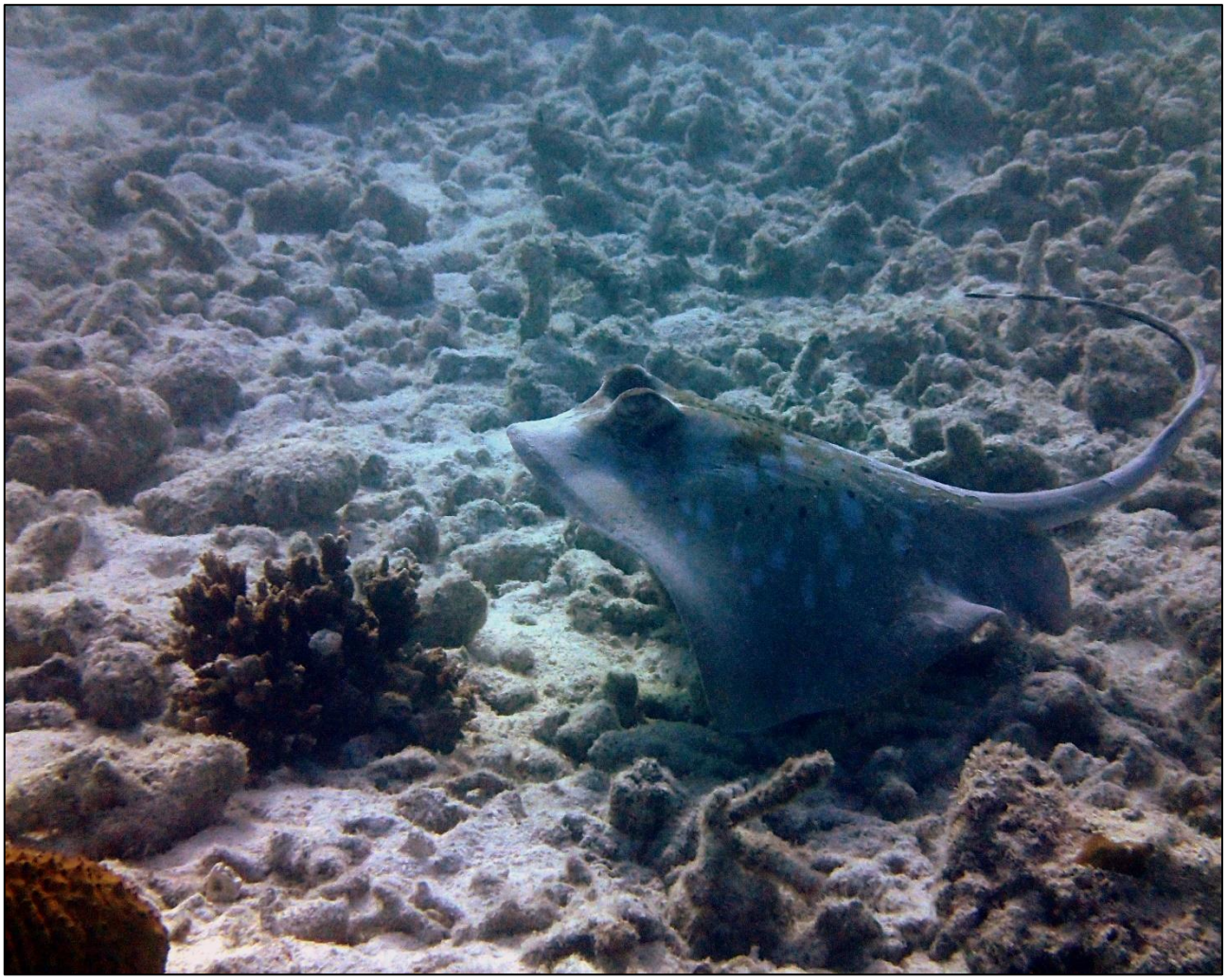

Abstract

This study investigated and compared the morphology of the electrosensory system of three species of benthic rays. *Neotrygon trigonoides*, *Hemitrygon fluviorum*, and *Maculabatis toshi* inhabit similar habitats within Moreton Bay, Queensland, Australia. Like all elasmobranchs, they possess the ability to detect weak electric fields using their ampullae of Lorenzini. Macroscopically, the ampullary organs of all three species are aggregated in three bilaterally paired clusters: the mandibular, hyoid and superficial ophthalmic clusters. The hyoid and superficial ophthalmic clusters of ampullae arise from both dorsal and ventral ampullary pores. The dorsal pores are typically larger than the ventral pores in all three species, except for the posterior ventral pores of the hyoid grouping. Ampullary canals arising from the hyoid cluster possessed a quasi-sinusoidal shape, but otherwise appeared similar to the canals described for other elasmobranchs. Ultrastructure of the ampullae of Lorenzini of the three species was studied using a combination of light, confocal and electron microscopy. All possess ampullae of the alveolar type. In *N. trigonoides* and *M. toshi*, each ampullary canal terminates in three to five sensory chambers, each comprising several alveoli lined with receptor and supportive cells, and eight to eleven sensory chambers in *H. fluviorum*. Receptor cells of all three species possess a similar organisation to those of other elasmobranchs and were enveloped by large, apically nucleated supportive cells protruding well into the alveolar sacs. The luminally extended chassis of supportive cells protruding dramatically into the ampullary lumen had not previously been documented for any elasmobranch species.

Introduction

The ampullae of Lorenzini of chondrichthyans facilitate passive electroreception and typically consist of an epithelial pore that opens to a mucopolysaccharide filled canal (Zakon, 1986; Jørgensen, 2005). Tight junctions and underlying desmosomes between adjacent canal wall cells are common to all ampullary organs, and have been demonstrated empirically to provide the canal wall with a high level of electrical resistance, restricting the loss of electrical potential along the length of the canal (Waltmann, 1966). These canals generally terminate in one or more ampullae proper, which in elasmobranchs usually comprise several alveoli, consisting of receptor and supportive cells (Zakon, 1986; Fishelson & Baranes, 1998; Whitehead, 2002b; Jørgensen, 2005; Wueringer *et al.*, 2009; Theiss *et al.*, 2011; Whitehead *et al*., 2015a). The major functions of passive electroreception are considered to be prey detection, detection of potential predators, electro-communication with conspecifics, and geomagnetic orientation (Dijkgraaf & Kalmijn, 1962; Kalmijn, 1974; Tricas *et al.*, 1995; Sisneros *et al.*, 1998; Collin & Whitehead, 2004).

Most stingrays are benthic, feeding on a variety of epifauna and infauna (Last & Stevens, 2009; Pierce *et al.*, 2009; Jacobsen and Bennett, 2010, 2012; Pardo *et al.*, 2015). The blue-spotted maskray is an Indo-Pacific maskray of up to 50 cm in disc width (W_D) (Last & Stevens, 2009). Currently recognised in the Catalog of Fishes as *Neotrygon trigonoides* (Castelnau 1873), in Australia it was previously named *Neotrygon kuhlii* and *Dasyatis kuhlii*; names that are now reserved for individuals of this species complex found in the Solomon Islands (Last *et al*., 2016a). This species inhabits soft substrate coastal environments, in association with coral and rocky reefs, to depths of 90 m (Last & Stevens, 2009; Pierce *et al.*, 2009; Jacobsen & Bennett, 2010, 2012; Last *et al.*, 2016a). The estuary stingray, *Hemitrygon fluviorum* (Ogilby, 1908) (previously known as *Dasyatis fluviorum*) is a medium to large stingray (exceeding 90 cm W_D) that is found in habitats ranging from shallow estuaries to fully marine waters throughout the coastal regions of Queensland (Last & Stevens, 2009; Last *et al.*, 2016b). The brown whipray, *Maculabatis toshi* (Whitley 1939) (previously known as *Himantura toshi*) is a medium-sized whipray that attains at least 74 cm W_D and is commonly found on muddy substrate and mangrove flats throughout coastal Queensland (Last & Stevens, 2009; Last *et al.*, 2016b). The distribution of these three dasyatids overlap; they all feed on the intertidal flats of Moreton Bay, but their diets differ significantly (Pardo *et al.*, 2015). *Neotrygon trigonoides* feeds primarily on polychaetes, *H.*

fluviorum on brachyurans and polychaetes, and *M. toshi* feeds predominantly on caridean shrimp (Pardo *et al.*, 2015).

Previous studies on the ampullae of Lorenzini of *N. trigonoides* and *H. fluviorum* identified three main clusters of ampullary organs around the head: the superficial ophthalmic, hyoid and mandibular clusters (Chu and Wen, 1979; Camilieri-Asch *et al.*, 2013). The focus of my investigation was primarily to document the ultrastructure of the ampullae of Lorenzini in each of these three species, using a combination of light, confocal, scanning and transmission electron microscopy. The second aim of this study was to compare the morphology of these ampullary organs across the three species and investigate any potential links to their favoured diet.

Methods

Specimen collection

A total of fifteen rays were used in this study, six *Neotrygon trigonoides*, six *Hemitrygon fluviorum*, and three *Maculabatis toshi.* Three *N. trigonoides* were captured by both seine and tunnel netting at Hays Inlet, Moreton Bay, Queensland, Australia (27°28′S, 153°02′E), and three specimens were captured from Jumpinpin, Queensland, Australia (27°44′S; 153°26′E); retained specimens had an even sex ratio, and disc widths (W_D) of 18.7 to 34.2 cm. Two *H. fluviorum* were captured from Jumpinpin, Queensland, Australia (27°44′S; 153°26′E) and four from Fisherman's Island, Queensland, Australia (27°23'S; 153°11'E). Retained specimens had an even sex ratio, with a W_D ranging from 33.0 to 67.0 cm. Three specimens of *M. toshi* from Moreton Bay were donated by a commercial fisher. Two specimens were female, the other male with a W_D ranging from 29.0 cm to 33.0 cm. Animals were euthanised on site using Aqui-S (concentration of 175 $mg.L^{-1}$ of seawater) or pithing (The University of Queensland (UQ) Animal Ethics Approval SBMS/406/14) and all the ampullary clusters removed and fixed appropriately in either 10% neutral buffered formalin or 2.5% glutaraldehyde in 0.1M phosphate buffer at pH 7.2. The non-fixed remains were then transported to the University of Queensland for studying the distribution of ampullary pores.

Ampullary pore distribution and gross measurements

Ampullary pore distribution in two specimens of each species was investigated by removal of the skin and placement onto a backlit plate to render the pores clearly visible. Ampullary pores were distinguished from lateral-line pores due to the presence of thickened canal walls in the latter, being readily visible and interconnecting adjacent pores of the lateral line. The ampullary pores were measured under a dissection microscope (using Nikon-BR Elements 4 software), for both the ventral and dorsal surfaces. For one specimen of each species, the total number of ampullary pores was quantified. Ampullary canals were fixed in 10% neutral buffered formalin (NBF) and processed for routine histology, sectioned at 6 µm thickness, and stained with Mayer's haematoxylin and eosin. The resulting slides were viewed under a Nikon 50i Eclipse compound microscope for gross measurements. Ampullary canal diameter was averaged from three transverse measures along the length of the canals, with each measurement separated by at least 1 mm along its length. All canal and ampullae proper measurements are reported as the mean and standard deviation of *n* measurements. All measurements were analysed using a two-way factorial ANOVA with a 95% confidence interval followed by a post-hoc Tukey test.

Confocal microscopy

Several ampullary organs were dissected out of the hyoid cluster, separated and prepared for bright-field confocal microscopy. Samples were fixed for 48 h in 10% formalin, followed by 3 x 20 min phosphate buffer rinses followed by dehydration in a graded ethanol series (20% to 100%), after which the ampullae were placed in a 50:50 mix of methyl benzoate and 100% ethanol for 24 h. This was followed by the following series: 100% methyl benzoate, 50% methyl benzoate/50% Canada balsam, 25% methyl benzoate/75% Canada balsam (24 h each) before mounting on glass slides in Canada balsam. Slides were viewed via a Diskovery spinning disk confocal microscope.

Scanning Electron Microscopy (SEM)

Five skin samples of approximately 1 cm^2 and up to 50 individual ampullary organs were removed from freshly euthanised animals and fixed in either 10% NBF, 2.5% glutaraldehyde in 0.1 M phosphate buffer, Karnovsky's or Bouin's fixative. The range of fixatives was used to investigate the presence of possible fixation artefacts. Following fixation, samples were

washed and then dehydrated in an ascending ethanol series (70%, 90%, and two changes 100% for 45 min each). Post-dehydration, specimens were dried fully using a critical point dryer, and then a selection of ampullary organs was bisected. Specimens were mounted on 12 mm diameter aluminium stubs with double-sided, carbon-impregnated tape and iridium coated (to ~10 nm thickness). Tissues were viewed and photographed in a JEOL 7001 field emission scanning electron microscope at a maximum of 15 kV.

Transmission electron microscopy (TEM)

Single ampullae were dissected free of surrounding tissues and fixed in either Karnovsky's fixative, containing 3% glutaraldehyde and 2% paraformaldehyde in 0.1 M phosphate buffer (pH 7.2), or 2.5% glutaraldehyde in 0.1M phosphate buffer. The samples were then processed and embedded following the protocol from Whitehead *et al.* (1999). Survey sections (1 µm thickness) were cut with a LKM UM III ultramicrotome, using a glass knife, and stained with 1% toluidine blue in 0.1 M phosphate buffer. Ultrathin sections of <100 nm thickness were cut with a Leica EM UC62 using a diamond knife, and mounted on 1 mm x 2 mm single-slot, carbon-stabilized collodion coated grids. The grids were then stained according to Daddow's double lead staining technique (Daddow, 1986). Sections were viewed and photographed in a JEOL 1010 transmission electron microscope at 80 kV.

Results

Ampullary pores (Fig. 2.1A) occured on both the ventral and dorsal surface of *Neotrygon trigonoides*, *Hemitrygon fluviorum*, and *Maculabatis toshi*, giving rise to ampullae in the superficial ophthalmic and hyoid functional groupings. In all three species, some of the pores on the dorsal snout tip led to the superficial ophthalmic cluster, while a majority extended to the hyoid cluster. Ampullary pores on the dorsal surface ranged from 110 to 247 µm in diameter in *N. trigonoides* (n = 40), while they ranged from 100 µm to 320 µm in *H. fluviorum* (n = 40) and 98 to 236 µm in *M. toshi* (n = 40). In comparison, pores of the ventral surface of *N. trigonoides* ranged from 28 to 257 µm in diameter (n = 80) and were generally smaller than those of the dorsal surface ($F_{1,234}$ = 133.7, p < 0.05), with a similar range found in the other two species, with pores measuring between 44 and 244 µm in *H. fluviorum* (n = 80), and 32 to 253 µm in *M. toshi* (n = 80). The ampullary pores of *H. fluviorum* were larger than those of both *N. trigonoides* ($F_{2,234}$ = 6.2, p < 0.05) and *M. toshi* ($F_{2,234}$ = 6.2, p > 0.05) but there were no differences between *N. trigonoides* and *M. toshi* ($F_{2,234}$ = 6.2, p > 0.05). There

were no significant differences in pore diameter between males and females ($F_{1,234} = 5.1$, $p > 0.05$). Within the hyoid cluster on the ventral surface of all three species, pores increased in diameter in a gradient from anterior to posterior, with posterior pores similar in diameter to dorsal pores. A total of 1152 pores were counted in *N. trigonoides*¸1204 in *H. fluviorum*¸ and 1074 in *M. toshi*.

In each of the three species, the ampullary pores gave rise to ampullary canals (Fig. 2.1B), the length of which varied with the size of the animal. These ampullary canals ranged from 3.2 to 164.0 mm in length and from 298 to 632 µm ($n = 10$) in diameter in *N. trigonoides*, from 4.6 to 160.0 mm in length and 213 to 599 µm ($n = 10$) in diameter in *H. fluviorum*, and from 3.0 to 158.0 mm in length and 280 to 596 µm ($n = 10$) in diameter in *M. toshi*. A common feature within each of these species was the quasi-sinusoidal shape of the infraorbital ampullary canals belonging to the hyoid cluster (Fig. 2.1C). The ampullary canal wall consisted of two layers of flattened squamous epithelial cells and was enveloped by a sheath of collagen fibres (Fig. 2.1D) in all three species. These two layers of squamous epithelial cells produced a relatively smooth luminal surface to the ampullary canal (Fig. 2.1C, 2.1D). Neighbouring flattened epithelial cells were adjoined by tight junctions with underlying desmosomes (Fig. 2.1E). At the terminal end of the ampullary canal, cuboidal cells replaced squamous epithelial cells producing a transition zone between the canal and the ampulla proper (Fig. 2.1F).

In *N. trigonoides* and *M. toshi*, ampullary canals led to alveolar ampullary organs, composed of three to five sensory chambers, each of which was further divided into five to seven alveolar sacs separated from each other by alveolar septa (Fig. 2.2A, 2.2B). The alveolar septa separating the receptor epithelia of adjacent alveoli consisted of dense epithelial tissues that were typically two cell layers thick, the surfaces of which appeared to be smooth in comparison to those of the sensory epithelia. The ampullae of *H. fluviorum* were similarly shaped, but comprised eight to eleven sensory chambers, each of which divided into five to seven alveolar sacs. After identifying the ampullae as being of the alveolar type, sensory chambers were counted only if a clear canal was observed branching off from the main ampullary canal using Z-stacks of 6 µm thickness obtained using the confocal microscope. The ampullae of *H. fluviorum* had an average diameter of 716 ± 93 µm ($n = 30$) and were significantly larger than both those of *N. trigonoides* with a diameter of 499 ± 96 µm ($n = 30$; $F_{2,84} = 74.7$, $p < 0.05$) and *M. toshi* with a diameter of 456 ± 71 µm ($n = 30$; $F_{2,84} = 74.7$, $p < 0.05$). There was no significant difference between the mean size of the ampullae of *N.*

trigonoides and *M. toshi* ($F_{2,84} = 74.7$, $p > 0.05$). There was no apparent sexual dimorphism in the mean diameter of the ampullae proper ($F_{1,84} = 0.2$, $p > 0.05$).

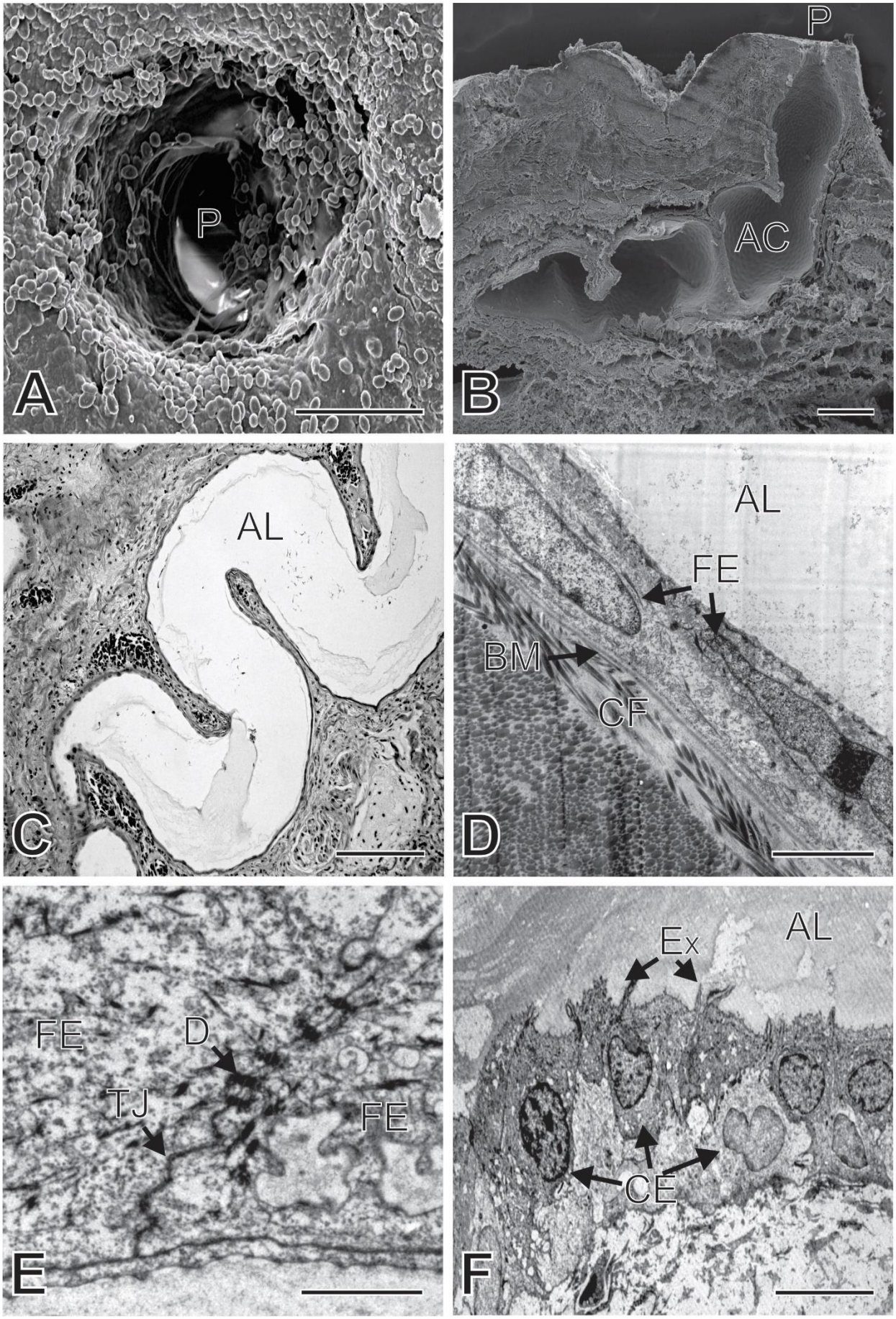
A
P
B
P
AC
C
AL
D
AL
FE
BM
CF
E
FE
D
TJ
FE
F
Ex
AL
CE

Figure 2.1. Micrographs of ampullary organs from all three studied species of dasyatids. **A.** Electron micrograph of a ventral ampullary pore (P) belonging to the hyoid cluster. *Neotrygon trigonoides*. SEM. Scale bar = 100 µm. **B.** Ampullary pore (P) leading to a quasi-sinusoidal ampullary canal (AC). *Neotrygon trigonoides*. SEM. Scale bar = 200 µm. **C.** Light micrograph of the quasi-sinusoidal route of the ventral, hyoid ampullary canals (AC). *Maculabatis toshi*. Light microscopy. Scale bar = 200 µm. **D.** Micrograph of the canal wall, composed of two layers of flattened epithelial cells (FE) located between the basement membrane (BM) and the ampullary lumen (AL), and enveloped by collagen fibres (CF). *Hemitrygon fluviorum.* TEM. Scale bar = 5 µm. **E.** Micrograph of two flattened epithelial cells of the canal wall adjoined by a tight junction (TJ) and underlying desmosomes (D). *Hemitrygon fluviorum.* TEM. Scale bar = 1 µm. **F.** Micrograph of a transition zone showing the enlarged cuboidal epithelial cells (CE). These cells show evidence of exocytosis (Ex) into the ampullary lumen (AL). *Hemitrygon fluviorum.* TEM. Scale bar = 10 µm.

Pear-shaped receptor cells lining the ampulla proper were similar in morphology among the three species and measure 15.5 ± 1.2 µm in height and 10.6 ± 0.3 µm in width (Fig. 2.2C) with a centrally located nucleus. These receptor cells extended from the basement membrane to the ampullary lumen where only a small portion of the cell, containing a single kinocilium, was exposed to the lumen (Fig. 2.2C, 2.2D). A basal body was identified for the kinocilia, yet no rootlet fibres were evident (Fig. 2.2B) in any of the species.

Within all three species, each receptor cell surveyed connected with one to three unmyelinated neural abutments in the basal region of the cell (Fig. 2.3A). These neural terminals contained numerous mitochondria and vesicles, and lay directly opposite to presynaptic bodies within the receptor cells (Fig. 2.3A). Presynaptic bodies were closely surrounded by numerous mitochondria (Fig. 2.3A).

In all species, receptor cells were adjoined to neighbouring supportive cells by tight junctions and underlying desmosomes (Fig. 2.3B). These apically-nucleated supportive cells extended from the basement membrane and protruded well into the ampullary lumen (Fig. 2.3C). This form of supportive cell appeared to structurally shelter the kinocilium of the receptor cells and supported several microvilli (Fig. 2.3D).

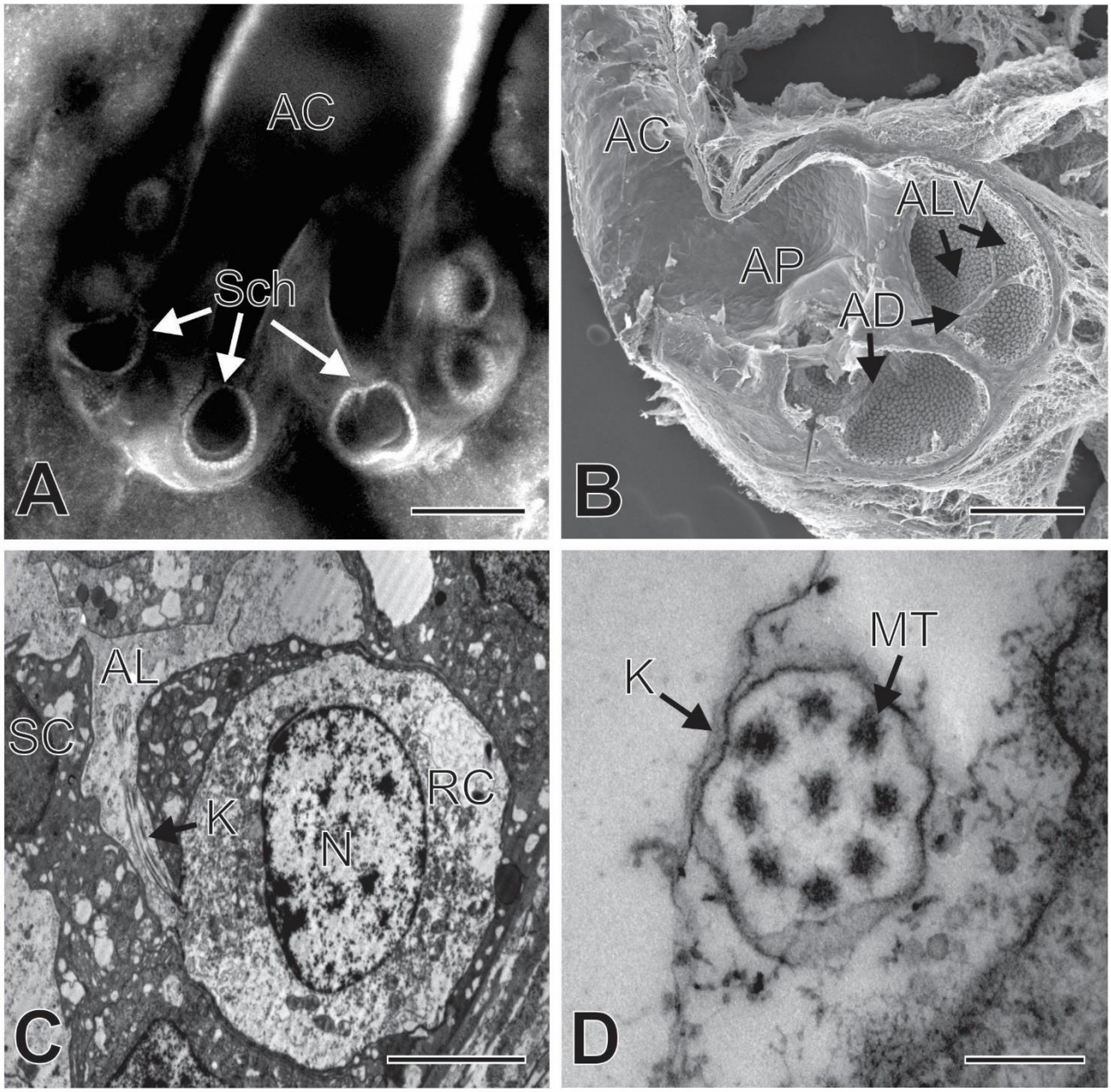

Figure 2.2. Micrographs of ampullary organs from all three studied species of dasyatids. **A**. Confocal image of an alveolar ampulla showing the ampullary canal (AC) splitting into smaller, narrower ducts, each leading to a single sensory chamber (Sch). *Maculabatis toshi*. Scale bar = 50 µm. **B.** Scanning electron micrograph of an ampullary canal (AC) opening into an ampulla proper (AP). Several alveoli (ALV) can be observed, each separated by alveolar divisions (AD). *Hemitrygon fluviorum.* SEM. Scale bar = 100 µm. **C**. Micrograph of two receptor cells (RC) with a centrally located nucleus (N) and a kinocilium (K) sticking out in the ampullary lumen (AL). The receptor cell is surrounded internally by supportive cells (SC) and externally by a sheath of collagen fibres. *Neotrygon trigonoides*. TEM. Scale bar = 5 µm. **D**. Cross section of a single kinocilium (K) showing an 8+1 arrangement of the microtubules (MT). *Neotrygon trigonoides.* TEM. Scale bar = 0.2 µm.

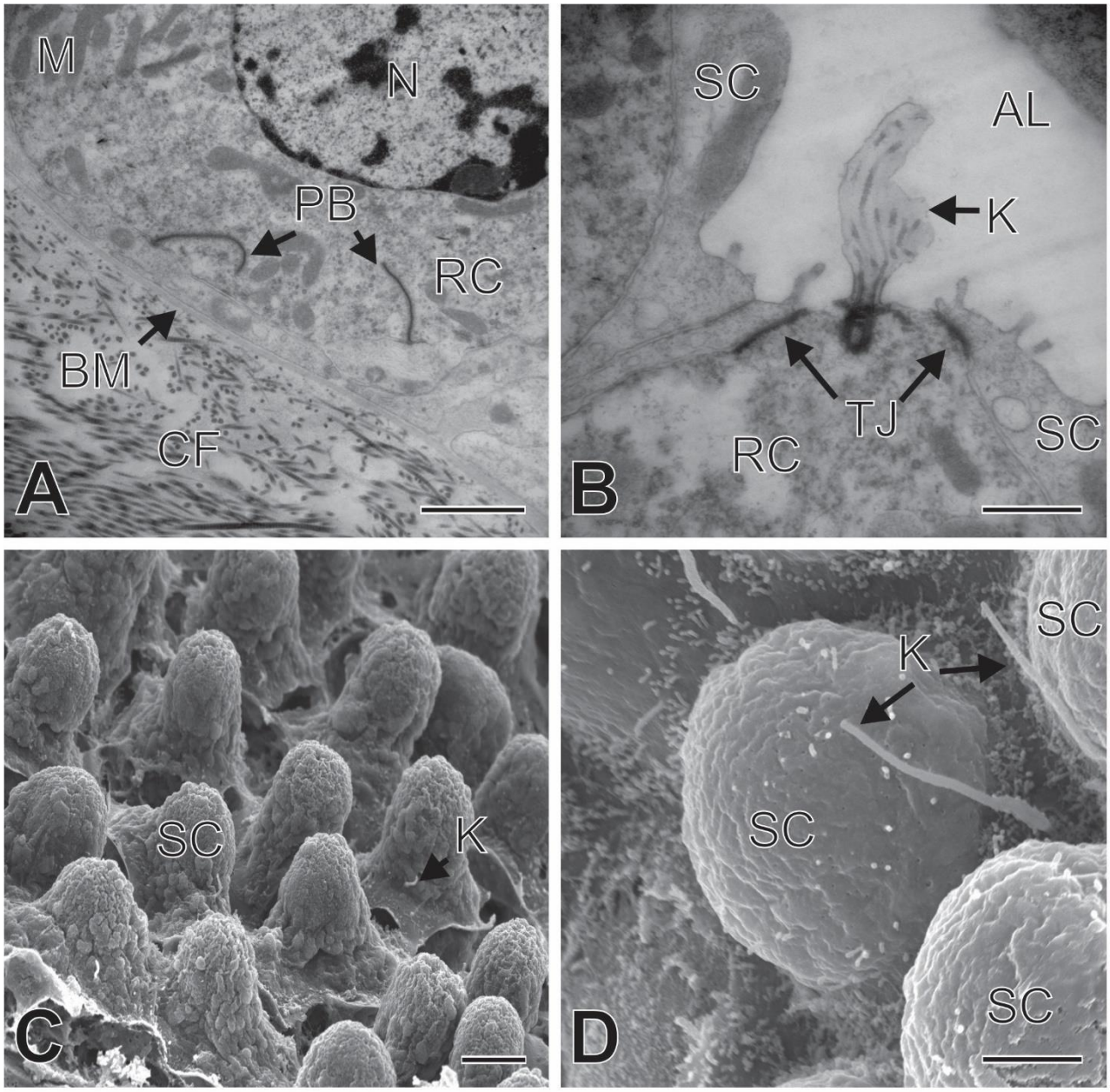

Figure 2.3. Micrographs of ampullary organs from all three studied species of dasyatids. **A.** Basal area of a receptor cell (RC) showing the base of the nucleus (N) numerous mitochondria (M) surrounding pre-synaptic bodies (PB). Collagen fibres (CF) are seen enveloping the ampulla proper separated by the basement membrane (BM). *Neotrygon trigonoides.* TEM. Scale bar = 2 µm. **B.** Apex of a receptor cell (RC) showing tight junctions (TJ) with adjacent supportive cells (SC) protruding into the ampullary lumen (AL), and a single kinocilium (K). *Neotrygon trigonoides.* TEM. Scale bar = 2 µm. **C.** Numerous supportive cells (SC) protruding well into the ampullary lumen. Kinocilia (K) can be observed sticking out near the base of the supportive cells. *Hemitrygon fluviorum.* SEM. Scale bar = 4 µm. **D.** Multiple kinocilia (K) located between supportive cells (SC). *Maculabatis toshi*. SEM. Scale bar = 1 µm.

Discussion

The distribution of ampullary pores on the ventral surface of *Neotrygon trigonoides*, *Hemitrygon fluviorum*, and *Maculabatis toshi* was similar to that described by both Chu & Wen (1979) and Camilieri-Asch *et al.* (2013); however, numerous ampullary pores were found on the dorsal surface of the snout leading to canals terminating in the superficial ophthalmic cluster, which has not been reported previously (Chu & Wen, 1979; Camilieri-Asch *et al.*, 2013). The total number of ampullary pores was only quantified in a single specimen of each species, but the final counts for both *N. trigonoides* and *H. fluviorum* matched those reported by Camilieri-Asch *et al.* (2013), with *M. toshi* in a similar range.

Similar to the findings of Camilieri-Asch *et al.* (2013), ventral ampullary pores were generally smaller than dorsal pores; however, the posterior ventral hyoid ampullary pores were similar in size to the dorsal pores and were much larger than previously described. Based on these findings, I suggest that the small ventral ampullary pores lead to ampullary organs primarily for point source localisation, directly associated with prey capture and feeding (Raschi, 1986). This interpretation is supported by reference to the diet of the three dasyatids, which feed primarily on infauna (Pardo *et al.*, 2015). These prey species include several families of polychaetes, such as Capitellidae and Eunicidae, and many crustaceans, particularly brachyurans and carideans, all of which are known to create shallow burrows in the sediment (Pardo *et al.*, 2015). A high density of small pores on the ventral surface of the rays may grant a higher sensitivity that is essential to detect buried prey. The larger pores on the dorsal surface, which seemingly mirror the distribution on the ventral surface, may assist in differentiating by reference larger electric or magnetic fields, such as the Earth's geomagnetic field, and be more useful for either navigation or predator detection (Kalmijn, 1974, 1978; Sisneros, 1998).

While Chu & Wen (1979) alluded to the quasi-sinusoidal shape of the ampullary canals in *Neotrygon trigonoides*, neither they nor Camilieri-Asch *et al.* (2013) clearly described the shape of the hyoid canals. The effect of the canal shape on the function of the ampullae is unknown, but it presumably results in a difference between an electrical signal that reaches the receptor cells via a more tortuous route compared to one that is conducted along a shorter, straight canal. Future studies should investigate whether the unusual canal morphology seen here in three dasyatids occurs in other species within the Dasyatidae, or in other families, and whether it is always associated with a diet comprising benthic or

infauna-based invertebrates. Despite the differences in shape, the overall cell composition of the ampullary canal wall was similar to descriptions previously published for other elasmobranchs (Whitehead, 2002b; Whitehead *et al.*, 2015a; Wueringer & Tibbetts, 2008; Wueringer *et al.*, 2009).

Confocal microscopy revealed that individual canals led to ampullae belonging to the alveolar type, similarly to those reported in *Squalus acanthias* (Jørgensen, 2005). Another feature of these species common to other elasmobranchs is the presence of multi-alveolate ampullae proper, with up to seven alveoli found in a single ampulla proper (Whitehead, 2002b; Jørgensen, 2005; Wueringer *et al.*, 2009; Theiss *et al.*, 2011; Whitehead *et al.*, 2015a).

This is the first report of the protrusion of the apically nucleated supportive cells well into the alveolar lumen; however, a similar but less exaggerated morphology occurs in *Carcharhinus leucas* (Whitehead *et al.*, 2015a). This marked protrusion of supportive cells occurs in all of the three studied benthic ray species, and raises the question as to their function. The only major morphological difference in the ampullae of Lorenzini among the three studied species was that *H. fluviorum* has larger ampullae and more sensory chambers. This characteristic may relate to the sensitivity of the electrosensory system, although how this would relate to the species' diet is unknown (Albert & Crampton, 2005; Pardo *et al.*, 2015). It is possible that the sensory chamber number is associated with large body size, as *H. fluviorum* specimens were larger in comparison to the other two species.

Overall, the electrosensory systems of these three sympatric dasyatids possessed remarkably similar morphological features that did not clearly reflect known differences in prey preference. Further studies involving comparisons between species feeding on benthic invertebrates and species with a primarily teleost diet may provide information on whether the morphology of the ampullae of Lorenzini is linked to diet.

Acknowledgements

I thank the Moreton Mixed Amateur Fishing Club, John Page, Drs. Tom Cribb and Scott Cutmore for their help in acquiring specimens. I also thank the University of Queensland Centre for Microscopy and Microanalysis, a node of the Australian Microscopy and Microanalysis Facility, for their assistance. Specimens were collected under The University

of Queensland Animal Ethics Approval SBMS/406/14 and General Fisheries Permit 165491 issued to MBB.

Chapter III

Distribution and morphology of the ampullae of Lorenzini in the bentho-pelagic ocellated eagle ray, *Aetobatus ocellatus.*

Abstract

This study investigated the morphology of the electrosensory system of the bentho-pelagic ocellated eagle ray, *Aetobatus ocellatus.* The species is common in coastal waters of the Indo-West Pacific, and feeds predominantly on benthic crustaceans and bivalve molluscs. As in other elasmobranchs, this species possesses ampullae of Lorenzini that enable detection of weak electric fields. The ampullary pores are densely located around the snout of the animal, with a relatively few pores on the rest of the body surface, and no ampullae on either surface of the pectoral fins. Most ampullary pores are similar in size with the exception of much larger pores that overlie and outline the visceral cavity on the ventral surface. There are no observable differences in pore morphology between those on the ventral and dorsal surfaces of the body, whereas some of the ampullary canals of the hyoid cluster have a quasi-sinusoidal shape. The ampullary organs are of the alveolar type, with six to eight sensory chambers. Similarly to benthic batoids previously studied, the supportive cells of all ampullae proper are apically nucleated and protrude markedly into the ampullary lumen, although the receptor cells are of similar shape to all other elasmobranchs.

Introduction

Chondrichthyes are capable of sensing weak electric fields in the water using their ampullae of Lorenzini (Kalmijn, 1966; 1971). This sense is referred to as electroreception and is used to locate prey or predators, navigate through the Earth's geo-magnetic field, and may be used for intra-specific communication (Tricas *et al*., 1995; Collin and Whitehead, 2004). With few exceptions, the ampullae of Lorenzini are generally restricted to the head region in sharks, while they are more widely dispersed on the bodies of rays (Chu and Wen, 1979; Kempster *et al*., 2012).

The ampullae of Lorenzini found in elasmobranchs typically consist of a somatic pore in the epidermis leading to an ampullary canal lined by two layers of flattened epithelial cells (Jørgensen, 2005). The ampullary canal is generally surrounded by a sheath of interlocking collagen fibres and is filled with a highly conductive mucopolysaccharide gel used to convey the electrical signal to the ampulla proper, which is located at the distal end of the canal (Waltmann, 1966; Jørgensen, 2005). The ampulla proper can comprise a single sensory chamber, or may be divided into several sensory chambers, each of which is lined by supportive and receptor cells. The number of sensory chambers may be dependent on the environment in which the animals live (Raschi, 1986; Jørgensen, 2005). A small area of the apex of each receptor cell is exposed to the ampullary lumen from which protrudes a single kinocilium, an arrangement which is thought to assist the reception of the electrical signals (Tricas, 2001). One or more neural terminals are present at the base of each receptor cell, connecting each cell to the central nervous system of the fish (Jørgensen, 2005).

The ampullary organs of rays have been studied in several species, but the main focus of most studies has been on the distribution and number of ampullary pores on the body (Chu & Wen, 1979; Jordan, 2008; Kempster *et al*., 2012). Benthic stingrays typically have a much higher concentration of ampullary pores on their ventral surface than on the dorsal surface. This presumably facilitates point source localisation, e.g. potential prey buried in the substrate, which is advantageous given the dorsal location of their eyes (Jordan *et al*., 2008; Kempster *et al*., 2012; Camilieri-Asch *et al*., 2013). Only two pelagic rays have been studied so far, *Pteroplatytrygon violacea* and *Myliobatis californica*, with the former showing a distribution of ampullary pores similar to that of benthic stingrays, but with a lower density (Jordan, 2008; Jordan *et al*., 2009). In the latter, most ampullary pores were concentrated

on the snout of the ray with relatively few pores located on the body, both dorsally and ventrally (Jordan, 2008).

Aetobatus ocellatus is a large bentho-pelagic eagle ray of coastal waters in the Indo-West Pacific (White *et al*., 2010). *Aetobatus ocellatus* has a predominantly pelagic lifestyle, but forages in the sediment using its elongated snout to feed on, primarily, molluscs and crustaceans (Last & Stevens, 2009; Schluessel *et al*., 2010). The distribution and morphology of ampullary organs in this species is currently unknown and the study of this species constitutes the first report on the morphology of the electrosensory system of a bentho-pelagic ray.

Methods

Animal collection

Four *Aetobatus ocellatus* (one male, three females, 550-870 mm disc width, W_D) were obtained from commercial fishers who operate on the western banks of Moreton Bay, Queensland, Australia. All specimens were euthanized by pithing, following The University of Queensland animal ethics guidelines (Animal ethics approval number: SBMS/406/14), and were dissected fresh. The skin from one individual was kept whole to study the pore distribution and obtain a total pore count, while ampullary clusters from all four individuals were fixed in either 10% neutral buffered formalin for histological analysis or 2.5% glutaraldehyde in 0.1M phosphate buffer at pH 7.2 for electron microscopy.

Tissue processing

To obtain gross measurements of the ampullae and canals, tissues were fixed in 10% Neutral buffered formalin and processed to paraffin wax, sectioned at 6 µm and stained with Mayer's Haematoxylin and eosin, according to the protocol described in Gauthier *et al*. (2018).

Similarly, the tissues for scanning (SEM) and transmission electron microscopy (TEM) were processed according to the methodology outlined in Chapter IV. Samples for SEM were coated with a thin layer of iridium and viewed with a JEOL7001 field emission scanning electron microscope. The TEM samples were embedded in EPON resin, sectioned at 90 nm

thickness and viewed with either a JEOL1011 or Hitachi HT7700 transmission electron microscope at 80 kV.

Statistics

A one-way ANOVA was used to compare the pore diameters in different locations of the body followed by a post-hoc Tukey test. Results are presented as mean and standard deviation, with significance accepted at $p < 0.05$.

Results

The ampullary pores of *Aetobatus ocellatus* are concentrated around the head of the animal, with few pores scattered on the rest of the body surface, and none on the pectoral fins (Fig. 3.1). The single specimen examined whole had 933 ampullary pores scattered over its body surface, with more ventral pores than dorsal (697 *vs* 236). These pores connect to three paired ampullary clusters: The superficial ophthalmic, hyoid, and mandibular clusters. The relatively few ventral pores situated on either side of the ventral cavity belong to the hyoid cluster. Ampullary pores vary greatly in size, ranging from 109 µm for those found on the snout, to 630 µm for those found on the ventral surface of the body.

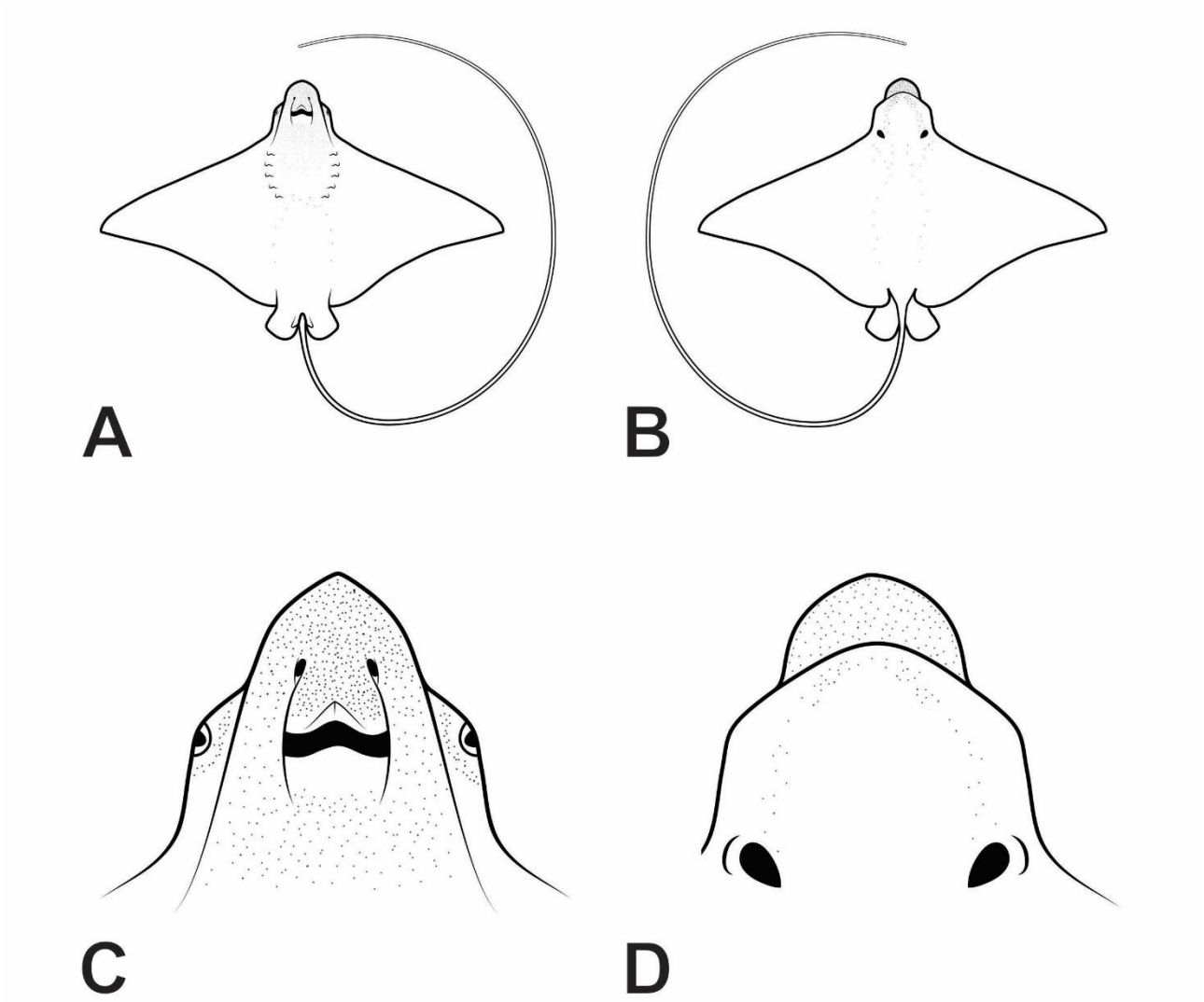

Figure 3.1. Ampullary pore distribution on the ventral (A, C) and dorsal (B, D) surfaces of *Aetobatus ocellatus.*

There was no significant size difference ($p > 0.05$) among ampullary pores on the ventral and dorsal surface of the snout (mean diameter = 210 ± 46 µm and 207 ± 51 µm respectively), in the infraorbital area (243 ± 72 µm) or dorsal surface of the body (250 ± 17 µm). Ampullary pores on the ventral surface of the body are significantly larger than the pores found in all other locations (479 ± 76 µm, $p < 0.05$; Fig. 3.2A).

Some, but not all, ampullary canals (mean diameter = 408 ± 117 µm) on both the ventral and dorsal surface of the ray's body leading to the hyoid cluster are quasi-sinusoidal in shape (Fig. 3.2B). Each ampullary canal wall comprises two layers of overlapping flattened epithelial cells connected by tight junctions, with underlying desmosomes (Fig. 3.2C).

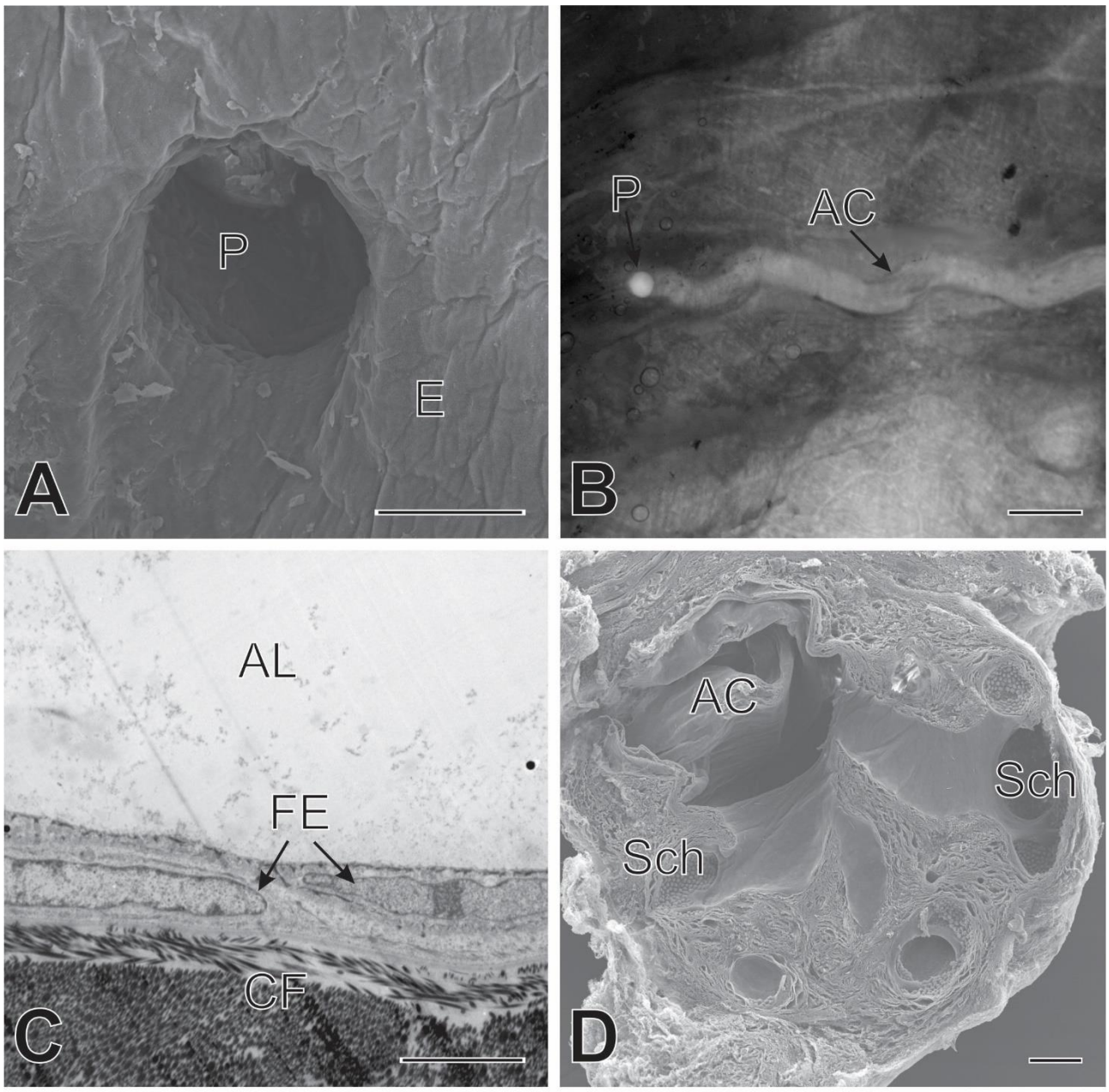

Figure 3.2. Micrographs of ampullae of Lorenzini from *Aetobatus ocellatus*. **A.** Ampullary pore (P) within the epidermis (E). SEM. Scale bar = 100 µm. **B.** Photograph of an ampullary pore (P) and the associated quasi-sinusoidal canal (AC) from the dorsal surface of *A. ocellatus*. Scale bar = 1000 µm. **C.** Ampullary canal wall of *A. ocellatus* showing two overlapping layers of flattened epithelial cells (FE). The canal wall is exposed to the ampullary lumen (AL) internally, while externally, the canal is surrounded by a sheath of collagen fibres (CF). TEM. Scale bar = 5 µm. **D.** Cross section through an ampulla proper showing the ampullary canal (AC) splitting off into smaller canals, each connected to a sensory chamber (SCh). SEM. Scale bar = 100 µm.

The distal end of the ampullary canal opens into an ampulla proper of the alveolar type, composed of 6 – 8 sensory chambers, which are further divided into multiple alveoli (Fig. 3.2D).

Ampullae proper average 674 ± 133 µm in diameter. The sensory epithelium is composed of apically nucleated supportive cells that protrude well into the lumen and envelop the receptor cells (Fig. 3.3A, B). The receptor cells are pear shaped with a round nucleus (Fig. 3.3B), with only a small portion of their apex exposed to the ampullary lumen, from which extends a single kinocilium (Fig. 3.3C). At the base of each receptor cell, pre-synaptic bodies can be observed lying opposite of a neural terminal (Fig. 3.3D). External to the basement membrane, the ampulla proper is surrounded by a sheath of interlocking collagen fibres (Fig. 3.3D).

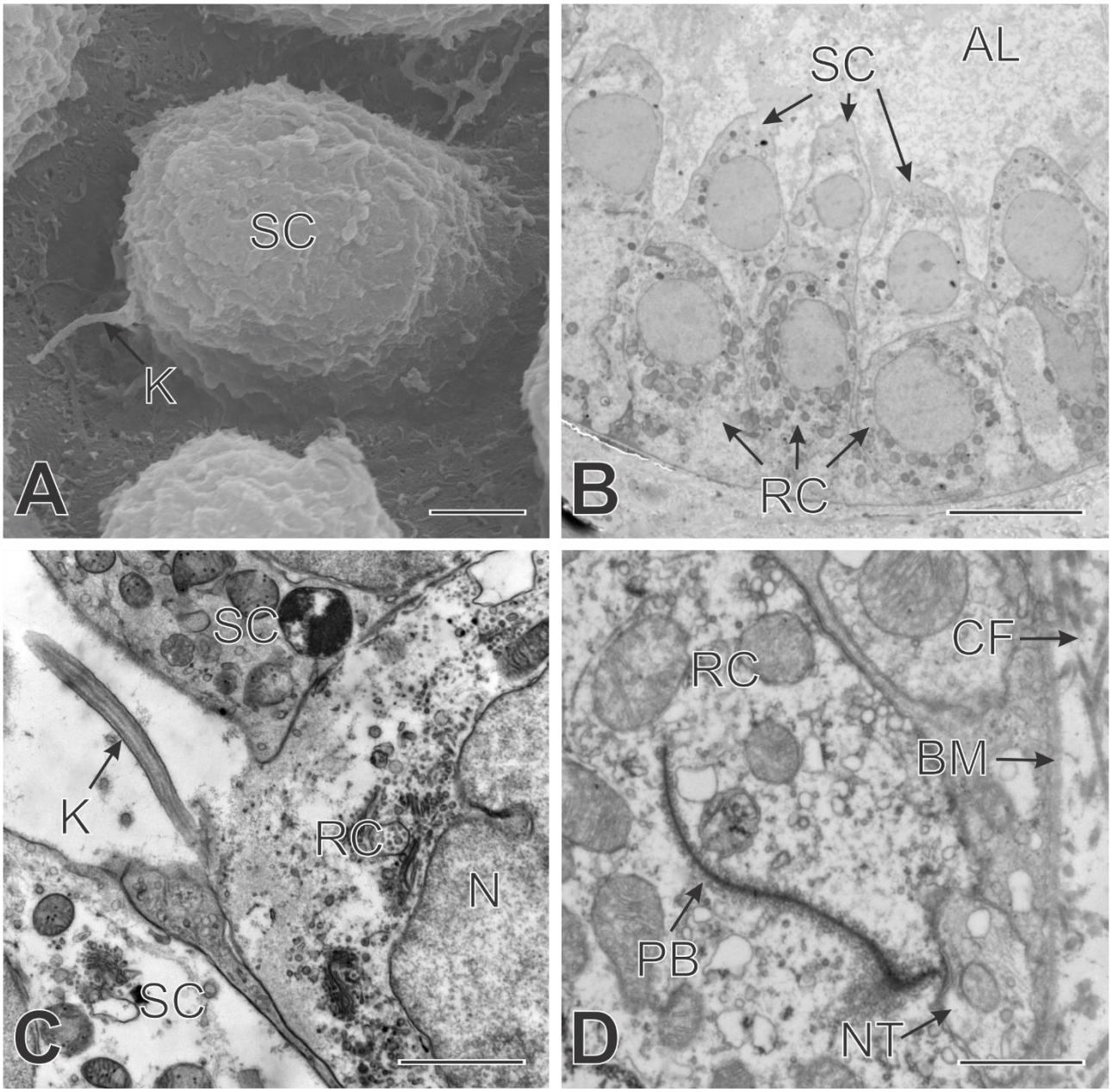

Figure 3.3. Micrographs of ampullae of Lorenzini from *Aetobatus ocellatus*. **A.** A supportive cell (SC) protruding into the ampullary lumen, with a single kinocilium (K) connected to a receptor cell near the base of the supportive cell. SEM. Scale bar = 2 µm. **B.** Sensory epithelium of *A. ocellatus*, showing the apically nucleated supportive cells (SC) protruding into the ampullary lumen (AL) and enveloping the receptor cells (RC). TEM. Scale bar = 10 µm. **C.** Apex of a receptor cell (RC) with part of the nucleus (N) visible, surrounded by two supportive cells (SC). A single kinocilium (K) extends out from the small surface area of the receptor cell exposed to the ampullary lumen. TEM. Scale bar = 2 µm. **D.** Basal area of a receptor cell (RC) showing a single pre-synaptic body (PB) connected to a neural terminal (NT). External to the basement membrane (BM), the ampulla proper is surrounded by a sheath of collagen fibres (CF). TEM. Scale bar = 1 µm.

Discussion

The pore distribution of *Aetobatus ocellatus* is unlike that of most elasmobranchs studied to date. While the distribution is generally similar to that of *Myliobatis californica*¸ the complete absence of ampullary pores on the pectoral fins had not been observed in any other rays previously studied, and could be linked to their pelagic nature or their feeding strategies (Jordan, 2008). In contrast to benthic stingrays, *A. ocellatus* is in constant movement through the water column and does not rest on the benthos for extended periods of time. It also uses an oscillatory pectoral fin mode of swimming, with a 'wingbeat' amplitude that is much greater than the undulation used by most benthic rays, which mostly only undulate the extremities of their pectoral fins (Rosenberg, 2001). The absence of pores on the pectoral fins may relate to this continuous, large amplitude movement, although the presence of a few ampullary pores on the pectoral fins of *M. californica* challenges this explanation. Alternatively, as elasmobranchs generate weak electric fields while swimming, they need to filter them out to focus on other external fields (Montgomery *et al*., 2012). An absence of ampullary pores on the pectoral fins may be an adaptation to avoid continuous filtering of this self-generated electrical noise, or the large amplitude movement renders the ampullae ineffective for localisation of the electric field source.

The high density of pores on the snout of *A. ocellatus* presumably relates to its foraging strategy, in which individuals swim over and close to the benthos in search of prey. While detection may occur through use of visual or olfactory senses, it is most likely that buried prey is detected by electroreception due to the electric fields that they produce. When foraging *A. ocellatus* generally swims relatively fast compared to benthic rays, and use their protrusible jaws and associated soft tissue structures to extract a prey item from a specific 'target region' of the sediment. In contrast, many benthic rays excavate a relatively large, body-sized pit to extract a prey item. I suggest that the snout of *A. ocellatus* is specialised to detect prey directly in front of the individual and to facilitate specific targeting.

This study constitutes the third observation of quasi-sinusoidal ampullary canals in elasmobranchs, but also the first known occurrence of this peculiar shape in canals present on the dorsal surface of a ray (Gauthier *et al*., 2018, Chapter II). Their occurrence in *Hemiscyllium ocellatum*, but not *Chiloscyllium punctatum*, two small demersal sharks with similar foraging behaviours, indicate that this canal morphology is unlikely to be driven by differences in diet (Chapter IV). In *A.* ocellatus, the fact that these quasi-sinusoidal canals

run parallel to the epidermis, a feature usually linked to the detection of uniform fields, and their presence on the dorsal surface supports the hypothesis that this canal morphology is not related to prey detection (Rivera-Vicente *et al*., 2011). However, the functional implications of this curious morphology remain obscure. The composition of the ampullary canal wall, two layers of interlocking flattened epithelial cells, is similar to all other elasmobranchs studied to date (Waltmann, 1966; Gauthier *et al*., 2018, Chapter II).

The ampullae proper of *A. ocellatus* are of the alveolar type, as those of three other species of batoids and the piked dogfish, *Squalus acanthias* (Jorgensen, 2005; Gauthier *et al*., 2018). This type of ampulla, while not widespread in selachimorphs, appears to be a common trait in batoids. Regarding the sensory epithelium, the pronounced protrusion of apically nucleated supportive cells into the ampullary lumen is similar to that seen in benthic stingrays. This morphology may allow for an increase in number of receptor cells per ampullae by having the large nuclei of the supportive cells away from the rest of the sensory epithelium. The receptor cells themselves do not differ from the common pear-shaped receptor cells found in other elasmobranchs.

Overall, the distribution of ampullary pores on the body of *A. ocellatus* seems to be heavily influenced by its bentho-pelagic nature and feeding strategies, but the ultrastructure of its ampullae of Lorenzini remains similar to that of benthic dasyatids. Questions remain about the occurrence of apically nucleated supportive cells and the quasi-sinusoidal shape of some of the ampullary canals, and further research on these features in different species may provide insight into their functional roles.

Acknowledgements

Thank you to Taylor Maggiacomo for drawing the outlines used in Figure 3.1, John Page, Dave Thomson, Russel Yong, Nicholas Wee, and Scott Cutmore for their help in acquiring the specimens used in this study, staff of the University of Queensland Centre for Microscopy and Microanalysis, a node of the Australian Microscopy and Microanalysis Facility, for their assistance, and all of the staff at the Moreton Bay Research Station for their help and the use of their facilities. Specimens were collected under The University of Queensland Animal Ethics Approval SBMS/406/14 and General Fisheries Permit 165491 issued to M.B.B..

Chapter IV

Comparative morphology of the electrosensory system of the epaulette shark, *Hemiscyllium ocellatum*¸ and the brown-banded bamboo shark, *Chiloscyllium punctatum*.

Abstract

Recent research into the distribution and morphology of the ampullae of Lorenzini has revealed that they may be influenced by a species' lifestyle and the habitat that it occupies. We compared the electrosensory system of two benthic elasmobranchs, *Hemiscyllium ocellatum* and *Chiloscyllium punctatum*. The distribution of the ampullary pores on the head was similar for both species, with a higher density of pores anteriorly and a lower density posteriorly, although *C. punctatum* generally possessed larger pores. Ampullary canals of the mandibular cluster were quasi-sinusoidal in *H. ocellatum*, a shape previously found in benthic rays only, whereas ampullary canals in *C. punctatum* were of a linear morphology as reported for many shark and ray species previously. The ampullae proper were of the lobular type, as occurs in most galean sharks. *Chiloscyllium punctatum* had six sensory chambers compared to the five per ampulla in *H. ocellatum*, which were generally smaller than those of *C. punctatum*. The sensory epithelium comprised flattened receptor cells, compared to the usual pear-shaped receptor cells encountered in other elasmobranchs, and their apically nucleated supportive cells did not protrude markedly into the ampullary lumen, unlike those in benthic rays.

Introduction

All chondrichthyans possess the ability to detect weak electrical fields in their environment (Zakon, 1986; Jørgensen, 2005). Electroreception is used in prey and predator detection, intra- and inter-specific communication, and orientation through the Earth's geomagnetic field (Kalmijn, 1974; Tricas *et al*., 1995; Collin & Whitehead, 2004). Passive electroreception is possible in elasmobranchs through use of ampullae of Lorenzini that typically comprise a somatic pore within the epidermis leading to a canal filled with a mucopolysaccharide gel (Jørgensen, 2005). The canal wall generally comprises squamous epithelial cells adjoined by tight junctions and underlying desmosomes (Waltmann, 1966; Jørgensen, 2005). The ampullary canal terminates in a bulb, the ampullae proper, which typically consists of several sensory chambers lined with receptor and supportive cells (Jørgensen, 2005).

Recent research into the morphology of the electrosensory system in elasmobranchs shows that the pore distribution varies among species, and may be influenced by their lifestyle and surrounding environment (Kempster *et al*., 2012). Wobbegong sharks (Orectolobidae) possess the highest number of ampullary pores on the dorsal surface of the head across all shark species studied to date. This arrangement of pores appears to match the requirements for detection of potential prey passing over the head, as these sharks are camouflaged, benthic predators that ambush prey from below (Theiss *et al*., 2011; Egeberg *et al*., 2014). In comparison, most pelagic sharks typically possess a much higher proportion of ampullary pores on the ventral surface of the head to facilitate close-range detection and localization of prey immediately prior to capture and ingestion (Cornett, 2006; Kempster *et al*., 2012).

The epaulette shark, *Hemiscyllium ocellatum* (Bonnaterre, 1788), and the brown-banded bamboo shark, *Chiloscyllium punctatum* (Müller & Henle, 1838), are benthic species (Order: Orectolobiformes) which, within Australia, occur in warm, northern waters (Last & Stevens, 2009). *Hemiscyllium ocellatum* is a small, slender shark (<110 cm total length, L_T) found on coral reefs, with a diet that comprises primarily benthic invertebrates, especially the polychaete *Eurythoe complanata* and Xanthid crabs (Heupel & Bennett, 1998; Last & Stevens, 2009). Recent research on their sensory system has resulted in a detailed description of the distribution of their mechano- and electrosensory systems, with the first report of ampullary pores on the body of a shark (Winther-Jason *et al*., 2012). However, no details were provided on the morphology of their ampullary organs. *Chiloscyllium punctatum* has a greater girth than does *H. ocellatum* for any given length, and grows to about 130 cm

L_T in Australian waters. The species is found in a variety of habitats, including coral reefs, intertidal flats, and seagrass beds (Last & Stevens, 2009), but information on its diet is lacking. Previous research on this species has shown late-stage embryos in the egg case may use their electroreceptive sense to detect potential predators. In response to an applied, simulated-predator sinusoidal electric field the embryos temporarily stop respiratory gill movements, presumably to lower their risk of being detected (Kempster *et al*., 2013). However, the pore distribution and morphology of their electrosensory system is unreported.

The aims of this project were to provide a detailed description of the ultrastructure of the ampullae of Lorenzini of both *H. ocellatum* and *C. punctatum*, and investigate potential morphological differences between these two closely related shark species. The dietary composition of *C. punctatum* is explored and contrasted with that of *H. ocellatum* to explore whether prey selection may relate to morphological differences between the electrosensory systems of the two shark species.

Methods

For analysis of the electrosensory system, five *Hemiscyllium ocellatum* (4 female, 1 male; 475-640mm L_T) were collected from Heron Island, Queensland Australia (23°26'33.3"S, 151°54'54.2"E). Six specimens of *Chiloscyllium punctatum* (3 female, 3 male; 470-1100mm L_T) were purchased from commercial fishers in various locations on the western banks of Moreton Bay, Queensland (27°32'21.8"S, 153°19'23.7"E).

Following euthanasia, the skin was removed from the head for investigation of the distribution and quantity of the ampullary pores. A sub-sample of the ampullary organs was dissected and fixed in either 10% neutral buffered formalin or 2.5% glutaraldehyde in 0.1M phosphate buffer for further investigation. All formalin-fixed material was processed for light, confocal, and scanning electron microscopy according to the methodology outlined in Gauthier *et al*. (2018).

Sizes of the ampullary pores, ampullary canals, ampullae proper and sensory chambers were recorded using a Nikon 50i Eclipse upright bright-field microscope and Nikon Basic Research 4.0 software. A Student's t-test compared the mean number of ampullary pores in *H. ocellatum* (n = 4) and *C. punctatum* (n = 4). For pore diameter, 10 representative pores from the head anterior to the eye, and 10 pores from posterior to this point were measured

on 3 individuals of each species. Similarly, 10 measurements for ampulla proper and sensory chamber diameters, and ampullary canal widths were made in four individuals of each species. A linear regression was used to investigate the effect of size of an individual on the ampullary organs. Results are presented as mean and standard deviation, with $p < 0.05$ being the test of significance.

Samples fixed in 2.5% glutaraldehyde were processed for transmission electron microscopy according to the following protocol: after fixation, the samples were rinsed 3 x 5 min in phosphate buffer, followed by a post-fixation in 2% osmium tetroxide + 1% potassium ferricyanide solution for 2 x 6 min in a Pelco Biowave set at 22 ºC, 80 watts (W), under vacuum (vac). Samples were then rinsed in deionised water (UHQ) (2 x 40 s, 22 ºC, 80 W, vac), followed by immersion in 1% tannic acid solution (2 x 6 min, 22 ºC, 80 W, vac), another rinse in UHQ water (2 x 40 s, 22 ºC, 80 W, vac), a secondary post-fixation in 2% osmium tetroxide (2*6 min, 22 ºC, 80 W, vac), a rinse in HQ water (2 x 40 s, 22 ºC, 80 W, vac), stained in 1% aqueous uranyl acetate (2 x 6 min, 45 ºC, 80 W, vac), rinsed in UHQ water (2 x 40 s, 45 ºC, 80 W, vac), stained in 0.6% lead aspartate (2 x 6 min, 45 ºC, 80 W, vac) followed by a final rinse in UHQ water (2 x 40 s, 45 ºC, 80 W, vac). Samples were then dehydrated in an ascending series of acetone (50%, 60%, 70%, 80%, 90%, 100%, 100%; 3 min, 22 ºC, 150 W), placed in an acetone:EPON mix (3:1, 2:1, 1:1, 1:2, 1:3; 3 min, 22 ºC, 150 W, vac) for infiltration, and then three changes of EPON (3 min, 22 ºC, 150 W, vac). The resin blocks were then left to polymerise for two hours at 90 ºC. Ultrathin sections (90 nm) were cut with a diamond knife (Leica EM UC62 ultramicrotome) and mounted on 1 mm x 2 mm three-slot, carbon-stabilized collodion coated grids. Sections were viewed and photographed with either a JEOL 1011 or Hitachi 7700 transmission electron microscope at 80 kV.

The stomach contents of an additional 14 specimens of *C. punctatum* obtained from Moreton Bay were analysed following the methodology described in Heupel & Bennett (1998). Briefly, prey items in the stomach contents were identified, and the frequency of occurrence (F_o; percentage of stomachs containing a particular prey group), numerical composition (N_c; number of items in each prey group expressed as a percentage of the total number of prey items) and volumetric composition (V_c; volume of prey items in each prey group expressed as a percentage of the total volume of prey) calculated. These data were used to calculate the Index of Relative Importance (IRI), where IRI = $(N_c + V_c)F_o$.

All research complied with The University of Queensland animal ethics committee approvals ANT/563/98/UQFG/URG and UQ/SBMS/406/14.

Results

Distribution and size of the ampullary pores

Ampullary pores of both species were restricted to the head, with the highest pore density in the anterior region of the snout (Fig. 4.1). There was no evidence of ampullary pores on the body of the sharks, and no ampullary canals originate posterior to the gill slits. Some pores of both species were partially or totally covered by the overlapping placoid scales (Fig. 4.2A). *Chiloscyllium punctatum* possessed significantly more ampullary pores than does *Hemiscyllium ocellatum* (584 *vs* 429, $p < 0.05$; Table 1). Mean pore diameter was significantly larger ($p < 0.05$) in *C. punctatum* (370 ± 50 µm) compared to that of *H. ocellatum* (261 ± 54 µm). There was no regional (anterior *vs* posterior) difference in pore size in *H. ocellatum* (267 µm *vs* 256 µm, $p > 0.05$), but anterior pores in *C. punctatum* were significantly smaller than the posterior ones (326 µm *vs* 413 µm, $p < 0.05$; Table 1).

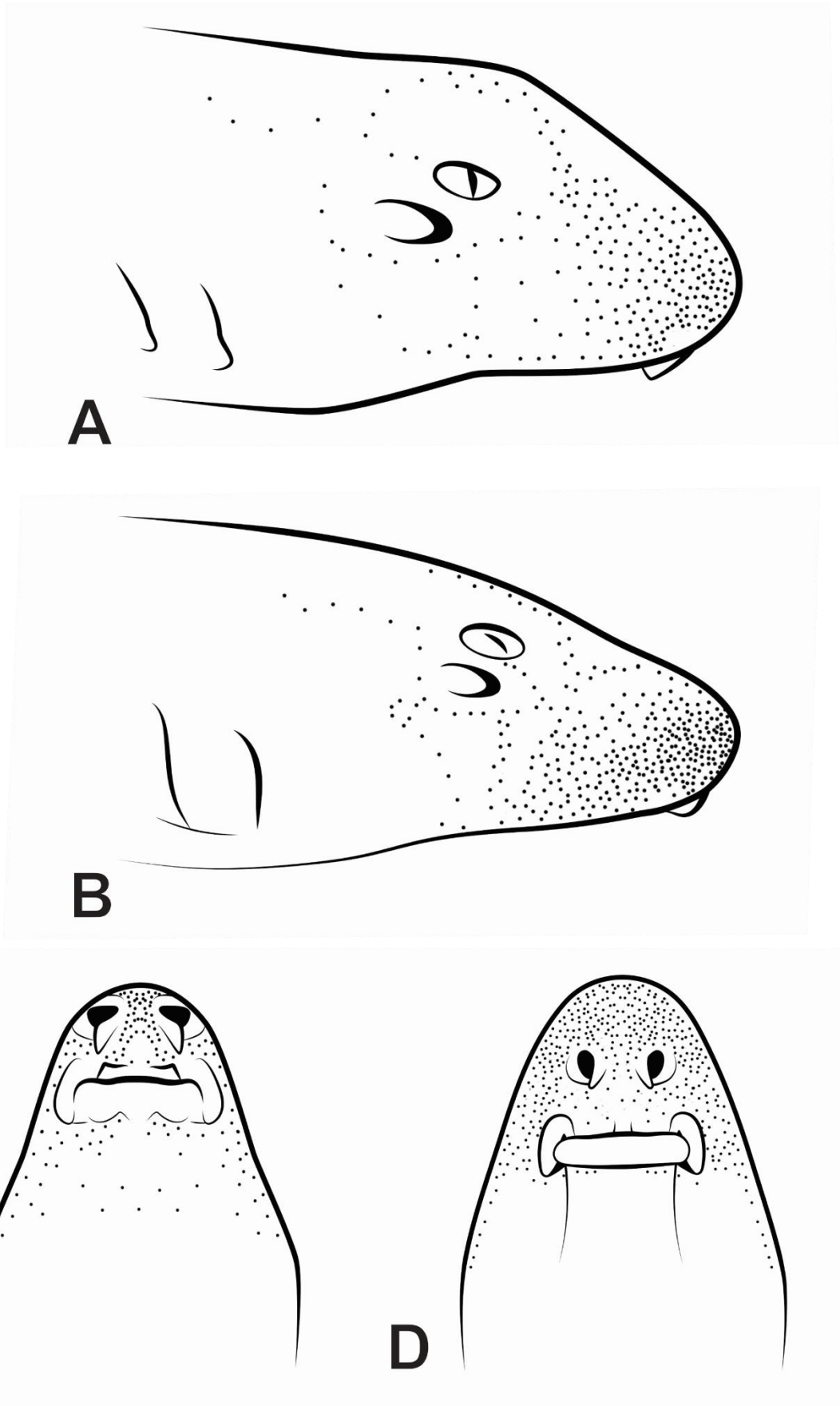

Figure 4.1. Ampullary pore distribution in *Hemiscyllium ocellatum* (A, C) and *Chiloscyllium punctatum* (B, D).

Table 4.1. Morphological measurements of the ampullae of Lorenzini of *Chiloscyllium punctatum* and *Hemiscyllium ocellatum*.

Species	Ampullary Pore Count	Pore Size Anterior (µm)	Pore Size Posterior (µm)	Ampulla Proper Diameter (µm)	Sensory Chamber Diameter (µm)	Ampullary Canal Width (µm)
Chiloscyllium punctatum	584 ± 50	326 ± 72	413 ± 89	581 ± 77	193 ± 38	494 ± 99
Hemiscyllium ocellatum	429 ± 54	267 ± 91	256 ± 64	454 ± 40	159 ± 28	338 ± 92

Morphology of the ampullary organs

Canals of the mandibular cluster in *H. ocellatum* were quasi-sinusoidal in shape (Fig. 4.2B), however, in *C. punctatum* they were more typically 'linear-shaped' (Fig. 4.2C). Mean ampullary canal diameter in *C. punctatum* was larger than that in *H. ocellatum* (494 µm *vs* 338 µm, $p < 0.05$; Table 1), and although considerable intra-individual variation was apparent, size of an individual did not influence the diameter of the ampullary canals for either species (Fig. S1). Canal walls of both species were composed of two layers of flattened epithelial cells adjoined by tight junctions and underlying desmosomes (Fig. 4.2D). The canal wall was supported by a collagen sheath along the entire length of the canal and immediately beneath the epithelial tissues.

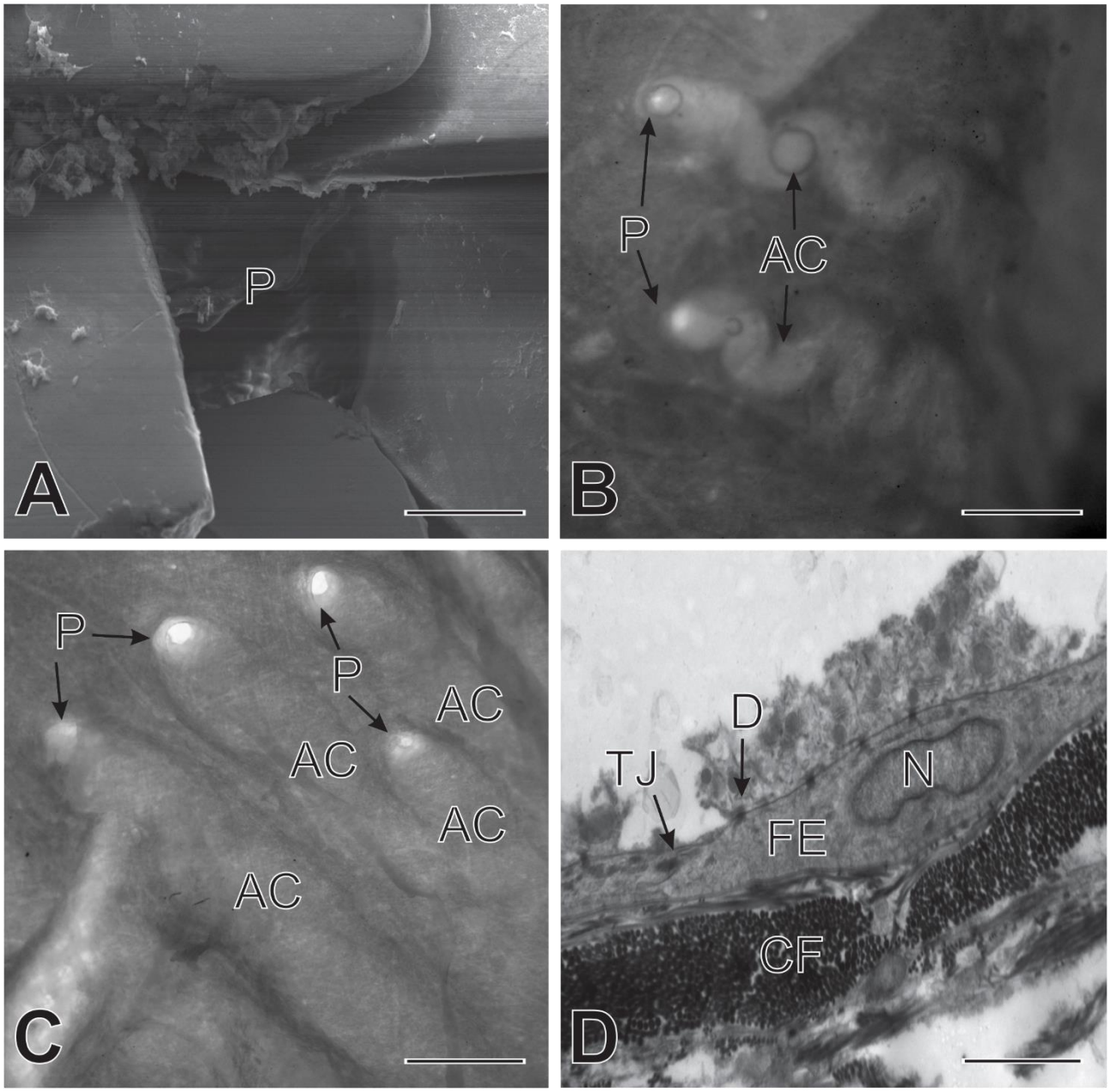

Figure 4.2. Micrographs of ampullae of Lorenzini from *Hemiscyllium ocellatum* and *Chiloscyllium punctatum*. **A.** Ampullary pore (P) from *H. ocellatum* partially covered by placoid scales. SEM. Scale bar = 50 µm. **B.** Photograph of ampullary pores (P) and the associated quasi-sinusoidal canals (AC) from the mandibular cluster of *H. ocellatum*. Scale bar = 400 µm. **C.** Photograph of ampullary pores (P) and the associated straight ampullary canals (AC) from the mandibular cluster of *C. punctatum.* Scale bar = 500 µm. **D.** Ampullary canal wall of *H. ocellatum* showing the two layers of flattened epithelial cells (FE) with their nuclei (N), the tight junctions (TJ) and underlying desmosomes (D) connecting the epithelial cells. Externally, the canal is surrounded by a sheath of collagen fibres (CF). TEM. Scale bar = 4 µm.

The ampullary canal wall transitioned from flattened squamous cells to cuboidal epithelial cells just proximal to the opening into the ampulla proper (Fig. 4.3A). The ampullae proper of *C. punctatum* were significantly larger than those of *H. ocellatum* (581 µm *vs* 454 µm, $p < 0.05$; Table 1). Confocal and scanning electron microscopy revealed that these ampullary organs had a lobular morphology, comprising five sensory chambers in *H. ocellatum* and six in *C. punctatum* (Fig. 4.3B). The sensory chambers of *C. punctatum* were larger than those of *H. ocellatum* (193 µm *vs* 159 µm, $p < 0.05$; Table 1). The size of an individual did not influence the diameter of the ampullae proper nor of the sensory chambers for either species (Fig. S1).

The sensory chambers of both species were lined with a smooth layer of apically nucleated supportive cells (Fig. 4.3C, 4.3D) as well as slightly flattened receptor cells (Fig. 4.3D) that extended from the basement membrane to the ampullary lumen. A single kinocilium protruded from the apex of each receptor cell and rootlet fibres were also apparent (Fig. 4.3E). A neural terminal adjoined the base of each receptor cell, and these receptor cells contained pre-synaptic bodies that lied opposite to the neural terminal (Fig. 4.3F).

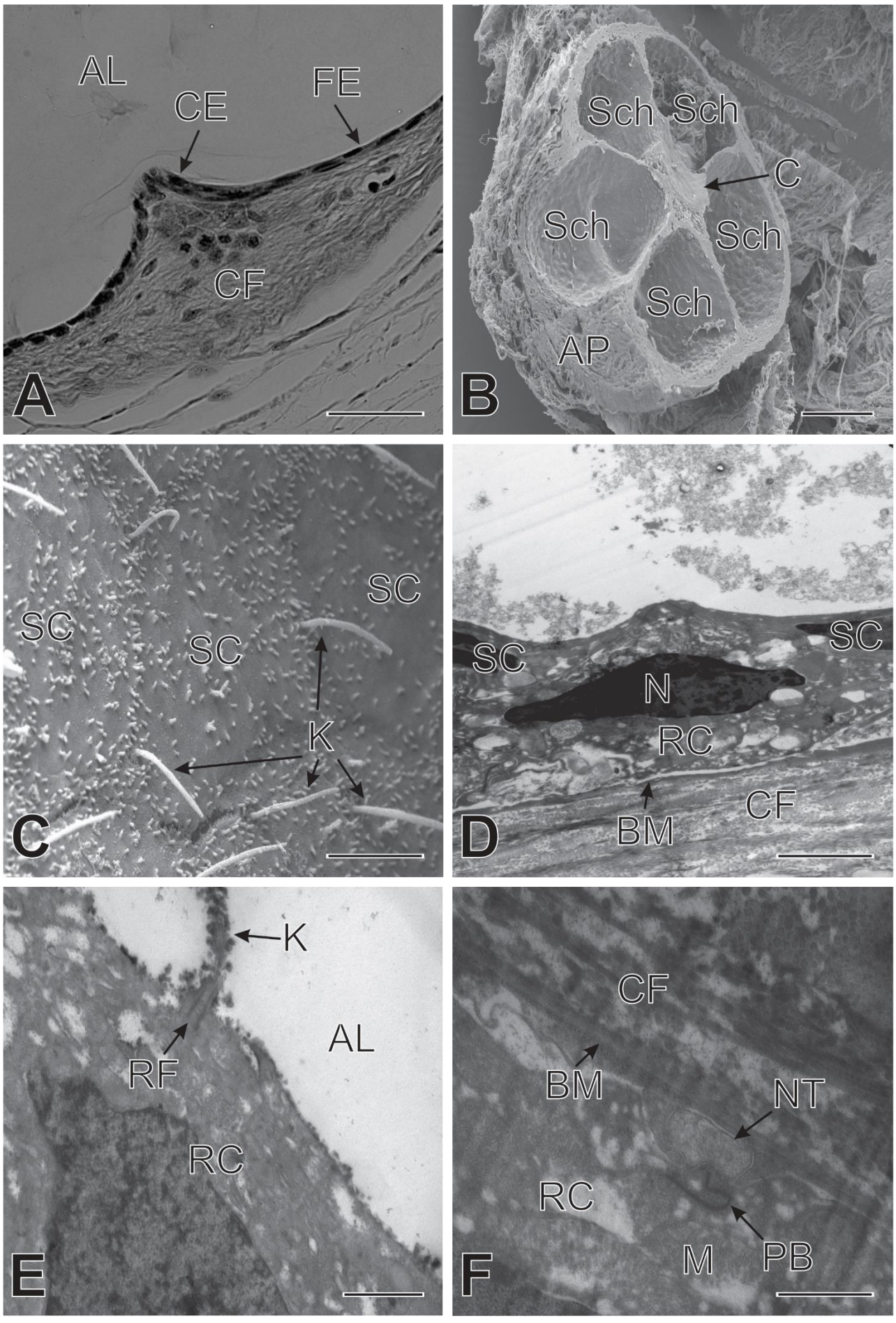
AL
CE
FE
CF
A
Sch
Sch
C
Sch
Sch
Sch
AP
B
SC
SC
SC
K
C
SC
SC
N
RC
BM
CF
D
K
AL
RF
RC
E
CF
BM
NT
RC
M
PB
F

Figure 4.3. Micrographs of ampullae of Lorenzini from *Hemiscyllium ocellatum* and *Chiloscyllium punctatum*. **A.** Light micrograph of the transition zone between the ampullary canal and ampulla proper in *C. punctatum*. Flattened epithelial cells (FE) of the ampullary canal wall widen and to give rise to cuboidal epithelial cells (CE) at the transition zone. The ampullary lumen (AL) is internal to the canal wall, while the ampullary canal is surrounded by a sheath of interlocking collagen fibres (CF). Scale bar = 20 µm. **B.** Cross section through an ampulla proper (AP) in *H. ocellatum* showing the five sensory chambers (SCh) and centrum (C). SEM. Scale bar = 100 µm. **C.** Smooth sensory epithelium in *C. punctatum* showing the supportive cells (SC) and kinocilia (K) extending into the lumen. SEM. Scale bar = 5 µm. **D.** Two apically nucleated supportive cells (SC) enclosing a slightly flattened receptor cell (RC) with a polymorphic nucleus (N) in *H. ocellatum*. A sheath of collagen fibres (CF) can be observed external to the basement membrane (BM). TEM. Scale bar = 2 µm. **E.** Apex of a receptor cell (RC) with a single kinocilium (K) extending out into the ampullary lumen (AL). Rootlet fibres (RF) are apparent at the base of the kinocilium. TEM. Scale bar = 1 µm. **F.** Base of a receptor cell (RC) with a neural terminal (NT) and pre-synaptic bodies (PB) as well as numerous mitochondria (M). External to the basement membrane (BM), a sheath of interlocking collagen fibres (CF) surrounds the ampulla. TEM. Scale bar = 1 µm.

Diet

Overall, both shark species targeted similar prey although the relative proportions differed markedly for some of the prey types. Crabs and teleost fishes (primarily the burrowing snake eel, *Malvoliophis pinguis* (Günther, 1872)) comprised the majority of the diet (87%IRI) of *C. punctatum*, whereas annelids and crabs formed most of the diet (91.4%IRI) in *H. ocellatum*, with teleost fishes a minor component (Table 2). The greater importance of fishes in the diet of *C. punctatum* may reflect the large body size of the specimens examined (body mass, M_B = 4.2 – 8.0 kg, L_T = 990-1175 mm) compared to *H. ocellatum* (M_B = c. 0.3 – 0.85 kg, L_T = c. 500 – 800 mm).

Table 4.2. Composition of the diet of *Chiloscyllium punctatum* and *Hemiscyllium ocellatum*, shown as frequency of occurrence (F_o), numerical composition (N_c), volumetric composition (V_c) and the Index of Relative Importance (IRI).

Species	Prey	Stomachs containing prey	F_o (%)	Number of prey items	N_c (%)	Volume of prey (cm^3)	V_c (%)	IRI	IRI (%)
Chiloscyllium punctatum	Annelids	3	25.0	15	26.8	55.5	16.9	1092.5	11.5
	Crabs	6	50.0	23	41.1	210.3	65.2	5315.0	56.0
	Shrimps	2	16.7	2	3.6	7.5	2.3	98.5	1.0
	Barnacles	1	8.3	1	1.8	14	4.3	50.6	0.5
	Fishes	9	75.0	15	26.8	40.6	12.4	2940.0	31.0
Hemiscyllium ocellatum	Annelids	35	68.6	159	50.2	76.5	47.1	6675.0	51.3
	Crabs	38	74.5	108	34.1	58.4	36.0	5217.9	40.1
	Shrimps	23	45.1	34	10.7	18.5	11.4	997.4	7.7
	Amphipods	7	13.7	8	2.5	0.6	0.4	39.7	0.3
	Fishes	6	11.8	8	2.5	8.4	5.2	90.5	0.7

Data for *H. ocellatum* are from Heupel & Bennett (1998).

Discussion

Ampullary pores of both *Hemiscyllium ocellatum* and *Chiloscyllium punctatum* follow a similar distribution, with a large number concentrated around the anterior of the head, and few pores posterior to the eyes. This higher density of ampullary pores located on the snout of the animals likely assists in prey detection by providing a higher spatial resolution than the fewer posterior pores, which are more likely to be used to detect uniform electric fields (Raschi, 1986; Rivera-Vicente *et al*., 2011). Contrary to other sharks studied to date, the pores of both species do not form highly-distinctive patterns (Raschi *et al*., 2001; Kempster *et al*., 2012). A previous study on the sensory systems of *H. ocellatum* by Winther-Jason *et al*. (2012) described the presence of up to six ampullary pores located between the first gill slit and the dorsal fin. While a single ampullary pore was observed just above the first gill slit in *H. ocellatum* in the present study, none were found posterior to that point. While the variation may represent intraspecific variability, both studies concur that ampullary pores are present at least above the first gill slit, which has not been recorded in any other shark species to date (Winther-Jason *et al*., 2012). Both studies also concur that far fewer pores occur posterior rather than anterior to the eyes, and that the overall total ampullary pore count is relatively low. *Chiloscyllium punctatum* also exhibits a relatively low total number of ampullary pores, which appears to be a common feature of demersal sharks. Similar results were found in the ornate wobbegong shark Orectolobus ornatus¸ and the nurse shark Ginglymostoma cirratum (Cornett, 2006; Theiss *et al*., 2011; Kempster *et al*., 2012). However, ampullary pore density on the snout is similar in both species, indicating that the higher number of pores in *C. punctatum* may be merely a function of the generally larger size of the specimens used in this study.

It is not clear whether the larger mean pore size in *C. punctatum*, when compared to *H. ocellatum*, was influenced by a larger body size: There was a suggestion that pore diameter increased with body size in *C. punctatum* only, but the sample size was insufficient to determine whether this was significant. Unlike *C. punctatum* and other elasmobranchs studied to date, the ampullary pores located posterior to the eyes in *H. ocellatum* were not significantly larger than the anterior pores (Camilieri-Asch *et al*., 2013; Gauthier *et al*., 2018).

The quasi-sinusoidal shape of the ampullary canals of the mandibular cluster in *H. ocellatum* resembles those documented in the ventral infraorbital canals of three benthic rays, Neotrygon trigonoides, Hemitrygon fluviorum, and Maculabatis toshi (Gauthier *et al*., 2018). This canal structure appears to be a feature common to benthic species, yet this peculiar shape of ampullary canals is not shared by *C. punctatum*. The diet of *H. ocellatum* predominantly comprises annelids and crustaceans (crabs and shrimps) (Heupel and Bennett, 1998), while in *C. punctatum* the greatest %IRI is represented by crabs (56%), followed by teleost fishes (31%) with annelids a relatively minor group. Given the broad similarities in their preferred prey, albeit taken in different proportions, the disparities in ampullary canal shape do not appear to be explained by differences in diet. Despite the differences in canal shape, the canal wall composition, aiming to conserve as much of the electrical signal as possible, remains the same between the two species, and similar to other elasmobranchs previously studied (Waltmann, 1966). The presence of quasi-sinusoidal canals in *H. ocellatum* and their absence in *C. punctatum*, both members of the family Hemiscylliidae, and the apparent lack of connection to prey detection may help in identifying their function in the future.

A lobular ampulla proper is common in sharks, and the larger size of the ampullae proper and of the sensory chambers may just be an artefact of the difference in size between the two species (Raschi *et al*., 2001; Jørgensen, 2005). The supportive cells of the ampullae of Lorenzini are typically basally nucleated, and this is the second observation of them being apically nucleated (Jørgensen, 2005; Whitehead *et al*., 2015; Gauthier *et al*., 2018). However, in contrast to the supportive cells observed in benthic rays, those found in both *C. punctatum* and *H. ocellatum* do not protrude far into the ampullary lumen, and the ampullae proper seem to possess a smooth sensory epithelium (Gauthier *et al*., 2018). The functional significance, should there be one, for the location of the nuclei of these cells and their protrusion remains to be explained. The typically pear-shaped receptor cells appear compressed or flattened in both species, with a polymorphic nucleus compared to the usually round nuclei found in any other species to date. Once again, whether there is a specific reason behind the different shape of the receptor cells and their nuclei remains unknown.

Overall, the electrosensory systems of *H. ocellatum* and *C. punctatum* are very similar, with the marked exception of the presence of quasi-sinusoidal canals in *H. ocellatum* that had previously only been observed in batoids. The pores and ampullae of *C. punctatum* also appear to be slightly larger than those of *H. ocellatum*, but whether this larger size relates to their overall larger bodies or because of differences in their environment and diet remains unknown.

Acknowledgements

Thank you to Taylor Maggiacomo for drawing the outlines of both species used in Figure 4.1. Thank you as well to both John Page and Dave Thomson for their help in acquiring several specimens. I also thank the University of Queensland Centre for Microscopy and Microanalysis, a node of the Australian Microscopy and Microanalysis Facility, for their assistance. And finally, thank you to all of the staff at both the Moreton Bay Research Station and the Heron Island Research Station for their help and the use of their facilities. The authors have no conflict of interest to declare. Specimens were collected under The University of Queensland Animal Ethics Approval SBMS/406/14 and General Fisheries Permit 165491 issued to M.B.B..

Chapter V

Distribution and ultrastructure of the ampullae of Lorenzini in ten species of galean sharks.

Abstract

Elasmobranchs detect weak electric fields in their surrounding environment through specific sensory organs, the ampullae of Lorenzini, which they use to detect potential prey, the Earth's geo-magnetic field, or even to communicate with conspecifics. Recent research has revealed that the distribution and morphology of these elasmobranchs electrosensors may be influenced by phylogeny, environmental factors, or the biology of a species. Here, I compare the distribution and morphology of the ampullae of Lorenzini in ten species of galean sharks: *Carcharhinus brevipinna*, *Carcharhinus cautus*, *Carcharhinus falciformis*, *Carcharhinus limbatus*, *Carcharhinus longimanus*, *Carcharhinus tilstoni*, *Galeocerdo cuvier*, *Hemigaleus australiensis*, *Isurus oxyrinchus*, and *Prionace glauca*. These coastal, oceanic, bentho-pelagic and pelagic species possess a range of diets and different foraging strategies. Yet, the ultrastructure of their ampullae of Lorenzini vary little. The larger species, *P. glauca*, *C. longimanus*, *C. falciformis*, and *I. oxyrinchus* tend to exhibit generally larger ampullary organs, with more numerous sensory chambers, and larger ampullary pores. These features seem to be influenced more by the size of the animal rather than its environment, lifestyle, or diet. However, clear differences were observed in the distribution and quantity of their ampullary pores, with members of the genus *Carcharhinus* displaying remarkably similar distribution patterns and counts, despite coming from different environments and lifestyles. On the other hand, *I. oxyrinchus* exhibit a markedly different distribution of ampullary pores, that seem to accord with its presumably high dependence on vision during prey capture.

Introduction

The ability to detect weak electric fields, electroreception, has appeared several times throughout evolutionary history, and can be found in fish, amphibians, and even mammals (Colin & Whitehead, 2004). In Chondrichthyes, the sensory organs associated with electroreception are the ampullae of Lorenzini, which are used for navigation, communication and foraging (Kalmijn, 1971; 1974; Tricas *et al*., 1995). The ampullary organs of many species of sharks and rays have been studied, although relatively few of these studies focus on the fine structure of the sensory organs in favour of behavioural responses to electric fields, or the distribution of the ampullary pores on the body of the animals (Kajiura & Holland, 2002; McGowan & Kajiura, 2009; Jordan *et al*., 2009; Kempster *et al*., 2012; Wueringer *et al*., 2012). An increasing number of variations in the morphology of the ampullae of Lorenzini are being documented, from specimens belonging to different families, living in environments of different salinities to specimens with different lifestyles (Kempster *et al*., 2012; Whitehead *et al*., 2015a; Gauthier *et al*., 2018).

Typically, the ampullae of Lorenzini consist of a somatic pore in the epidermis invaginating into a canal filled with a highly conductive mucopolysaccharide gel, the wall of which is generally two cells thick and composed of flattened squamous epithelial cells (Waltmann, 1966; Josberger *et al*., 2016). These epithelial cells are adjoined by tight junctions with underlying desmosomes to ensure the transmission of the electrical signals from the external environment along the length of the canal with minimal loss of intensity (Waltmann, 1966; Jørgensen, 2005). Each canal terminates into a single ampulla proper that is typically divided into several sensory chambers, that may each further divide into alveoli depending on the type of ampulla proper. The ampullae proper are lined by supportive cells and receptor cells, the apices of which are exposed to the ampullary lumen and are covered in microvilli as well as a single protruding kinocilium (Jørgensen, 2005; Whitehead *et al*., 2015a; Gauthier *et al*., 2018). At the base of each receptor cell, one or several neural terminals are connected to unmyelinated neurons originating from the anterior lateral line lobe of the brain (Jørgensen, 2005).

Variation in ampullary organ structure within elasmobranchs has been documented in a range of species. For example, the ocellate river stingray, *Potamotrygon motoro*, has very short micro-ampullae with few receptor cells (Szabo *et al*., 1972), whereas those found in most marine specimens may have ampullary canals that extend to over 20 cm in length and

thousands of receptor cells (Raschi, 1986; Whitehead *et al*., 2015a; Gauthier *et al*., 2018). Marine benthic rays possess apically nucleated supportive cells that protrude heavily into the ampullary lumen, a phenomenon not observed in any other elasmobranchs. They also have a peculiar quasi-sinusoidal shape of some ampullary canals, the functional role of which has yet to be determined (Gauthier *et al*., 2018). Variation also occurs in the distribution and number of ampullary pores, for example, the ornate wobbegong shark, *Orectolobus ornatus*, has a higher concentration of ampullary pores on the dorsum of its head compared to pelagic sharks (Theiss *et al*., 2011), with the differences most likely related to the species' different foraging strategies. In *O. ornatus* the greater concentration of dorsal pores, leading to the ampullae, would facilitate detection of potential prey items passing over the head of this camouflaged, ambush predatory (Theiss *et al*., 2011; Kempster *et al*., 2012). Ampullary canals of the euryhaline bullshark, *Carcharhinus leucas*, display a peculiar "clover leaf" shape, and the ampullae proper are lined with apically nucleated supportive cells (Whitehead *et al*., 2015a). This "clover leaf" shape has been observed in a fossilized specimen of *Carcharias amonensis*, but so far has not been detected in any other extant elasmobranch (Vulo & Guinot, 2015).

Here, I report the distribution and fine scale structure of the ampullae of Lorenzini in ten species of galean sharks, *Carcharhinus brevipinna*, *C. cautus*, *C. falciformis*, *C. limbatus*, *C. longimanus*, *C. tilstoni*, *Galeocerdo cuvier*, *Hemigaleus australiensis*, *Isurus oxyrinchus*, and *Prionace glauca*, which occur variously in coastal and oceanic environments, and with bentho-pelagic or purely pelagic lifestyles. They possess a range of different life history traits, behaviours, diets, and biology, which allows me to explore how these factors may relate to the distribution and morphology of the species' electrosensory systems.

Methods

Sample collection & preservation

A total of 34 specimens comprising 10 shark species were collected with the help of recreational, commercial, and game fishers from locations on the East coast of Australia, in both Queensland (QLD) and New South Wales (NSW) waters (Table 1). Ampullary organs were dissected free from the body and fixed, either in 10% neutral buffered formalin (NBF) for light microscopy (LM) and scanning electron microscopy (SEM), or 2.5% glutaraldehyde in 0.1M phosphate buffer for transmission electron microscopy (TEM). Specimens that had died more than two hours prior to collection of ampullae were not used for TEM. Where possible, the skin of the head was retained to allow ampullary pore distributions to be mapped. If sharks had been frozen prior to sampling, only the skin was kept to investigate the size, number, and distribution of ampullary pores.

Pore distributions, *counts*, *and measurements*

The skin removed from the head of sharks, and the resulting epidermis and overlying scales, was placed on a backlit plate for observation. The number and distribution of ampullary pores was recorded following the methodology described in Chapter IV. Ampullary pore diameters were measured (Nikon 50i Eclipse compound microscope; Nikon Basic Research 4.0 imaging software), with 20 measurements taken of the pores located anterior to the eye socket and, when possible, 20 measurements were taken of pores located posterior to the eye socket.

Light microscopy

Some of the tissues fixed in 10% NBF were processed through to paraffin wax following routine histological procedures, sectioned at 10 µm thickness, and stained using Mayer's haematoxylin & eosin (Chapter IV). Gross measurements were obtained for 10 ampullae proper, canals, and sensory chambers from each individual shark.

Table 5.1. Size range, sex ratio, and site of capture of all species examined in this chapter.

Species	Total length (cm)	Sex	Site of capture
Carcharhinus brevipinna	85-88	F:2 ; M:0	Gold Coast (QLD)
Carcharhinus cautus	60-80	F:1 ; M:5	Moreton Bay (QLD)
Carcharhinus falciformis (Adult)	212	F:1 ; M:0	Port Stephens (NSW)
Carcharhinus falciformis (Embryos)	56	F:1 ; M:1	Port Stephens (NSW)
Carcharhinus limbatus	78-92	F:0 ; M:3	Moreton Bay (QLD)
Carcharhinus longimanus	232	F:0 ; M:1	Port Stephens (NSW)
Carcharhinus tilstoni	78-86	F:4 ; M:1	Moreton Bay (QLD)
Galeocerdo cuvier	336-342	F:1 ; M:1	Port Stephens (NSW), Port Hacking (NSW)
Hemigaleus australiensis	76-107	F:3 ; M:2	Moreton Bay (QLD)
Isurus oxyrinchus	194-260	F:3 ; M:2	Port Stephens (NSW), Port Hacking (NSW), Watson's Bay (NSW)
Prionace glauca	233-279	F:2 ; M:1	Watson's Bay (NSW), Broken Bay (NSW)

Electron microscopy

Tissues fixed in 10% NBF for SEM were critical-point dried, mounted on carbon tape on a 12 mm stub, and coated with a 10 nm layer of iridium (Chapter IV). The samples were viewed under a JEOL 7001 Field Emission Microscope at 10 kV. The samples fixed in 2.5% glutaraldehyde in 0.1M phosphate buffer were processed for TEM following the methodology described in Chapter IV. Samples were then embedded in EPON resin, sectioned at 90 nm thickness on a Leica UC 62 Ultramicrotome, viewed and imaged under either a JEOL1011 or a Hitachi 7700 transmission electron microscope.

Statistical analysis

Pore measurements were compared between anterior and posterior pores for each species using a series of paired t-tests, and among species using nested one-way ANOVAs. All gross measurements were analysed with a series of nested one-way ANOVAs for each characteristic, followed by a post-hoc Tukey test if required. Results are presented as mean and standard deviation. Linear regression was used to examine whether the diameter of the ampullae proper was correlated with animal size, in *Isurus oxyrinchus*, *Carcharhinus cautus*, and *Hemigaleus australiensis*. Significance accepted at $p < 0.05$.

Results

Pore distributions, *counts*, *and measurements*

The distribution of ampullary pores varies across all nine species for which the skin was collected (Fig. 5.1-9). Carcharhinids generally have a similar pore distribution pattern across all seven species studied. *Carcharhinus limbatus*, *C. longimanus*, and *C. tilstoni* have about equal numbers of ventral and dorsal pores, whereas *C. brevipinna*, *C. falciformis*, and *G. cuvier* all have a much higher proportion of ventral than dorsal pores. *Carcharhinus cautus* is the only carcharhinid that displays a much higher number of dorsal pores than ventral pores (Table 2). The pore distribution pattern of the two embryonic *C. falciformis* closely resembles that of their mother, albeit with only about half of the number of ampullary pores (Fig. 5.3; Table 2). Ampullary pores occur at about 40 pores.cm^{-2} on the snout of the embryos, compared to 20 pores.cm^{-2} in the mother. Embryos also display a more even distribution of ampullary pores on their dorsal and ventral surface than the adult, although with a bias in favour of ventral pores. Of the mature specimens, *I. oxyrinchus* (Family: Lamnidae) and *H. australiensis* (Hemigalidae) have the fewest pores, with around half as many as occurs in the other species (all Carcharhinidae). The pore distribution in *I. oxyrinchus* is markedly different from the other species, with few pores posterior to the eye socket, and a “V”-shaped pattern of pores on the dorsal surface of the head (Fig. 5.9; Table 2).

Ampullary pores are located solely on the head of all species involved in this study, with pores absent from the trunk of the sharks. Pores in *C. longimanus* and *G. cuvier* are nested between placoid scales, some of which appear to differ in shape from normal scales (Fig. 5.10A); whereas in all other species the pores are partially covered by overlapping placoid scales (Fig. 5.10B). Some of the ampullary pores located posterior to the eyes have an oval appearance (Fig. 5.10C), unlike the circular openings of the anterior pores. Within each species, the mean posterior pore diameter is larger than the mean diameter of the anterior ones (444 – 1961 µm and 263 – 883 µm respectively, excluding the embryonic specimens) ($p < 0.05$; Fig. 5.11).

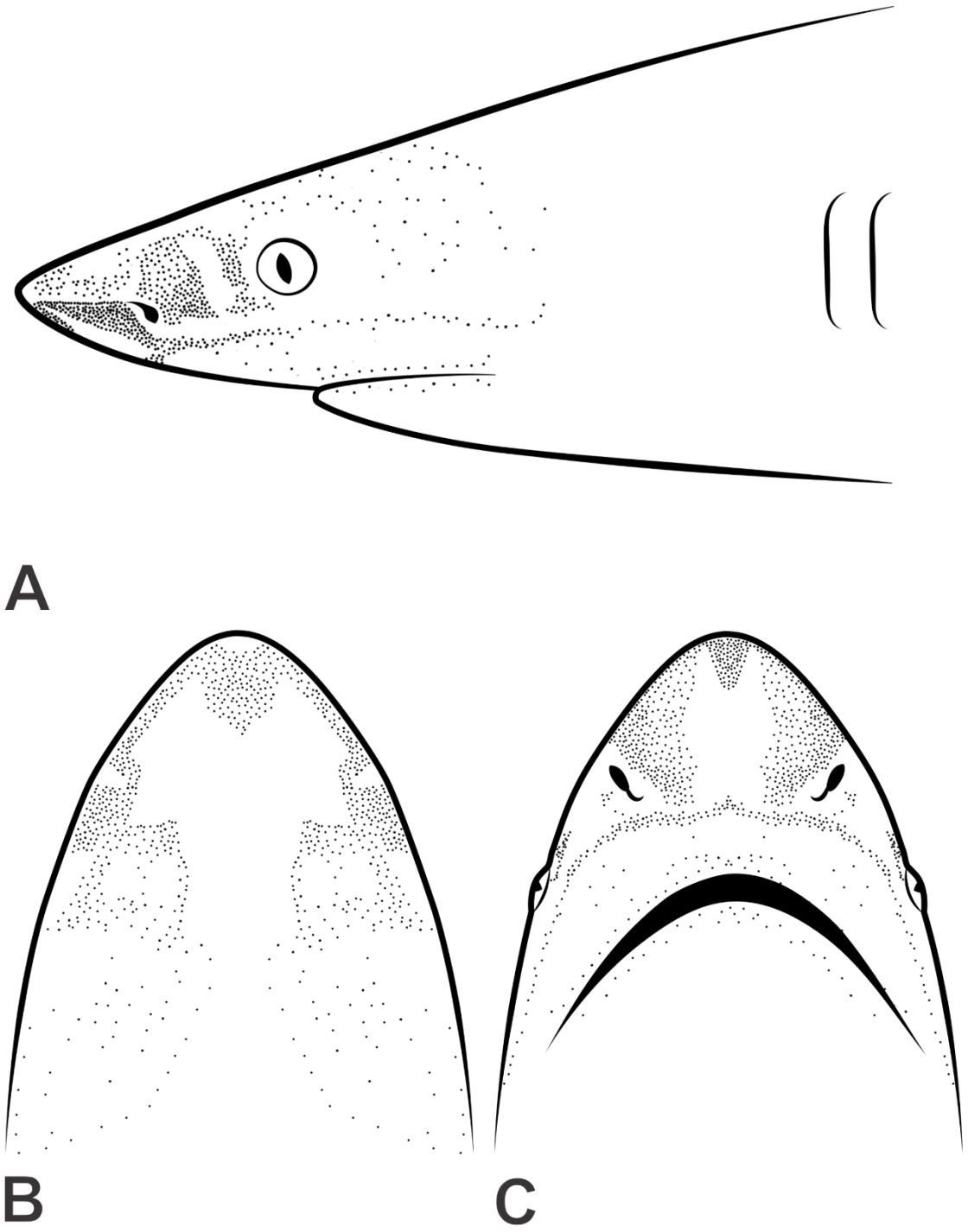

Figure 5.1. Lateral (A), dorsal (B), and ventral (C) view of the distribution of ampullary pores on the head of *Carcharhinus brevipinna.*

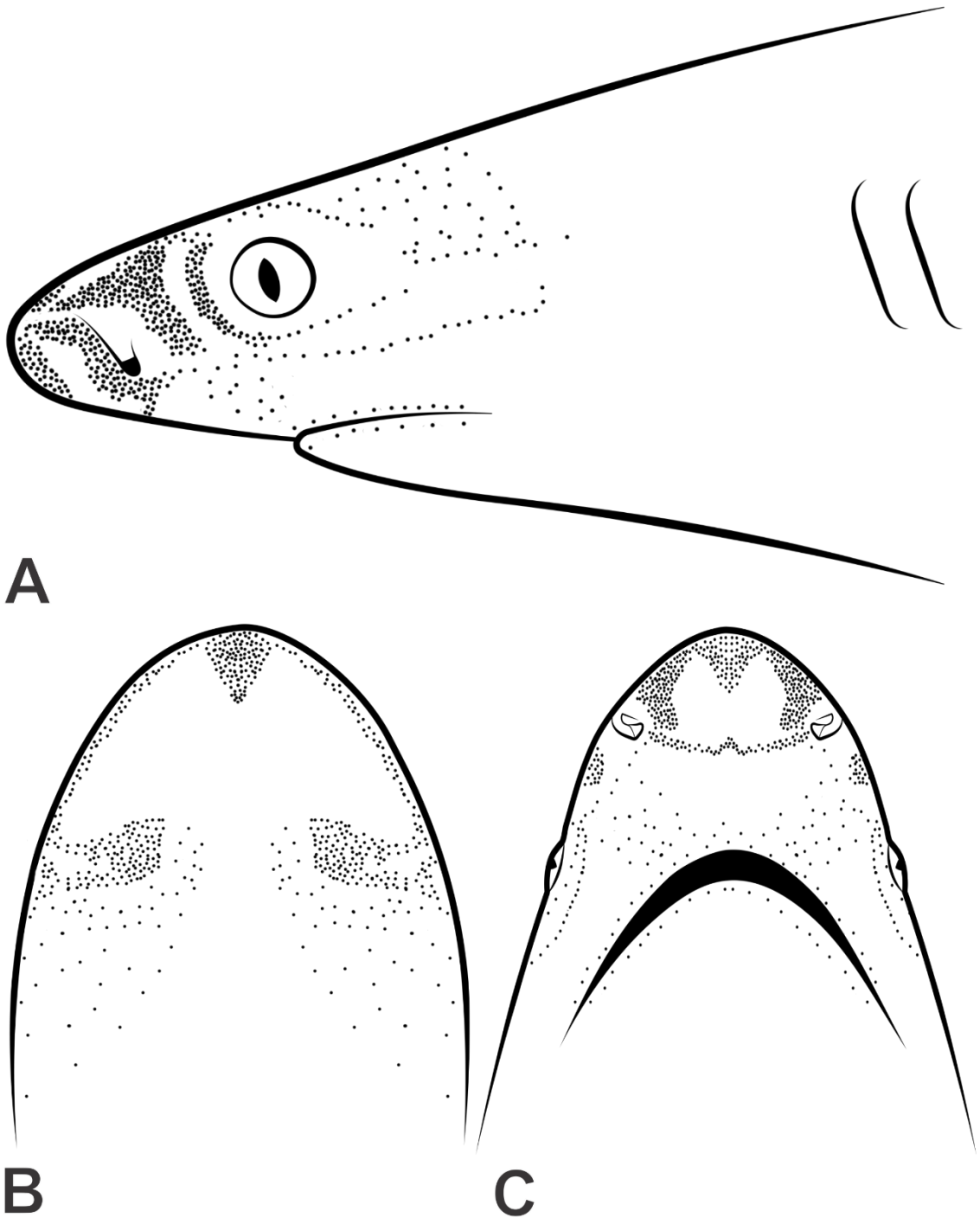

Figure 5.2. Lateral (A), dorsal (B), and ventral (C) view of the distribution of ampullary pores on the head of *Carcharhinus cautus.*

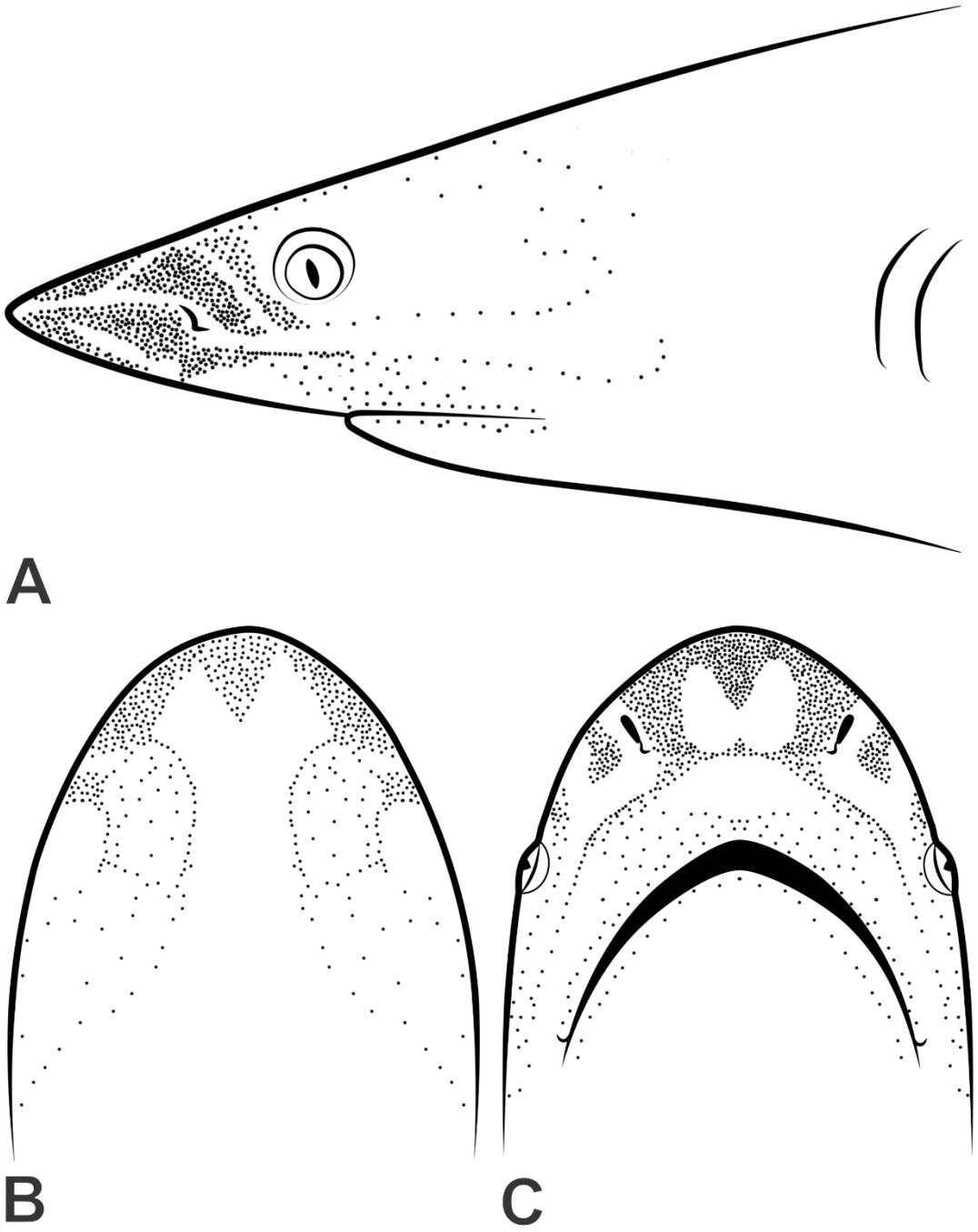

Figure 5.3.1. Lateral (A), dorsal (B), and ventral (C) view of the distribution of ampullary pores on the head of *Carcharhinus falciformis* (Adult).

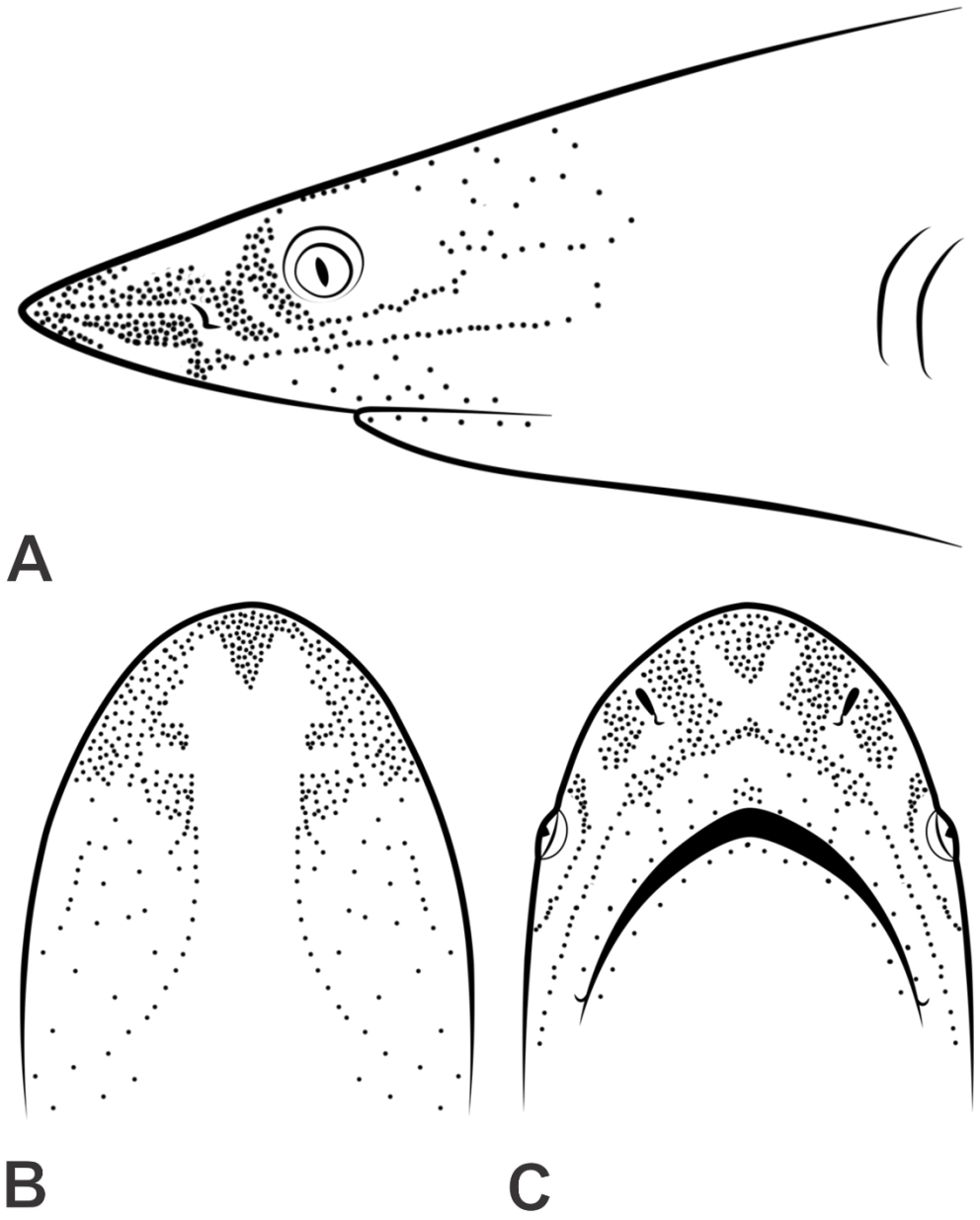

Figure 5.3.2. Lateral (A), dorsal (B), and ventral (C) view of the distribution of ampullary pores on the head of *Carcharhinus falciformis* (Embryo).

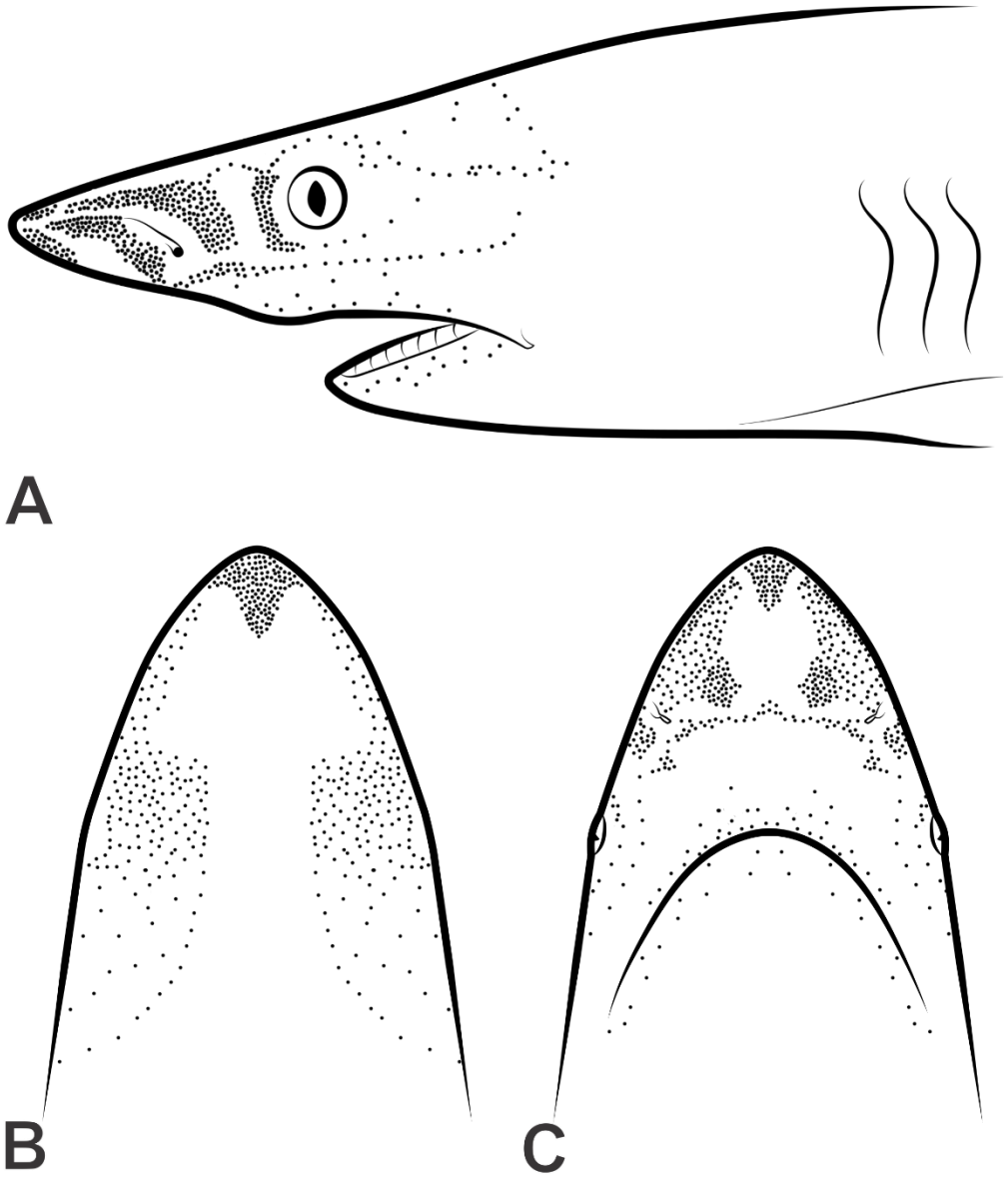

Figure 5.4. Lateral (A), dorsal (B), and ventral (C) view of the distribution of ampullary pores on the head of *Carcharhinus limbatus.*

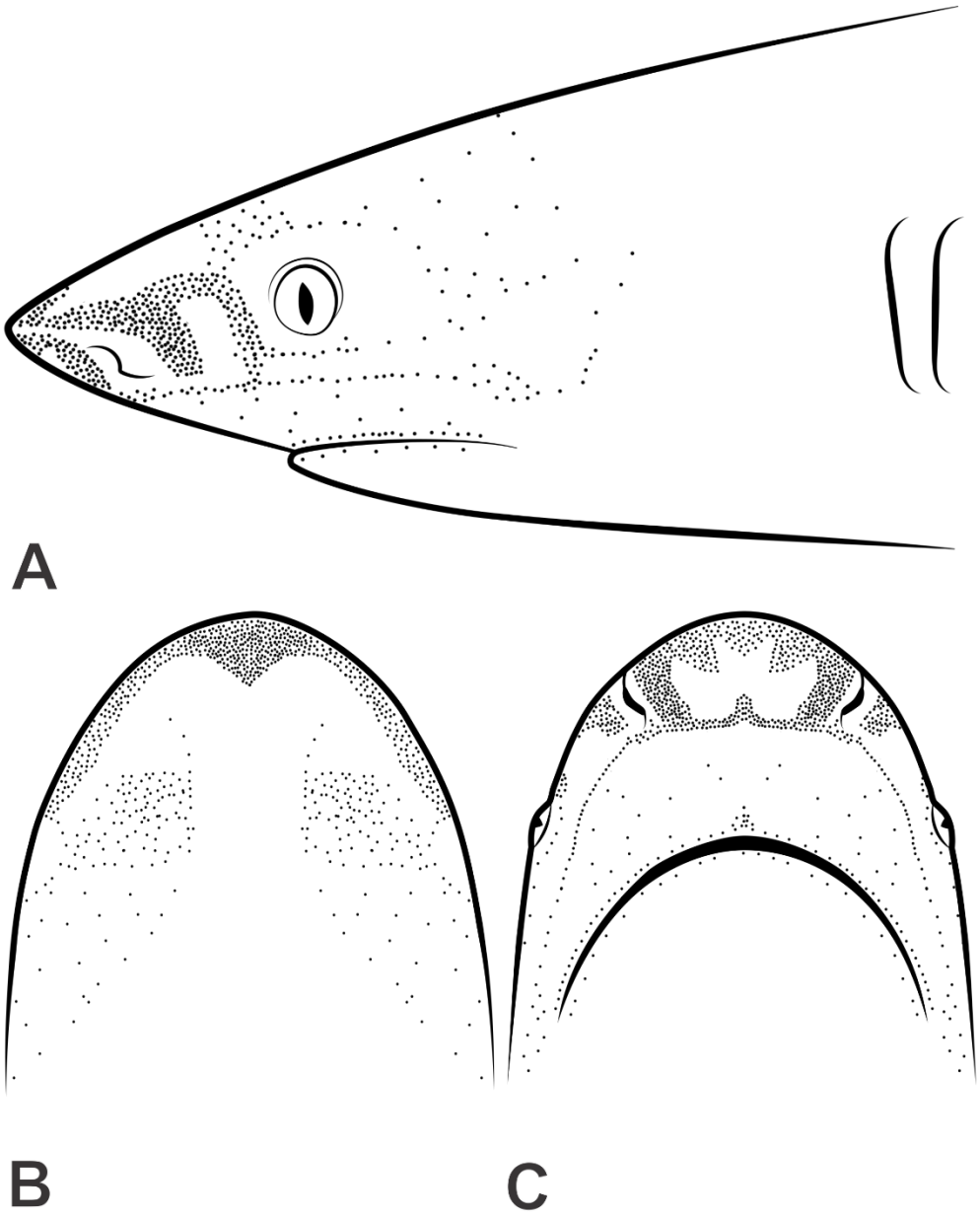

Figure 5.5. Lateral (A), dorsal (B), and ventral (C) view of the distribution of ampullary pores on the head of *Carcharhinus longimanus.*

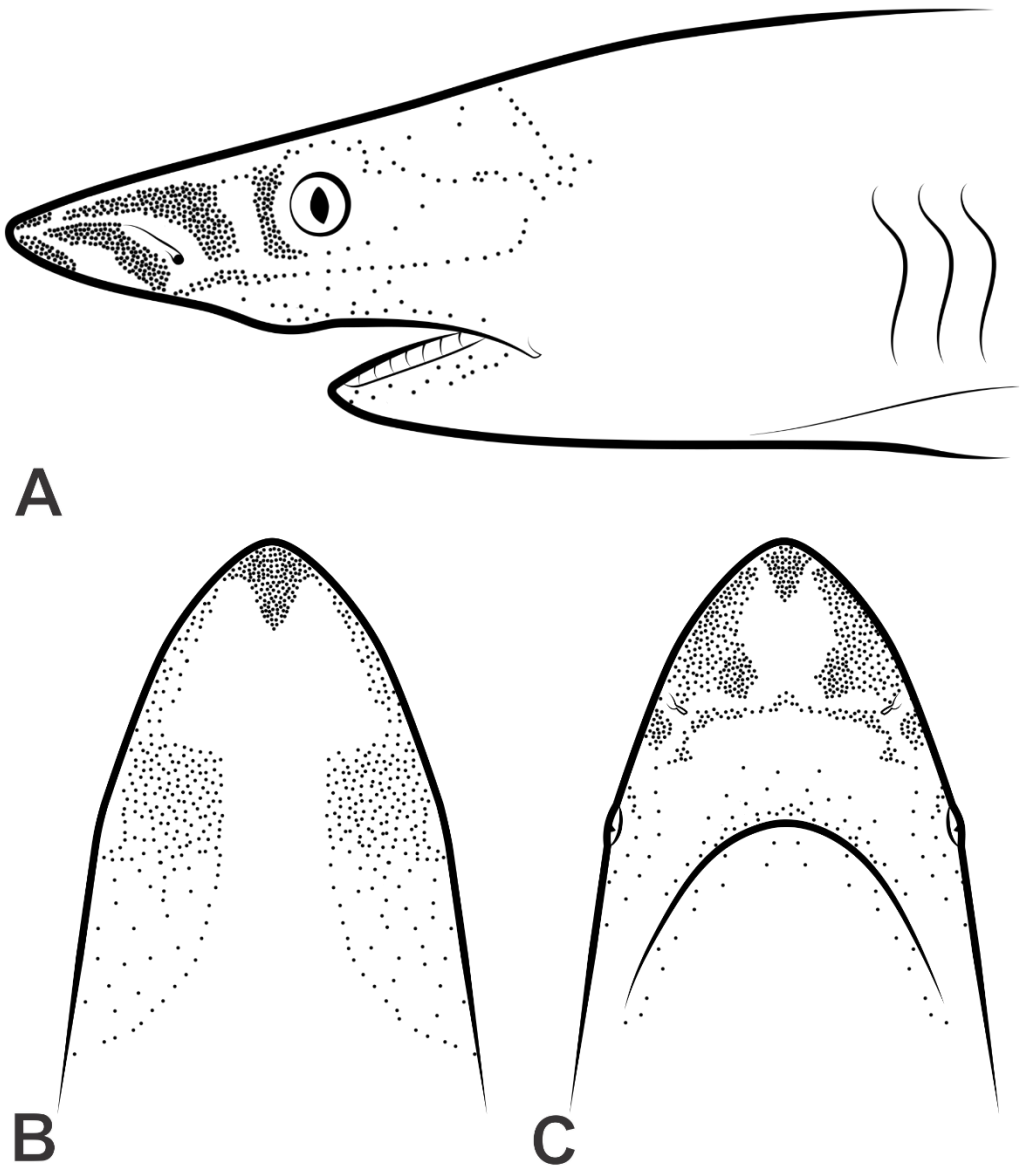

Figure 5.6. Lateral (A), dorsal (B), and ventral (C) view of the distribution of ampullary pores on the head of *Carcharhinus tilstoni.*

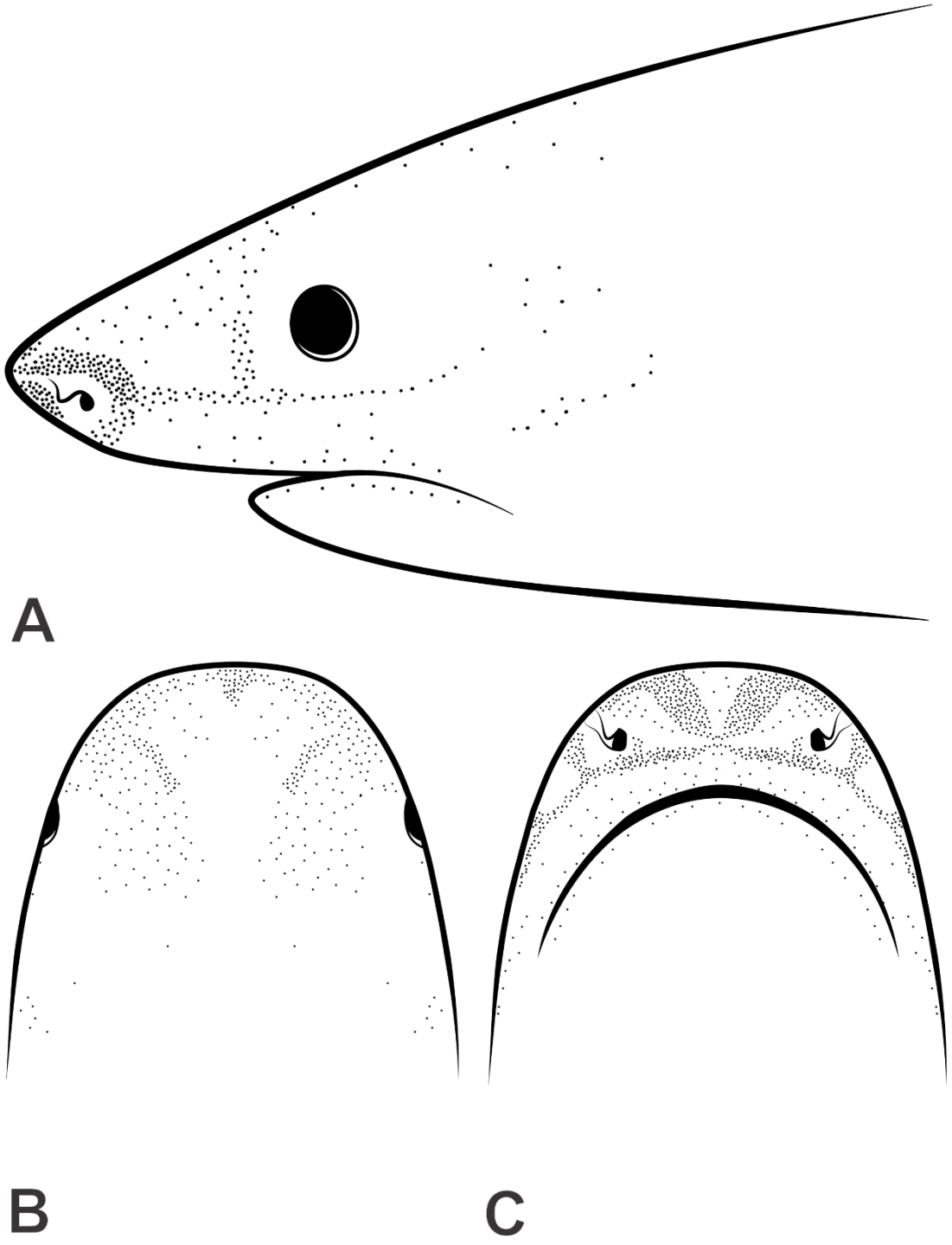

Figure 5.7. Lateral (A), dorsal (B), and ventral (C) view of the distribution of ampullary pores on the head of *Galeocerdo cuvier.*

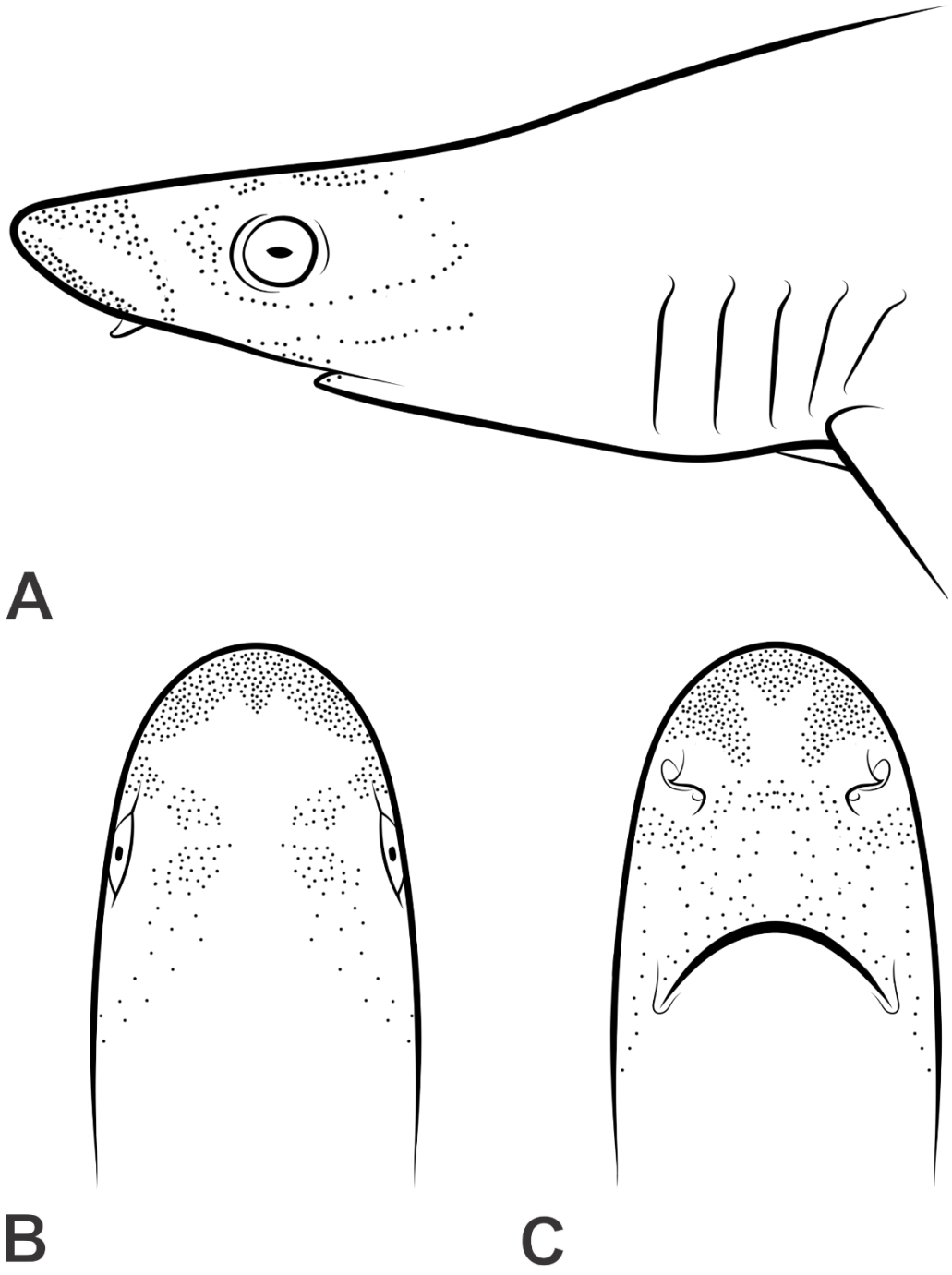

Figure 5.8. Lateral (A), dorsal (B), and ventral (C) view of the distribution of ampullary pores on the head of *Hemigaleus australiensis.*

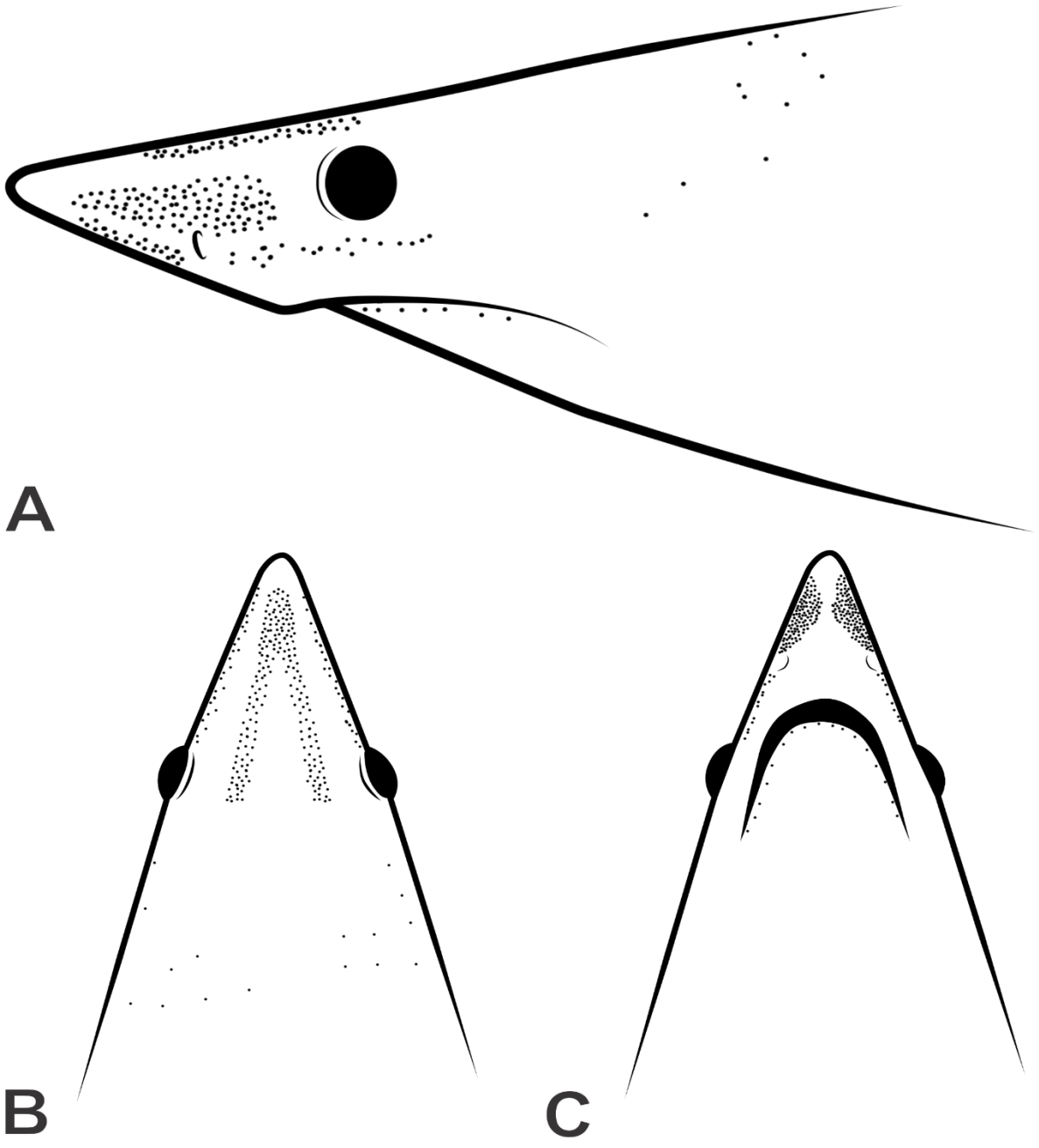

Figure 5.9. Lateral (A), dorsal (B), and ventral (C) view of the distribution of ampullary pores on the head of *Isurus oxyrinchus.*

Table 5.2. Gross measurements and counts of the ampullary pores, canals, ampullae proper and sensory chambers of the ampullary organs of the species used in this study.

Species	Ampulla Proper diameter (µm)	Sensory chamber number	Sensory chamber diameter (µm)	Ampullary canal diameter (µm)	Anterior ampullary pore diameter (µm)	Posterior ampullary pore diameter (µm)	Pore count	%Ventral	%Dorsal
Carcharhinus brevipinna	-	-	-	-	263 ± 42	518 ± 105	1834 ± 14	56.8	43.2
Carcharhinus cautus	662 ± 55	5-6	203 ± 29	335 ± 53	303 ± 45	481 ± 58	1408 ± 247	42.0	58.0
Carcharhinus falciformis (Adult)	1452 ± 158	6-8	251 ± 55	793 ± 82	737 ± 105	2146 ± 307	1800	59.9	40.1
Carcharhinus falciformis (Embryo)	445 ± 33	6-8	136 ± 20	331 ± 42	254 ± 28	376 ± 32	905 ± 27	47.0	53.0
Carcharhinus limbatus	584 ± 38	5-6	177 ± 36	422 ± 75	338 ± 40	444 ± 75	1735 ± 243	49.9	50.1
Carcharhinus longimanus	906 ± 116	6-8	215 ± 48	752 ± 95	839 ± 84	1478 ± 333	1992	48.1	51.9
Carcharhinus tilstoni	578 ± 64	5-6	174 ± 24	467 ± 84	345 ± 41	491 ± 54	1961 ± 64	49.3	50.7
Galeocerdo cuvier	1246 ± 226	7-8	325 ± 55	1115 ± 305	883 ± 160	1278 ± 342	1726	67.5	32.5
Hemigaleus australiensis	665 ± 90	6-7	190 ± 36	438 ± 55	320 ± 59	631 ± 117	865 ± 88	55.2	44.8
Isurus oxyrinchus	1295 ± 183	7-8	321 ± 67	1276 ± 230	847 ± 180	1192 ± 220	834 ± 108	34.7	65.3
Prionace glauca	1197 ± 106	7-8	308 ± 54	996 ± 104	-	-	-	-	-

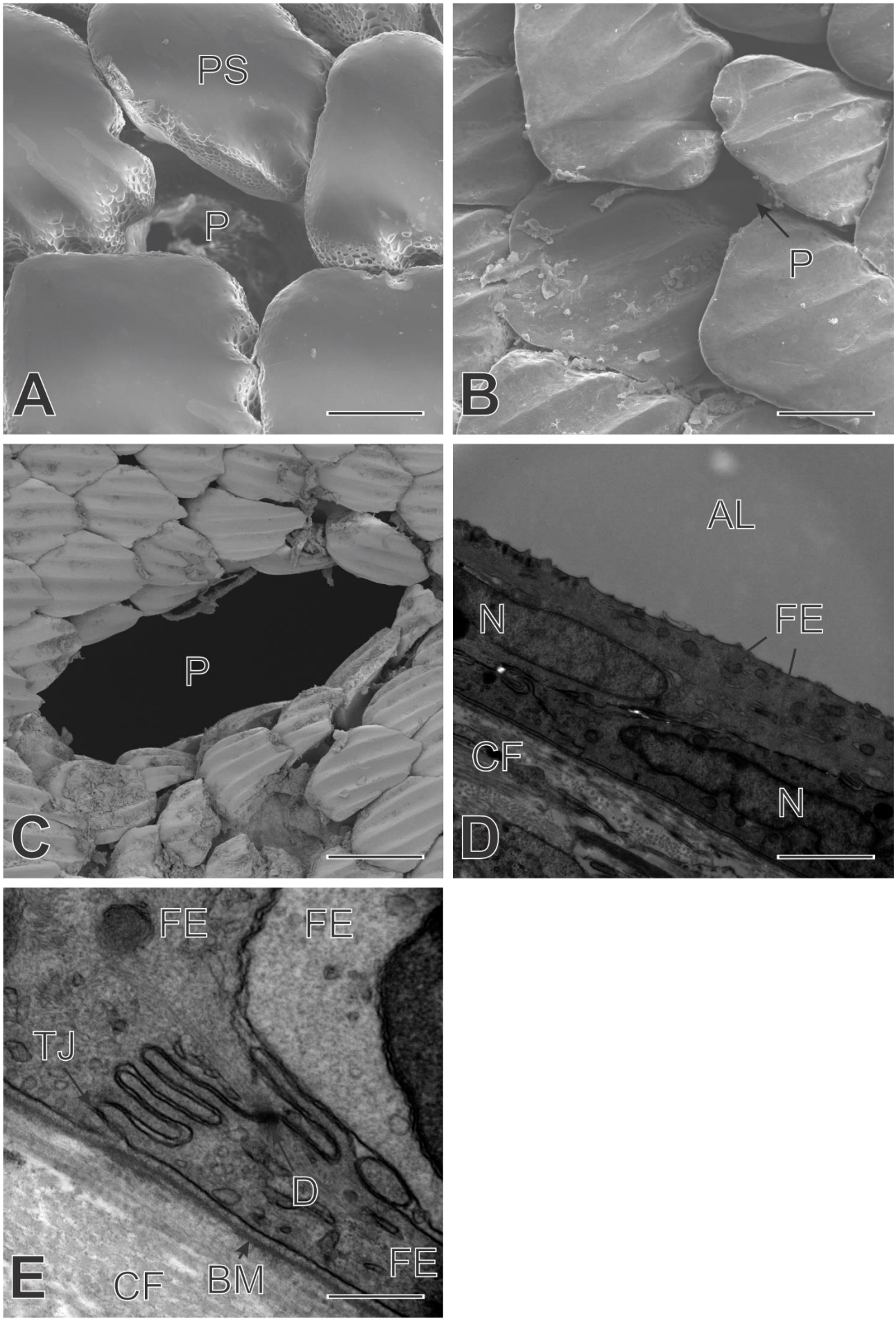
PS
P
A
P
B
P
C
AL
N
FE
CF
N
D
FE
FE
TJ
D
E
CF
BM
FE

Figure 5.10. Micrographs of ampullae of Lorenzini from different species of selachimorphii. **A.** Ampullary pore (P) located between placoid scales (PS). Evidence of structural deformities can be observed in the scales to accommodate the presence of the pore. *Carcharhinus longimanus*. SEM. Scale bar = 100 µm. **B.** Ampullary pore (P) partially covered by overlapping placoid scales. *Hemigaleus australiensis*. SEM. Scale bar = 100 µm. **C.** Elongated posterior ampullary pore (P). *Carcharhinus falciformis*. SEM. Scale bar = 200 µm. **D.** Ampullary canal wall showing two overlapping layers of flattened epithelial cells (FE) with elongated nuclei (N). Internally, the canal wall is exposed to the ampullary lumen (AL), while externally, a sheath of interlocking collagen fibres (CF) supports the canal. *Carcharhinus limbatus*. TEM. Scale bar = 2 µm. **E.** Micrograph of the junction between two adjacent flattened epithelial cells (FE) in the ampullary canal wall. The flattened epithelial cells are adjoined by an interdigitating tight junction (TJ) with underlying desmosome (D). External to the basement membrane (BM), the sheath of collagen fibres (CF) can be observed. TEM. Scale bar = 0.5 µm.

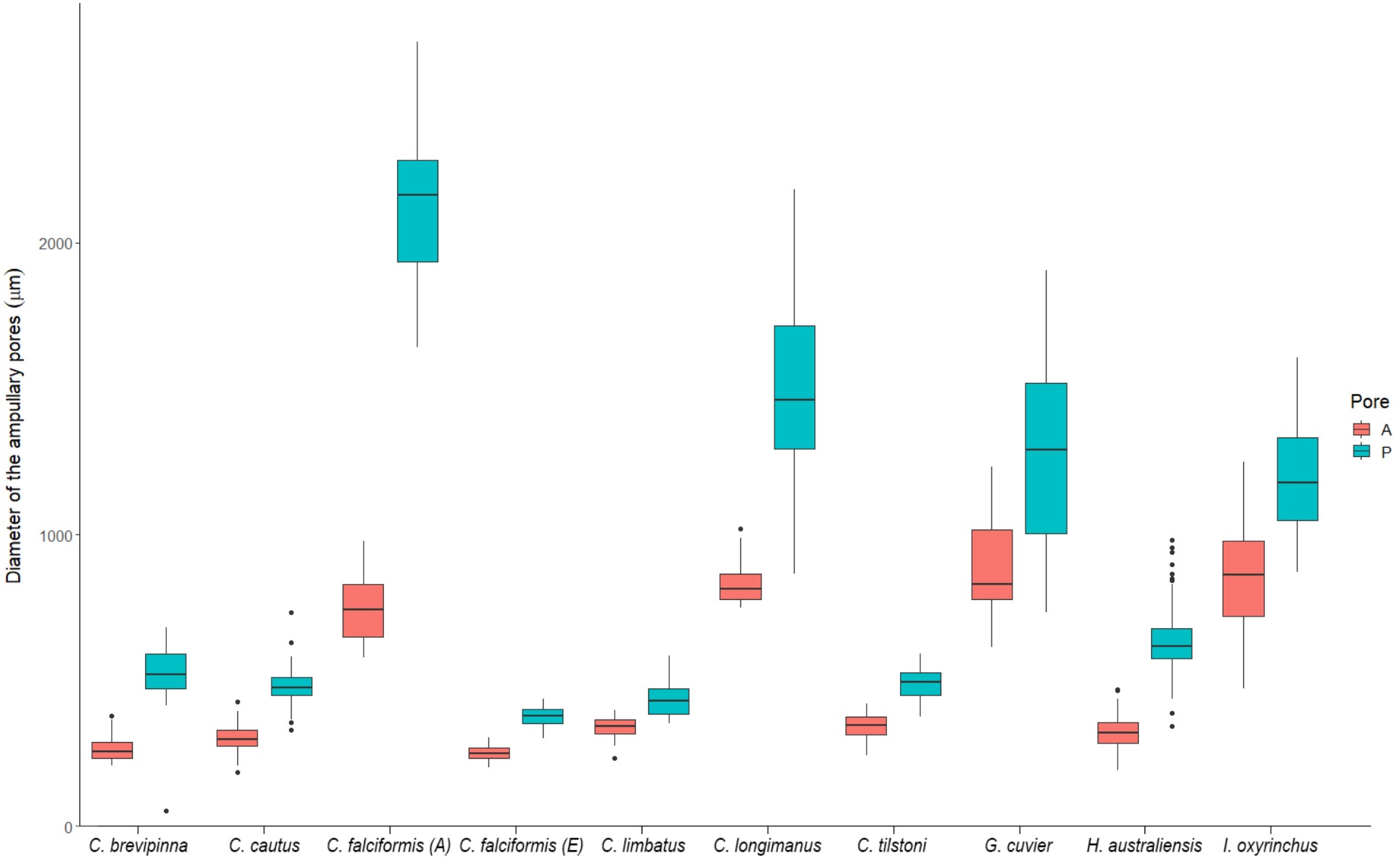

Figure 5.11. Box plot comparing the variation in diameter of the anterior (red) and posterior (blue) ampullary pores of *C. brevipinna, C. cautus, C. falciformis, C. limbatus, C. longimanus, C. tilstoni, G. cuvier, H. australiensis,* and *I. oxyrinchus.*

Gross morphology & ultrastructure

Ampullary pores lead to linear ampullary canals of significantly different mean diameter among the species ($F_{22,288} = 4.2$, $p < 0.05$; Fig. 5.12). Mean canal diameter varies four-fold, from 335 µm in *C. cautus* to 1276 µm in *I. oxyrinchus*. In all species, the ampullary canal wall is composed of two layers of interlocking flattened epithelial cells, adjoined by tight junctions with underlying desmosomes (Fig. 5.10D, 5.10E).

Ampullary canals open into ampullae proper of the lobular type for every species, but of significantly different diameters ($F_{22,288} = 4.6$, $p < 0.05$; Table 2, Fig. 5.13A). The blacktip sharks, *C. tilstoni* and *C. limbatus*, have small ampullae proper (c. 580 µm diameter) compared to the adult specimen of *C. falciformis* with a mean diameter of 1452 µm (Table 2; Fig. 5.14). Intraspecific differences in ampulla size in relation with a specimen L_T were absent, with the exception of *I. oxyrinchus* and *C. cautus* where a small but significant relationship occurs between pore diameter and body size ($p < 0.05$, $R^2 = 0.36$; Fig. 5.15A and $p < 0.05$, $R^2 = 0.13$; Fig. 5.15B respectively).

Carcharhinus cautus, *C. limbatus*, and *C. tilstoni* typically have 5-6 sensory chambers, *H. australiensis* has 6-7, while *C. falciformis* (adult and embryos), *C. longimanus*, *G. cuvier*, *I. oxyrinchus*, and *P. glauca* all have 6-8 sensory chambers (Table 2). Size differences of the sensory chambers occurred among species ($F_{22,288} = 1.7$, $p < 0.05$; Fig. 5.16). The smallest sensory chambers occur in *C. tilstoni* and the largest in *G. cuvier* (Fig. 5.16).

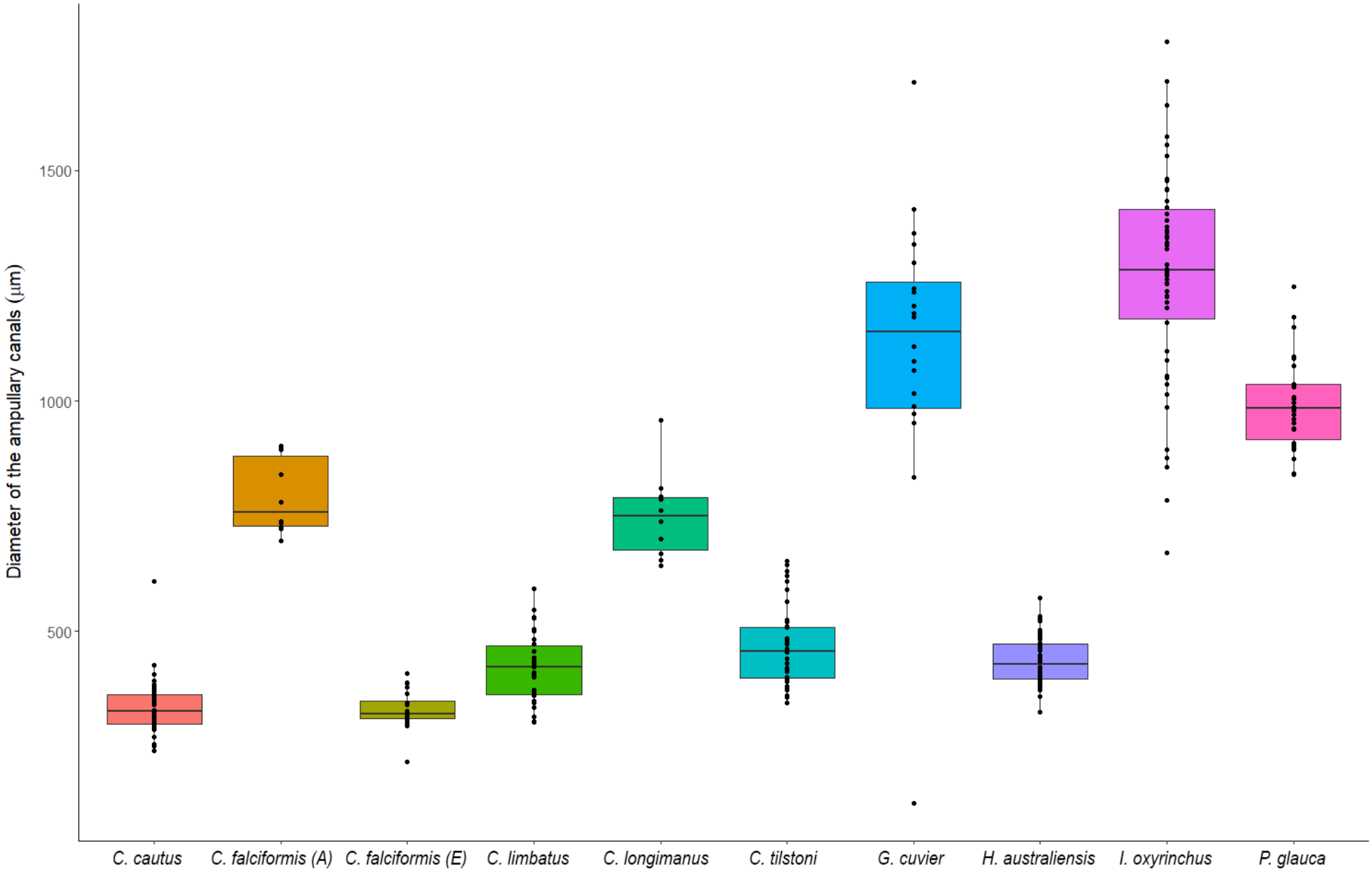

Figure 5.12. Box plot comparing the variation in diameter of the ampullary canals of *C. cautus, C. falciformis, C. limbatus, C. longimanus, C. tilstoni, G. cuvier, H. australiensis, I. oxyrinchus,* and *P. glauca*.

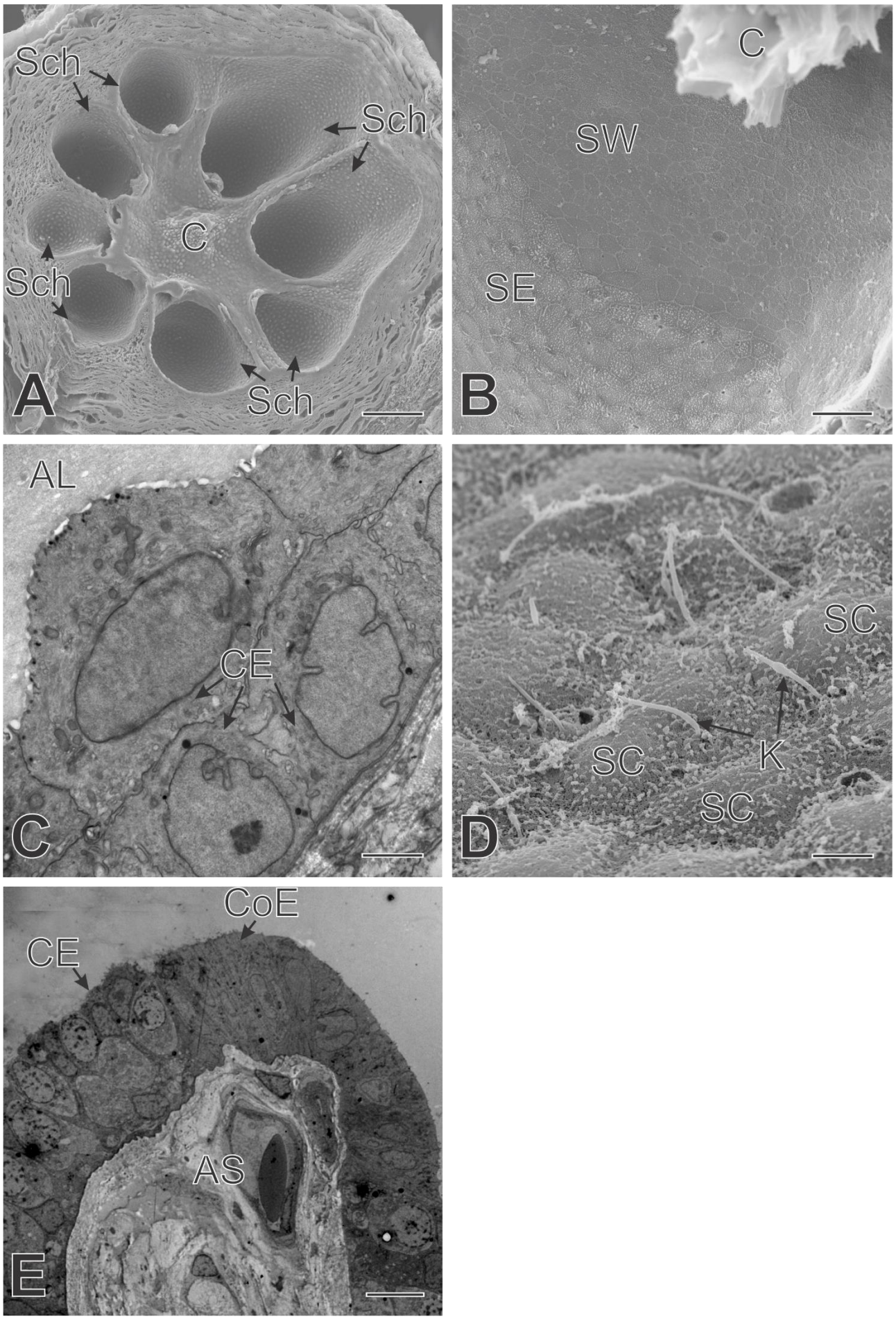
Sch
Sch
C
Sch
Sch
A
C
SW
SE
B
AL
CE
C
SC
K
SC
SC
D
CoE
CE
AS
E

Figure 5.13. Micrographs of ampullae of Lorenzini from different species of selachimorphii. **A.** Transverse section through a lobular ampulla showing the centrum (C) and eight sensory chambers (SCh). *Carcharhinus longimanus*. SEM. Scale bar = 100 µm. **B.** Micrograph of a single sensory chamber showing the transition between the wall of the sensory chamber (SW) to the sensory epithelium (SE). The centrum (C) is visible and covering parts of the sensory chamber. *Isurus oxyrinchus*. SEM. Scale bar = 20 µm. **C.** Section through the wall of the sensory chamber before reaching the sensory epithelium. The chamber wall is composed of two layers of overlapping cuboidal epithelial cells (CE). The cuboidal cells from the luminal layer are exposed to the ampullary lumen (AL) and appear to have a distorted cell wall. *Carcharhinus tilstoni*. TEM. Scale bar = 2 µm. **D.** Surface layer of the sensory epithelium, with kinocilia (K) extending out into the lumen at the junction between supportive cells (SC). *Isurus oxyrinchus*. SEM. Scale bar = 3 µm. **E.** Section through one of the alveolar septae (AS) showing several layers of cuboidal epithelial cells (CE) transitioning into a single layer of columnar epithelial (CoE) at the tip of the septae. *Hemigaleus australiensis*. TEM. Scale bar = 10 µm.

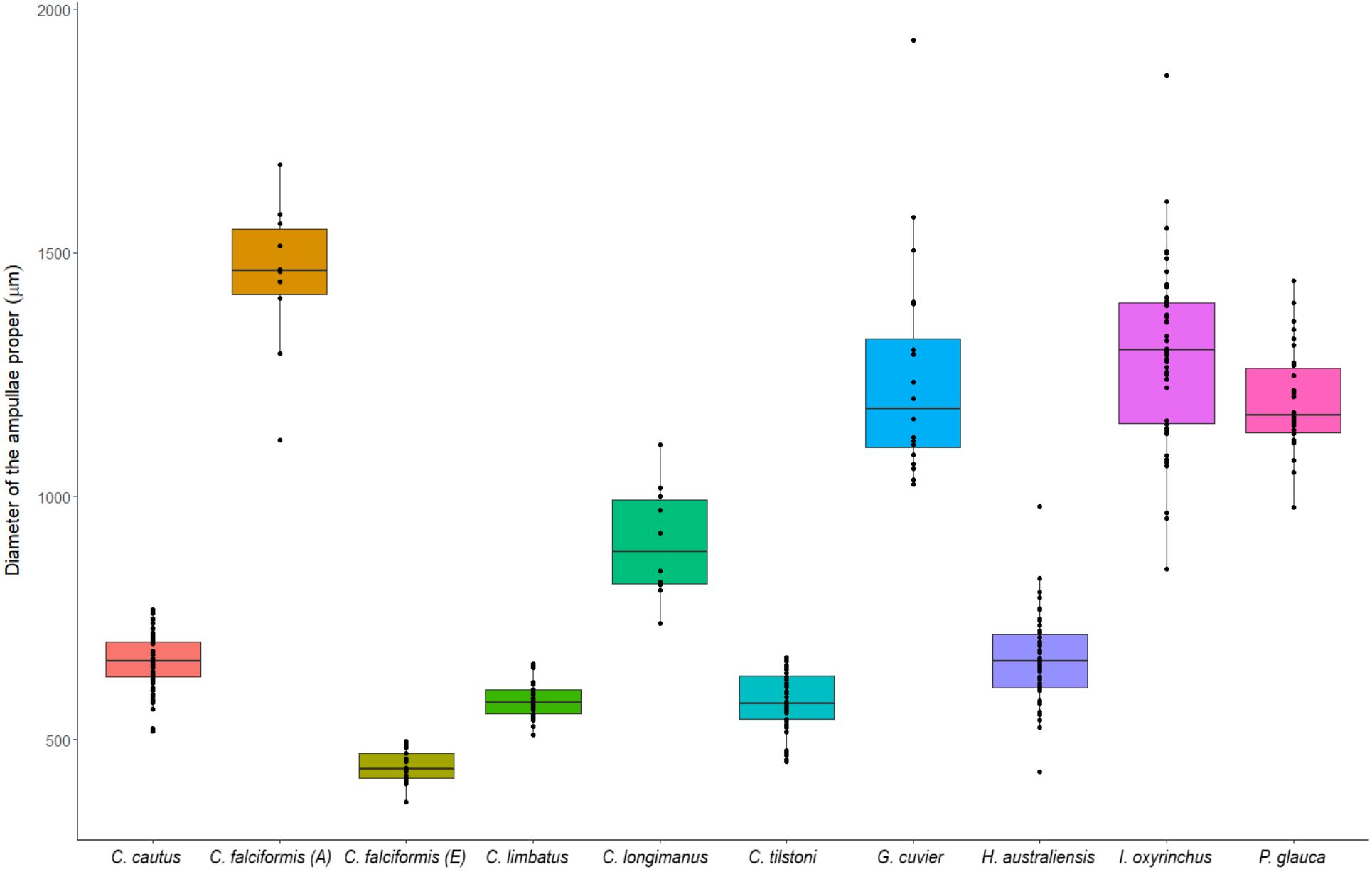

Figure 5.14. Box plot comparing the variation in diameter of the ampullae proper of *C. cautus, C. falciformis, C. limbatus, C. longimanus, C. tilstoni, G. cuvier, H. australiensis, I. oxyrinchus,* and *P. glauca*.

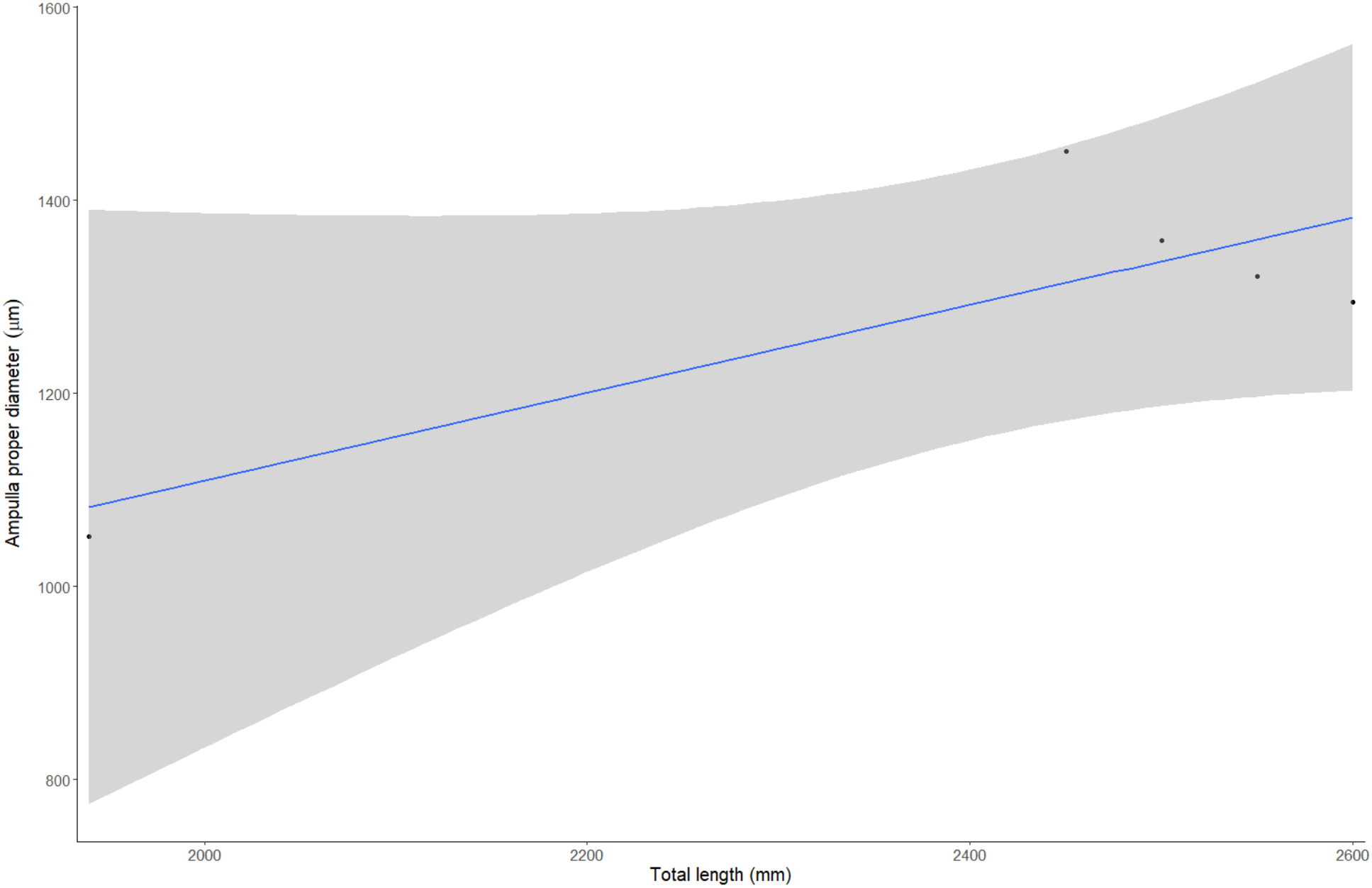

Figure 5.15A. Plot of the linear regression comparing the mean diameter of the ampullae proper of a specimen with its total length in *I. oxyrinchus* with a 95% confidence interval.

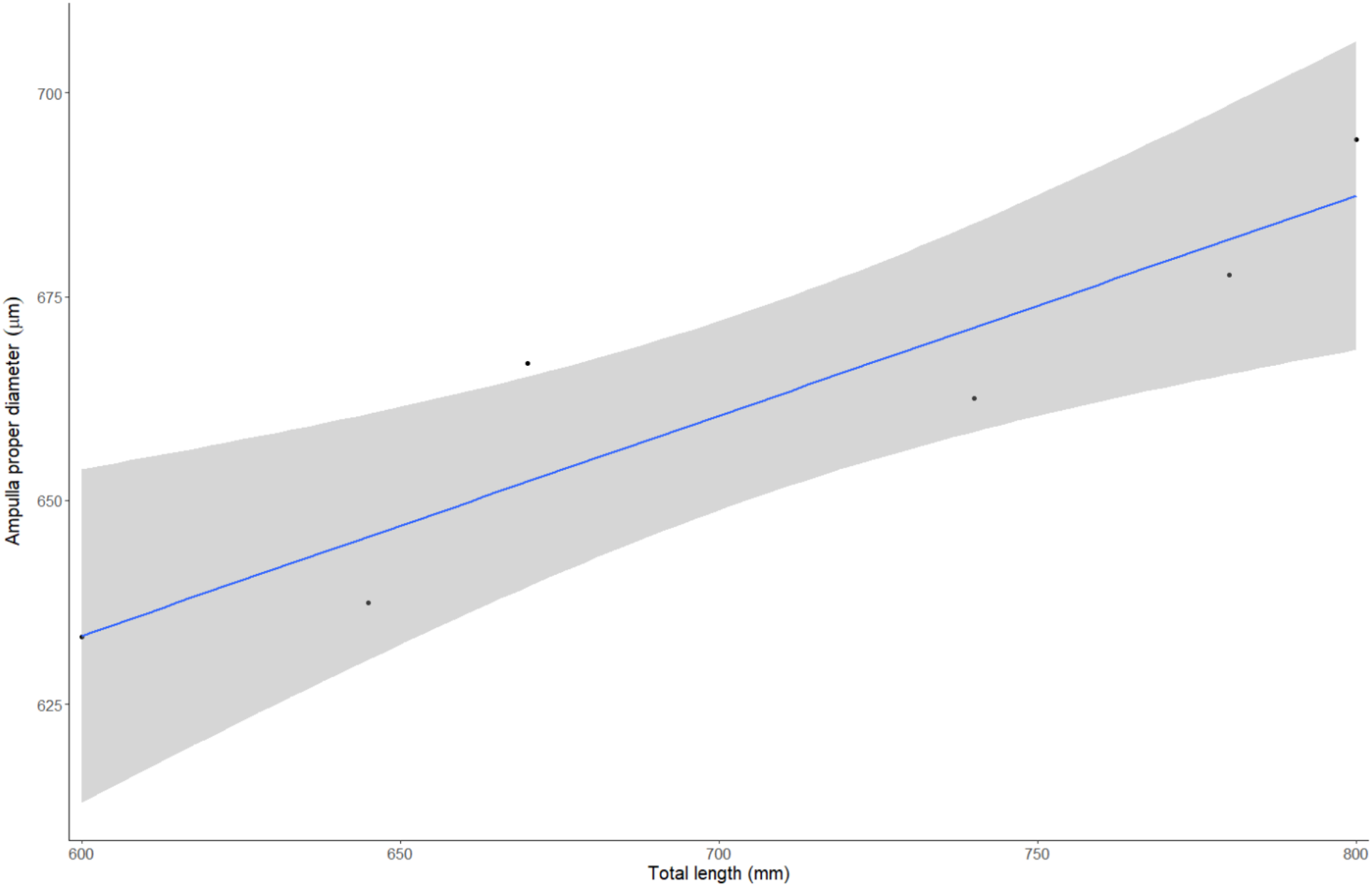

Figure 5.15B. Plot of the linear regression comparing the mean diameter of the ampullae proper of a specimen with its total length in *C. cautus* with a 95% confidence interval.

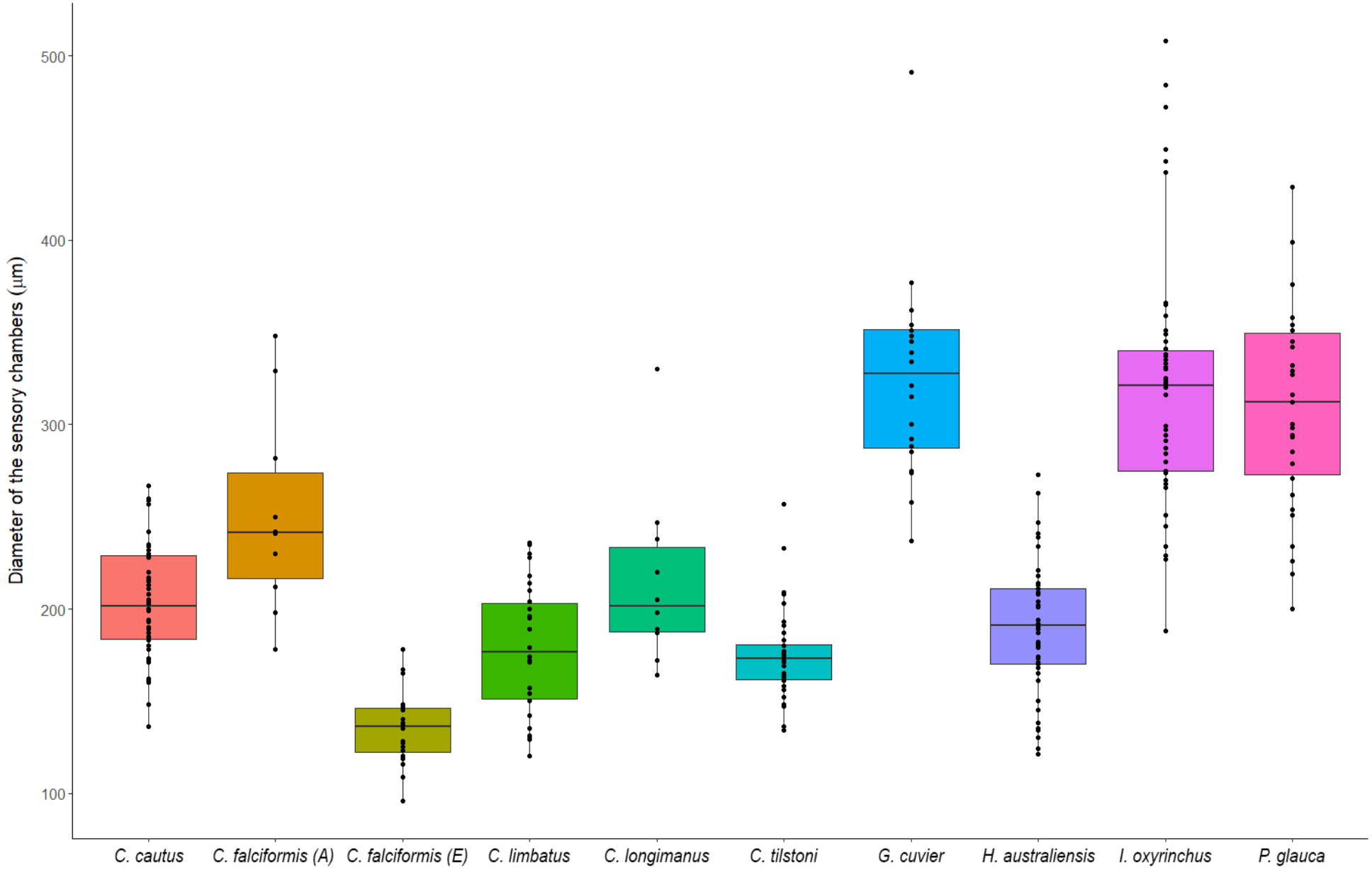

Figure 5.16. Box plot comparing the variation in diameter of the sensory chambers of *C. cautus, C. falciformis, C. limbatus, C. longimanus, C. tilstoni, G. cuvier, H. australiensis, I. oxyrinchus,* and *P. glauca*.

There are no observable structural variations in the sensory epithelium among the species examined in this study. There is a clear transition between the epithelial cells of the upper part of the ampulla proper and the deeper-lying sensory epithelium (Fig. 5.13B). The wall of the sensory chamber, before it reaches the sensory epithelium, is composed of two layers of cuboidal epithelial cells (Fig. 5.13C). The sensory epithelium is smooth, but microvilli cover the supportive cells, and kinocilia extend from receptor cells (Fig. 5.13D). The alveolar septae comprise both cuboidal and columnar epithelial cells (Fig. 5.13E). The base of each sensory chamber is composed of both apically and basally nucleated supportive cells, with the position of the nuclei alternating in no discernible pattern (Fig. 5.17A, 5.17B). External to the basement membrane, the ampulla proper is enveloped by a sheath of interlocking collagen fibres (Fig. 5.17B). Supportive cells are adjoined to receptor cells by tight junctions with underlying desmosomes, physically isolating receptor cells from each other, and extending all the way from the basement membrane to the ampullary lumen. Receptor cells are pear shaped with a central round nucleus (Fig. 5.17A, 5.17B). A small area of the apex of each receptor cell is exposed to the ampullary lumen, where a single kinocilium extends into the lumen (Fig. 5.17C, 5.17D). Rootlet fibres are evident and the kinocilia are arranged in an 8+1 structure (Fig. 5.17D, 5.17E). At the base of each receptor cell, pre-synaptic bodies lie opposite of a neural terminal (Fig. 5.17F). Neural terminals are typically filled with a high concentration of mitochondria (Fig. 5.17F).

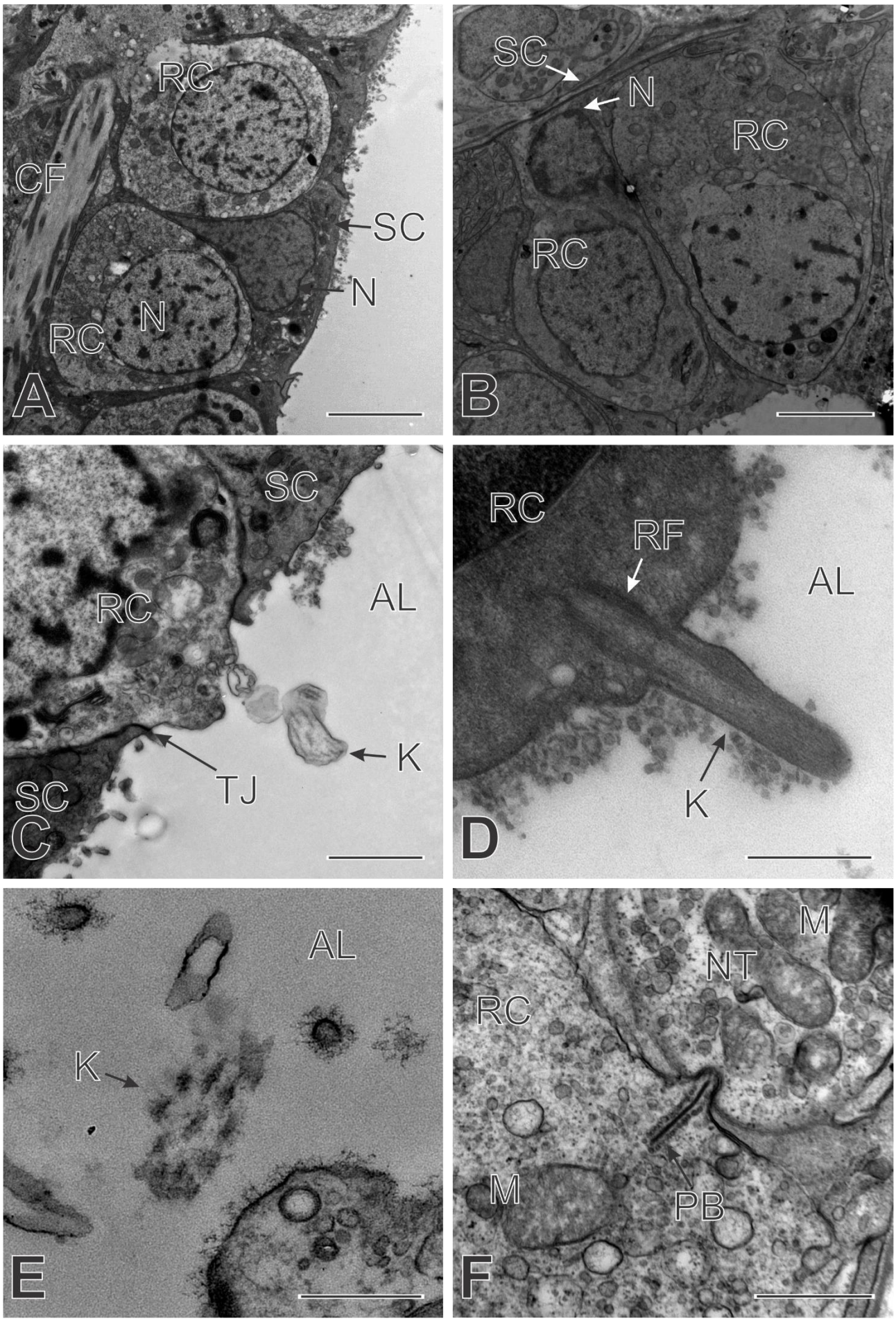
RC
CF
SC
N
N
RC
A
SC
N
RC
RC
B
SC
RC
AL
TJ
K
SC
C
RC
RF
AL
K
D
AL
K
E
M
NT
RC
M
PB
F

Figure 5.17. Micrographs of ampullae of Lorenzini from different species of selachimorphii. **A.** Sensory epithelium showing two receptor cells (RC) with round nuclei (N) and covered by an apically nucleated supportive cell (SC). Externally, the ampulla is surrounded by a sheath of collagen fibres (CF). *Galeocerdo cuvier*. TEM. Scale bar = 5 µm. **B.** Section through the same ampulla proper as Figure 5.17A. The supportive cell (SC) separating the receptor cells (RC) has a basally located nucleus (N). *Galeocerdo cuvier*. TEM. Scale bar = 5 µm. **C.** Apex of a receptor cell (RC) adjoined by two supportive cells (SC) by tight junctions (TJ). A single kinocilium (K) extends into the ampullary lumen (AL). *Carcharhinus longimanus*. TEM. Scale bar = 2 µm. **D.** Apex of a receptor cell (RC) with a single kinocilium (K) extending into the ampullary lumen (AL). Rootlet fibres (RF) are evident at the area where the kinocilium is connected to the receptor cell. *Carcharhinus falciformis*. TEM. Scale bar = 0.5 µm. **E.** Cross section of a kinocilium (K) in the ampullary lumen (AL) showing the microtubules in an 8+1 structure. *Carcharhinus cautus*. TEM. Scale bar = 0.5 µm. **F.** Basal area of a receptor cell (RC) with a pre-synaptic body (PB) lying adjacent to a neural terminal (NT) where a high concentration of mitochondria (M) is evident. *Galeocerdo cuvier*. TEM. Scale bar = 1 µm.

Discussion

In accordance with previous studies, the distribution of the ampullary pores in elasmobranchs appears to be affected by an animal's lifestyle and environment. However, aspects of the gross morphology of ampullary organs seems to only be affected by the size of an individual, while their ultrastructure appears to be unaffected by a species' lifestyle or environment.

Pore distribution

There were various differences and similarities in the distribution, number and shape of ampullary pores among the nine species studied. Some of the ampullary pores were nested between placoid scales, with some of the scales located around the pore showing structural variation, most likely related to their proximity to the pore. Differences in scale morphology at a gross level have been described in relation to the habitat that shark species occupy. For example, prominently ribbed scales occur in species that swim constantly, as this morphology is considered to reduce drag (Raschi *et al*., 1992). In relation to the ampullae of Lorenzini, it is suggested that ridge patterns on scale crowns direct water flow away from pore openings (Reif, 1978). Generally, members of the *Carcharhinus* genus exhibit a remarkable similarity of pore number and the pattern of distribution across the head. In the present study, all seven species studied favour teleosts in their diet, are all pelagic animals, but species vary somewhat in preference for coastal or oceanic environments. The larger and more oceanic species, *Carcharhinus falciformis* and *C. longimanus*, have a similar number of pores to the much smaller *C. tilstoni* and *C. brevipinna*. As there is a difference in size that is not matched by an increase in pore number there is presumably a decrease in target resolution associated with having a lower density of ampullary pores on the snout. However, the pores of the bigger species tend to be much larger which may be offset by having a greater sensitivity to weak electric fields that can be produced by their prey. This hypothesis is seemingly supported by the differences observed in the ampullary pore distribution between adult and embryonic *C. falciformis*. While the distribution pattern was mostly similar, albeit with a heavier concentration of pores on the ventral surface of the adult specimen compared to the embryo, the density of ampullary pores in the adult specimen was half that of the embryos. The roughly equal distribution between ventral and dorsal pores for most species fits well with the diets consisting mostly of teleosts (and cephalopods,

mainly in *C. cautus*, and *Hemigaleus australiensis*) and their use of electroreception during the final stages of prey capture (Stevens, 1984, White *et al*., 2004; Taylor & Bennett, 2008). The much larger concentration of ampullary pores on the ventral side of the head in *Galeocerdo cuvier* compared to its dorsal side also seems to fit well with its highly diverse diet, composed of teleosts, elasmobranchs, birds, mammals, reptiles, and benthic crustaceans (Stevens, 1984; Last & Stevens, 2009). *Galeocerdo cuvier* is also well-known for being a scavenger, but this feeding strategy is unlikely to affect the distribution of ampullary pores. They will likely not use electroreception for detection and feeding on carcasses as they do not emit the electric fields of a live animal. The number of ampullary pores found in the one specimen studied here is much higher than the 798-895 pores previously reported for this species. The specimens examined in previous studies were smaller (although their total lengths were not reported, but information gleaned from the articles' figures suggest they were no longer than 200 cm L_T) which could have impacted the total ampullary pore count (Raschi, 1986; Cornett, 2006). However, the difference in pore counts between the previous studies and this one is large, even for animals of different size (cf. *C. falciformis*), but there are no clear reasons behind the discrepancies. Despite this difference in pore counts, their distribution across the head, and the relative proportion of dorsal to ventral pores were similar in all studies (Raschi, 1986; Cornett, 2006).

The shortfin mako shark, *Isurus oxyrinchus*¸ has a relatively low ampullary pore count; fewer than any other species presented in this study and as might be expected from a purely pelagic, highly visual predator that theoretically does not rely on electroreception for foraging (Yopak & Lisney, 2012). The observed intraspecific difference in ampullary pore count may be a size-effect, with 758 pores observed in a 194 cm L_T specimen, and 958 in a 255 cm L_T specimen. The few specimens of this species examined in previous studies also had a slightly lower pore count (834 ± 108 in the present study vs 635 (Cornett, 2006) and 690 ± 109 (Kempster *et al*., 2012)), but the size of the animals was not reported (Aadland, 1991; Cornett, 2006; Kempster *et al*., 2012). A low ampullary pore count is also shared by other lamniformes, such as *Cetorhinus maximus* and *Megachasma pelagios*, with 300 or fewer pores observed in either species (Kempster & Collin, 2011a; Kempster & Collin, 2011b). However, the peculiar distribution observed in *I. oxyrinchus* is not present in either species. The combination of relatively low abundance of ampullary pores and the highly visual nature of *I. oxyrhinchus* could indicate a low reliance on its electrosensory system. However, lack of a nictitating membrane, which results in a rolling of the eyes back into the skull for protection during the final stages of attack, and the presence of a 'V'-shaped pattern of

ampullary pores on the dorsum of the head may suggest otherwise. Reports from game fishers (*Pers. comm.)* indicate that *I. oxyrinchus* is often observed swimming below prey items before striking, most likely relying on those pores distributed on their dorsal surface to determine the location of their prey before and during the strike. The absence of ampullary pores immediately anterior to the eye sockets, like those observed in every other species studied here, may also relate to the foraging strategy. I suggest that the pores (leading to ampullae) immediately anterior to the eyes in other species are used to detect laterally oriented escape attempts by prey in the final moments of an attack. With the shark's vision being limited during those final moments before a strike, the detection of movement through the ampullary organs associated with these pores would allow the shark to swing its head and catch their prey. A high attack speed and/or an attack on their prey from below may obviate the need for these lateral pores in *I. oxyrinchus*.

Ampullary pores located anterior to the eyes are much smaller and more numerous than the ones located posterior to the eyes; both trends were observed in every species studied here. The posterior pores give rise to long canals that run parallel to the epidermis, a morphology usually associated with the detection of uniform fields, whereas prey detection is associated with shorter canals in the snout that run perpendicular to the epidermis (Rivera-Vicente *et al*., 2011). The smaller, more numerous pores on the snout would presumably provide for a level of spatial resolution, to allow the position of close prey to be determined accurately, that is not necessary for the detection of uniform fields.

Gross morphology & ultrastructure

The ultrastructure of the ampullae of Lorenzini was remarkably similar across the species examined in this study. The ampullary canal walls are composed of two interlocking cell layers, adjoined with tight junctions and desmosomes, to preserve the electrical signal travelling through the ampullary canal, and is a feature conserved across all elasmobranchs studied to date.

The differences observed in the size of the ampullary canals, ampullae proper, and sensory chambers appear to be influenced both by the size of the specimens, and their phylogeny. Apart from *G. cuvier*, the coastal species studied are all relatively small and similar in size to one another, with minor differences in the gross measurements of their ampullary organs. In the larger, more oceanic species the differences in these measurements were more

obvious, especially with *C. falciformis* having the largest ampullae proper, despite being much smaller than the specimens of *G. cuvier* examined. The significant difference in the size of all of these features in the smaller specimen of *I. oxyrinchus* compared to its larger conspecifics, and in the embryonic *C. falciformis* compared to the adult suggest that ampullary organs may change in size through ontogeny, but the magnitude of change may differ from species to species. Larger *C. cautus* typically had larger ampullae proper as revealed by a linear regression. Larger sample sizes are required to resolve possible relationships between L_T and the various measured variables as applied to ampullary organs, which could also eliminate the variability observed in the larger specimens of *I. oxyrinchus*. The larger size of the ampullary organs of *C. falciformis* could result in a higher sensitivity to weak electrical fields (Raschi, 1986). However, there are no obvious differences in the diet, behaviour, or lifestyle of this species compared to the other oceanic sharks that would justify the need for this increase in sensitivity. While the overall measurements of the ampullary organs of the *C. falciformis* embryos are generally smaller than that of the adult specimen, and that of the other species examined, the presence of a similar number of sensory chambers between the embryo and adult specimen indicate that their electrosensory system is most likely functional. These embryos were most likely close to being born: The cited size at birth of *C. falciformis* is 56 – 87 cm, depending on the location (Bonfil, 2008). Kempster *et al*. (2013) observed functional ampullae of Lorenzini by stage 32 of the development of *Chiloscyllium punctatum*¸ where changes to respiratory movements were correlated to changes in applied electric fields. The use of oviparous species provides opportunities to examine the early ontogenetic development, and function, of the electrosensory system that are effectively unavailable in viviparous species. However, analysis of a representative ontogenetic sequence of individuals for any species should be considered in order to resolve the question of changes in size and number of ampullae with growth.

The epithelium in the sensory chambers rapidly transitions from smooth cuboidal epithelial cells to the sensory epithelium, composed of both supportive and receptor cells. The alveolar septae separating each sensory chamber are composed of both cuboidal and columnar epithelial cells. The alternation between basally and apically nucleated supportive cells is of interest but probably has a negligible – if any – impact on the sensitivity of the receptor cells. Supportive cells have typically been reported as either basally, or apically nucleated, but never before in this alternating pattern (Whitehead *et al*., 2015a; Gauthier *et al*., 2018). This alternation is unlikely to occur only in the species that are part of this study, and may have

gone un-noticed or un-reported in the past. The receptor cells themselves are pear-shaped, with a central, round nucleus, as has generally been reported for selachimorphs. They all possess a single kinocilium that extends into the ampullary lumen and is thought to help detect the electric fields, and are abutted by a basal neural terminal. Interestingly, these similarities occur across species that use different lifestyles, occupy different habitats, rely differently on their other senses (e.g. a likely greater emphasis on vision in *I. oxyrinchus*, and olfaction in *G. cuvier*), and presumably have different sensitivities to surrounding electric fields, all of which do not affect their electrosensory system other than the distribution and number of their ampullary pores. Any differences in sensitivity to weak electric fields described in various shark behavioural studies, or responses to shark deterrent devices that use pulsed electric fields, are most likely not a direct result of the morphology of their ampullae of Lorenzini (Kalmijn, 1982; Marcotte & Lowe, 2008; Kempster *et al*., 2016). In order to get a better understanding of the origin of these variations in sensitivity and response to electric stimulus, a more thorough investigation into how the dorsal octavolateralis nucleus, a cerebellum-like structure, receives and processes the information coming from the ampullae of Lorenzini would be required (Montgomery, 2012).

Overall, the main difference observed in the electrosensory system of the ten species of sharks studied in this project was that of ampullary pore distribution. While pores of species within a genus have a similar distribution pattern, different patterns occur at a broader phylogenetic level (intra- and inter-familial variation). However, phylogeny and specific behaviours, abilities and habitat-use are linked, and it is likely that similar pore and ampullae distributions could evolve independently among sharks that have a similar functional use for their electrosensory system.

Apart from the general size of the ampullae, which appears to depend on the size of the organism, the ultrastructure of the electrosensory system was identical across all species examined in this study and appeared to not be influenced by a species' diet, phylogeny, or lifestyle.

Acknowledgments

This research would not have been possible without the tremendous help of John Page and Dave Thomson to acquire samples from Moreton Bay, as well as Sam Williams, Julian Pepperell, Gary Chenoweth and the entire New South Wales Game Fishing Association

who kindly let me collect samples during game fishing tournaments. Thank you as well to the staff of the Moreton Bay Research Station for accommodating me, and The University of Queensland’s Centre for Microscopy and Microanalysis for their assistance.

Chapter VI

Lack of phenotypic plasticity in the teleost ampullary organs of a euryhaline silurid, *Neoarius graeffei*.

Abstract

Siluriforms can detect weak electric fields in their surrounding environment using ampullary organs. The morphology of these ampullary organs typically depends on the salinity environment the fish inhabits. Freshwater species generally possess micro-ampullae with short ampullary canals and few receptor cells, whereas marine species have macro-ampullae with longer canals and more numerous receptor cells per ampullae. *Neoarius graeffei* is a euryhaline species of catfish commonly found in freshwater, estuarine, and marine areas of south east Queensland, Australia. The morphology of the *N. graeffei* electrosensory system has been examined previously, and differs in wild animals originating from environments of different salinities. In this study, I tested the phenotypic plasticity of the ampullary organs of these species by collecting specimens from a mostly freshwater area, and raising them in tanks of different salinities (0, 17, and 34 ppt), mimicking the conditions they can be exposed to in the wild. After six months, I examined their ampullary organs, and found no significant differences in their gross morphologies, despite evidence of new ampullae being formed through budding. The lack of observable differences between treatment groups challenges the hypothesis of electrosensory system phenotypic plasticity. If such plasticity does exist then what are the: factors that drive change, time-course and magnitude of change for change, mechanisms for change, and is there a critical window of opportunity during development for change?

Introduction

In 1917, the ability of catfishes (Order: Siluriformes) to detect galvanic fields was discovered (Parker & van Heusen, 1917). Further investigation has shown that catfish possess ampullary organs (henceforth called teleost ampullary organs), similar in shape to those found in elasmobranchs. These teleost ampullary organs consist of a somatic pore within the epidermis that opens to a canal that terminates in a single ampulla proper. The ampullary canal wall may be composed of squamous, cuboidal, or columnar epithelial cells (Mullinger, 1964; Wachtel & Szamier, 1969; Whitehead *et al*., 1999; 2000; 2015; Jørgensen, 2005; Gauthier *et al*., 2015). These epithelial cells are adjoined by tight junctions with underlying desmosomes ensuring minimal loss of electric current through the canal (Waltman, 1966; Josberger *et al*., 2016). The ampullary canal itself is filled by a highly conductive mucopolysaccharide gel (Waltman, 1966; Obara & Sugawara, 1984; Kramer, 1996; Josberger *et al*., 2016). In species with an elongated canal, a sheath of interlocking collagen fibres can be observed enveloping the canal (Zakon, 1986; Whitehead *et al*., 1999; Gauthier *et al*., 2015). Situated at the distal end of the canal is the ampulla proper, which is lined by receptor and supported cells. The receptor cells of teleost ampullary organs are typically pear-shaped, their apex is exposed to the ampullary lumen and covered in microvilli (Mullinger, 1964; Whitehead *et al*., 1999, 2000, 2003; Raschi & Gerry, 2003; Gauthier *et al*., 2015). Unmyelinated neural terminals abut the basal region of each receptor cell, and individual neurons connect each receptor cell to a branch of the anterior lateral line nerve and to the anterior lateral line lobe of the central nervous system (Bretschneider & Peters, 1992).

Significant morphological differences have been observed in the ampullary organs of species originating from habitats with different salinities (Kalmijn, 1974). Freshwater species have micro-ampullae with short ampullary canals that stay within the limits of the epidermis, few receptor cells per ampulla, lack an enveloping collagen sheath (Herrick, 1901; Wachtel & Szamier, 1969; Andres & von Düring, 1988; Jørgensen, 1992; Whitehead *et al*., 2000; 2003). The marine catfish *Plotosus lineatus* (= *P. anguillaris*) possesses macro-ampullae, with much longer ampullary canals and a surrounding collagen sheath. The ampullae proper of this species contain numerous receptor cells and tend to form clusters, similar to an elasmobranch's ampullae of Lorenzini (Friedrich-Freska, 1930; Bauer & Denizot, 1972). The longer canals are required to create the potential difference needed to detect weak electric fields (Kalmijn, 1974). However, the estuarine *Plicofollis argyropleuron* possesses the

longest ampullary organs of all recorded teleosts, which raises the question of the importance of the effects of environmental salinity on the morphology of teleost ampullary organs (Whitehead *et al*., 2015b). Additionally, this species also has numerous micro-ampullae, scattered on the body of the fish, but not over the head (Whitehead *et al*., 2015b). In the siluriform family Ariidae, *Neoarius graeffei* (previously referred to as *Arius graeffei*) is a euryhaline species commonly found in marine waters, estuaries, and freshwater rivers of the Moreton Bay catchment in south east Queensland, Australia. This species can reproduce in freshwater impoundments and freshwater lakes, and may travel among or be otherwise exposed to environments of differing salinities (Stuart & Berghuis, 2002; Stuart *et al*., 2007; Oughton, 2014). The osmoregulatory capabilities of this species allow it to be used as a model for observational and experimental investigation on the phenotypic plasticity of teleost ampullary organs in relation to environmental salinity. Previous research on this species documented significant morphological differences in the ampullary organs of freshwater, estuarine and marine individuals (Whitehead *et al*., 1999, 2000; Gauthier *et al*., 2015). As was expected, freshwater individuals possessed short ampullary canals with few receptor cells, while marine individuals possessed much longer canals with numerous receptor cells (Gauthier *et al*., 2015). However, the ampullary canals of the marine individuals were not as long as those reported for *P. lineatus* or even the estuarine *P. argyropleuron*.

The present study aimed to investigate the hypothesised phenotypic plasticity of teleost ampullary organs in *Neoarius graeffei*. Adaptive change in ampullary organ morphology would be determined in response to long-term exposure to controlled, constant salinity environmental conditions.

Methods

Specimen collection & Experimental protocol

Twenty-eight juvenile *Neoarius graeffei* were captured over two-days in November 2015 by angling and netting in the Brisbane River between Kookaburra Park and Colleges Crossing (27°32'30.9"S, 152°50'28.8"E). Shortly after capture on both days, the collected fish were transported in aerated Brisbane River water to The University of Queensland's Moreton Bay Research Station on North Stradbroke Island. Four fish were taken at random to act as time-zero controls and euthanised (175 mg L^{-1} of Aqui-S in river water: University of Queensland's

Animal Ethics Committee Certificate: SBMS/406/14). The remaining fish were randomly sorted into three groups, and each group assigned a different salinity: 0 parts per thousand (ppt), 16-18 ppt, and 34-36 ppt, representing freshwater, estuarine and marine environments respectively. The fish were progressively acclimated to their new environment over two weeks, after which four fish were taken from each environment as Day 0 samples. Fish were then kept at their respective salinities for a period of six-months, after which they were euthanised. All fish were immersion fixed in 10% neutral buffered formalin immediately following euthanasia.

Pore measurements

To measure the diameter of the ampullary pores, the skin from two fish per time point per treatment was removed, scraped of any remaining flesh, and placed under a Nikon SMZ745T dissection microscope with a backlight. A total of 20 pores per fish were measured using the Nikon BR 4.0 Basic Research software.

Light microscopy & gross measurements

After fixation, the tissue samples containing teleost ampullae were processed to paraffin wax following routine histology procedure, serial sectioned on a Leica rotary microtome RM 2245 at 6 µm thickness, and stained with Mayer's haematoxylin & eosin following the protocol outlined in Gauthier *et al*., (2015). The resulting slides were examined under a Nikon 50i Eclipse compound microscope and measurements realised through the Nikon BR 4.0 Basic Research software. A total of 10 ampullae proper and 10 ampullary canals were measured per fish, and the receptor cells of 10 ampullae were counted.

Statistical analysis

The measurements were compared between different treatments and analysed using a series of nested one-way ANOVAs, results are presented as mean ± standard deviation. Linear regression analysis was used to investigate possible effects of an animal size on each of the measurements taken. Significance for all tests was accepted at $p < 0.05$.

Results

Ampullary pore mean diameter ranged from 189.9 ± 37.1 to 201.2 ± 25.0 µm across all specimens studied, with no significant differences between treatments ($p > 0.05$; Table 1; Fig. 6.1). Ampullary canal mean length ranged from 236.6 ± 38.7 to 258.0 ± 46.8 µm, with no significant differences between treatments ($p > 0.05$; Table 1; Fig. 6.2, 6.3, 6.4).

Across all individuals, the mean diameter of the ampullae proper ranged from 80.1 ± 7.6 to 86.3 ± 11.4 µm, with no significant differences between treatments ($p > 0.05$; Table 1; Fig. 6.2, 6.3, 6.5). The number of receptor cells per ampulla varied from 49.1 ± 8.6 to 54.6 ± 10.3 µm on average, with no significant differences between treatments ($p > 0.05$; Table 1; Fig. 6.2, 6.3, 6.6). In all specimens from every treatment, evidence of budding ampullae could be observed (Fig. 6.3D).

Linear regression analysis showed a small, but significant relationship between ampullary canal length and specimen total length (L_T) ($p < 0.05$, $R^2 = 0.04$; Fig. 6.7A). Similarly, there was a significant relationship between the diameter of the ampullae proper and L_T ($p < 0.05$, $R^2 = 0.05$; Fig. 6.7B). Ampullary pore diameter and the number of receptor cells per ampulla were independent of L_T over the range of fish size in this study.

Table 6.1. Morphological measurements of several of the teleost ampullary organs characteristics. The F, E, and M denominations respectively refer to Freshwater (0ppt), Estuarine (16-18ppt), and Marine (34-36ppt) environments. The F0, E0, and M0 samples correspond to the samples taken after the two-week acclimation period, considered Day 0 of the experiment. The F180, E180, and M180 correspond to the samples collected on Day 180 of the experiment.

Specimen	Environment	Total Length (range, cm)	Canal length (µm)	Ampulla proper diameter (µm)	Number of receptor cells	Pore diameter (µm)
Control	Brisbane River*	112-155	236.6 ± 38.7	80.1 ± 7.6	52.3 ± 9.7	191.8 ± 24.2
F0	Freshwater	115-195	249.9 ± 41.1	83.7 ± 9.8	54.6 ± 10.3	200.2 ± 36.6
E0	Estuarine	115-170	241.7 ± 37.3	80.7 ± 8.5	49.1 ± 8.6	201.2 ± 25.0
M0	Marine	150-220	238.1 ± 33.0	86.3 ± 11.4	52.5 ± 8.9	193.8 ± 35.2
F180	Freshwater	170-205	242.4 ± 43.8	84.3 ± 7.8	51.0 ± 10.8	189.9 ± 37.1
E180	Estuarine	180-250	258.0 ± 46.8	83.3 ± 11.9	51.0 ± 9.9	193.9 ± 31.2
M180	Marine	190-260	253.0 ± 28.5	85.3 ± 8.4	50.7 ± 7.7	191.0 ± 27.0

*The Brisbane River at the site of collection is primarily freshwater, but the tide might bring in a layer of saltwater that *Neoarius graeffei* might be exposed to.

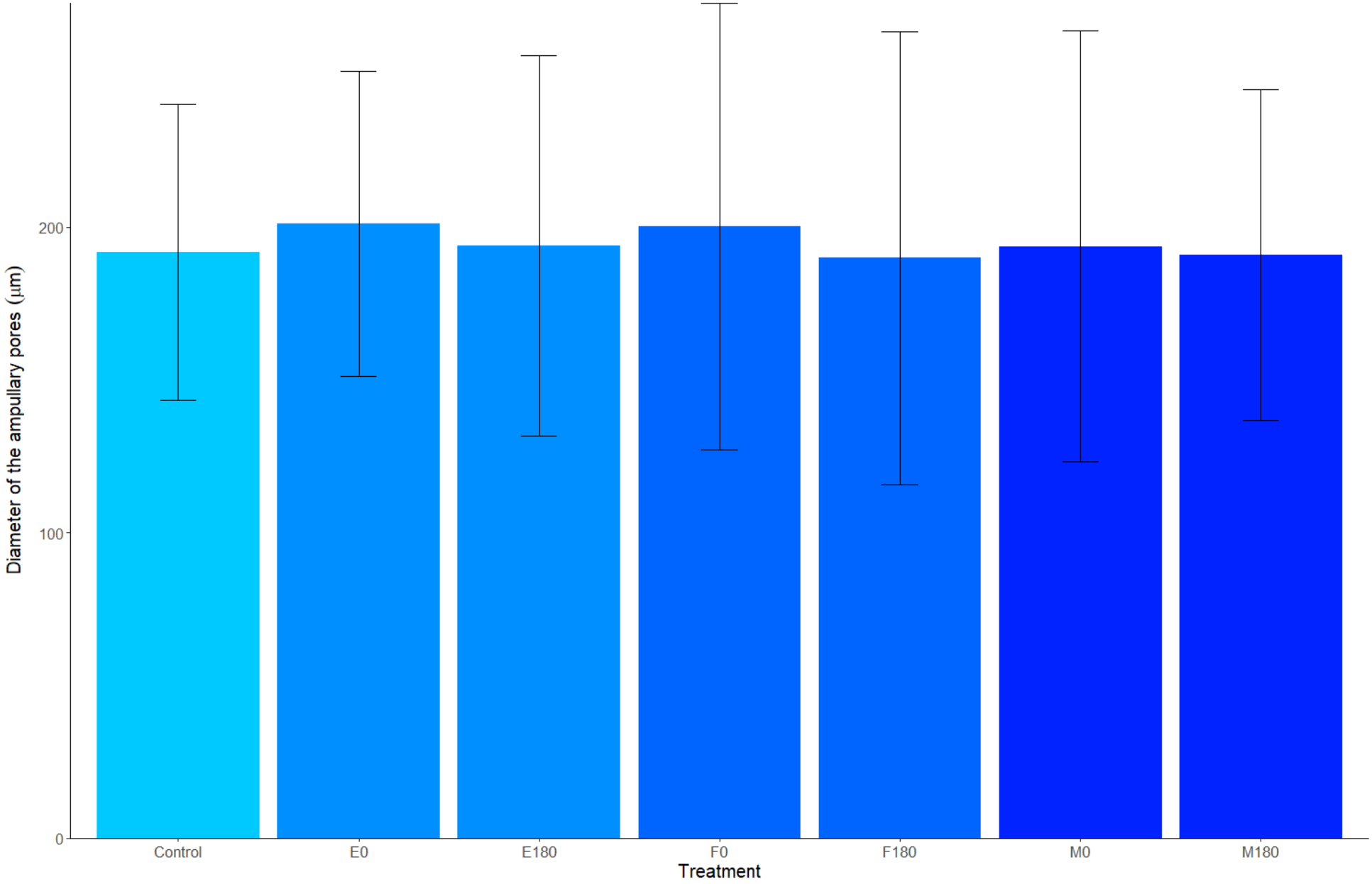

Figure 6.1. Bar graph comparing the mean standard deviation of the diameter of the ampullary pores across treatments.

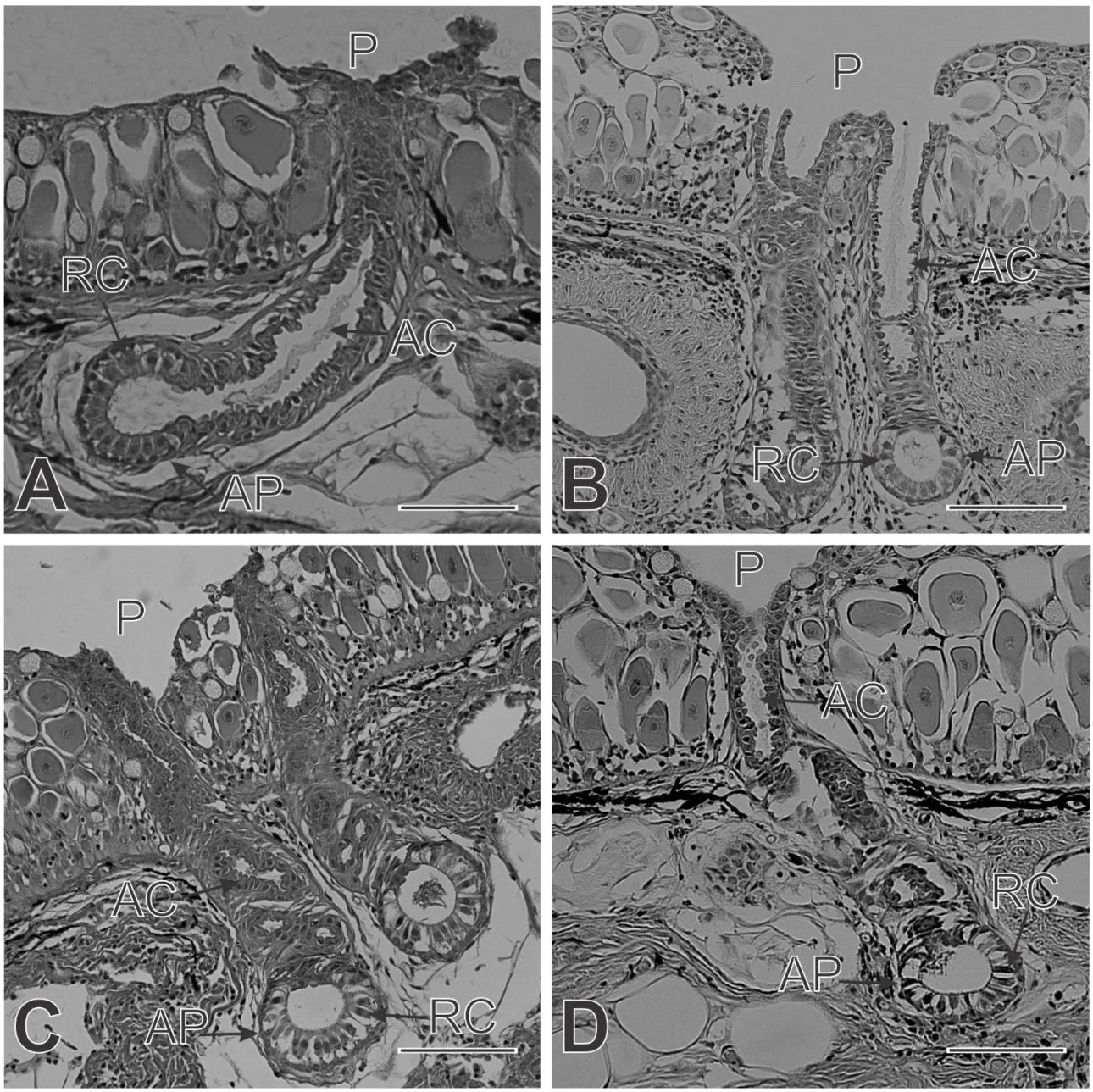

Figure 6.2. Micrographs of ampullary organs from *Neoarius graeffei* from different treatments showing the ampullary pore (P) invaginating into an ampullary canal (AC) that terminates in an ampulla proper (AP) lined with receptor cells (RC). **A.** Control. Scale Bar = 80 µm. **B.** Freshwater on Day 0. Scale Bar = 100 µm. **C.** Estuarine on Day 0. Scale Bar = 80 µm. **D.** Marine on Day 0. Scale Bar = 80 µm.

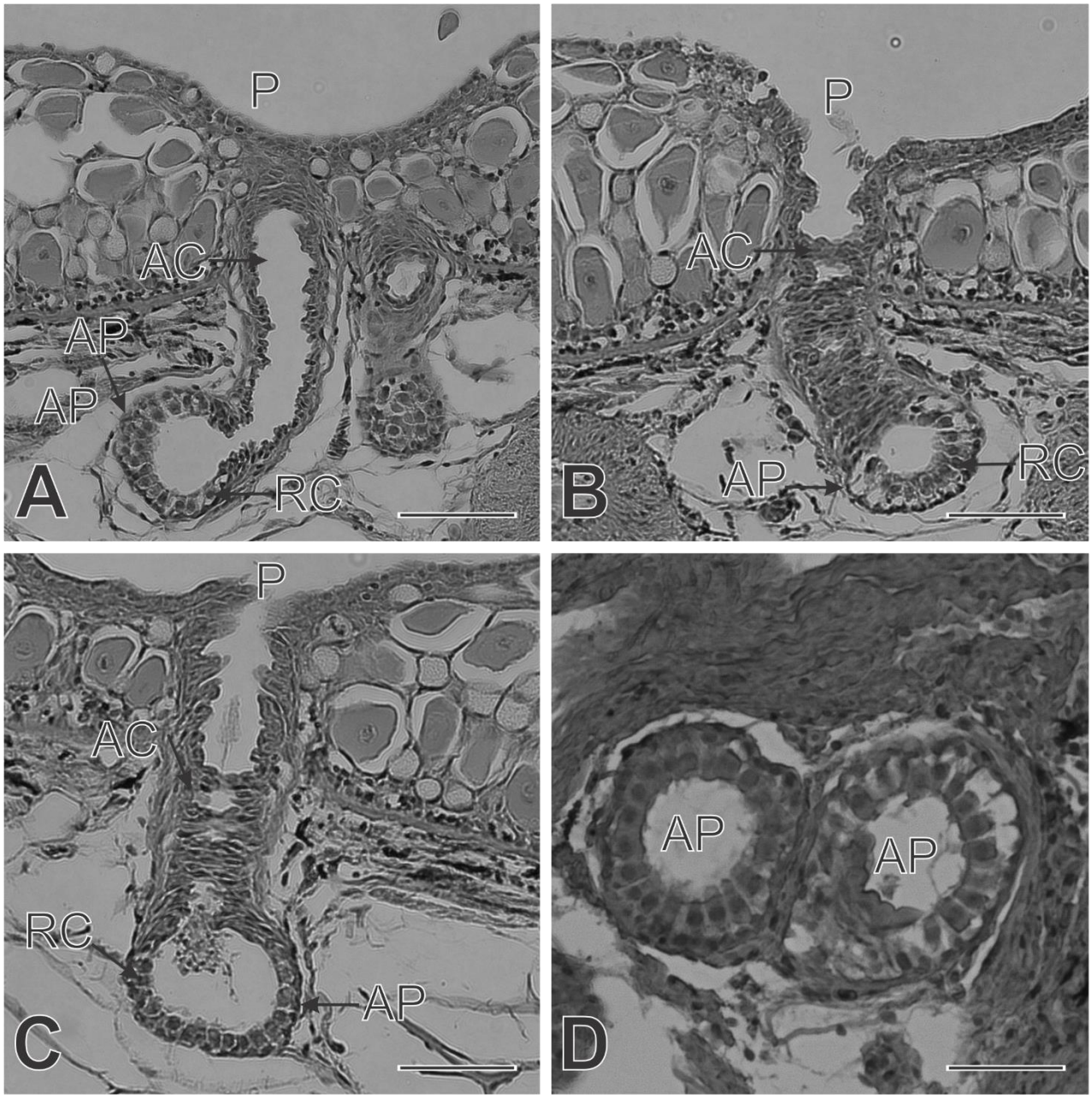

Figure 6.3. Micrographs of ampullary organs from *Neoarius graeffei* from different treatments showing the ampullary pore (P) invaginating into an ampullary canal (AC) that terminates in an ampulla proper (AP) lined with receptor cells (RC). **A.** Freshwater on Day 180. Scale Bar = 80 µm. **B.** Estuarine on Day 180. Scale Bar = 80 µm. **C.** Marine on Day 180. Scale Bar = 70 µm. **D.** Budding ampullary organs from a freshwater *N. graeffei* on Day 180. Scale Bar = 60 µm.

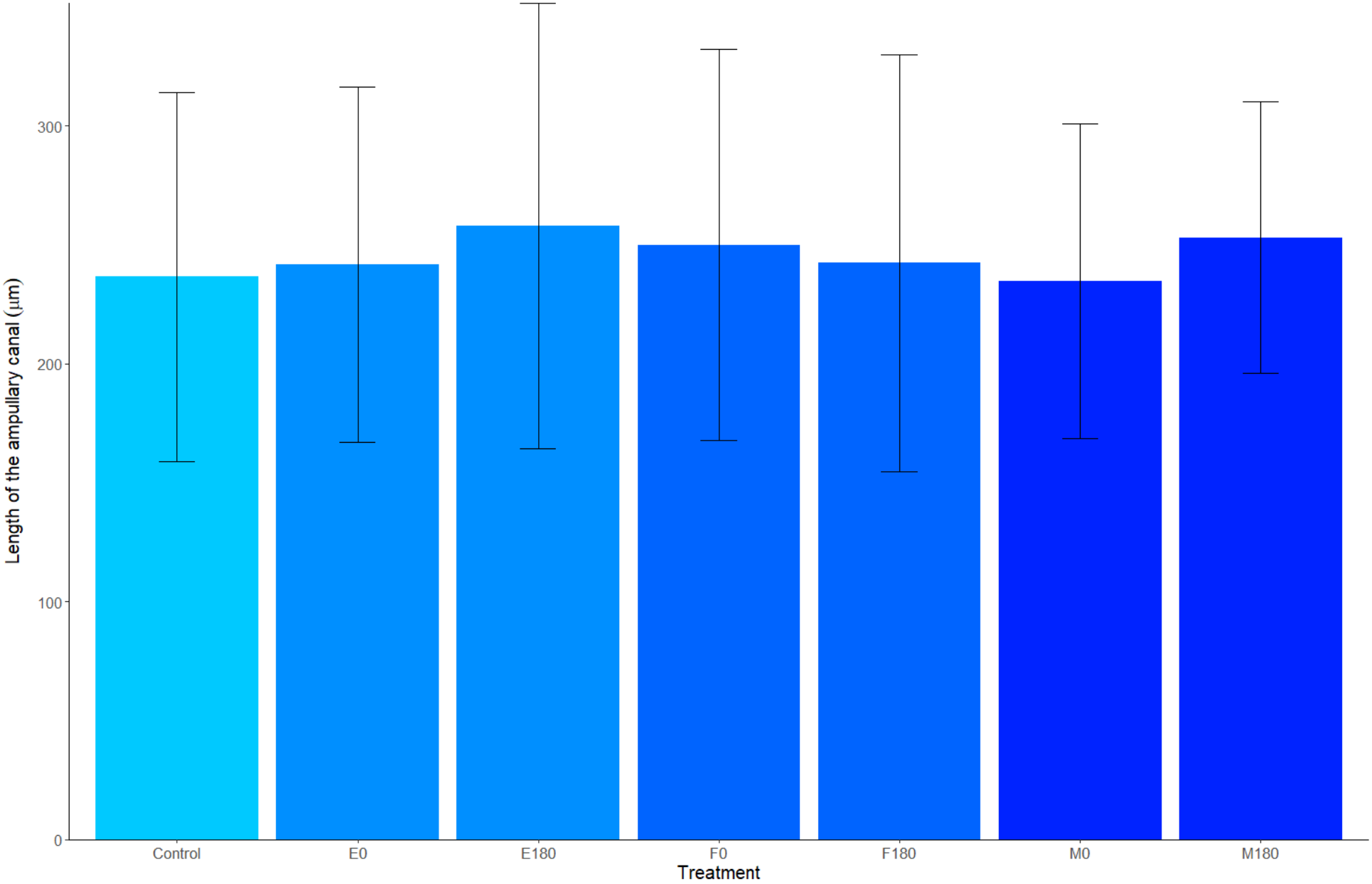

Figure 6.4. Bar graph comparing the mean standard deviation of the length and of the ampullary canals across treatments.

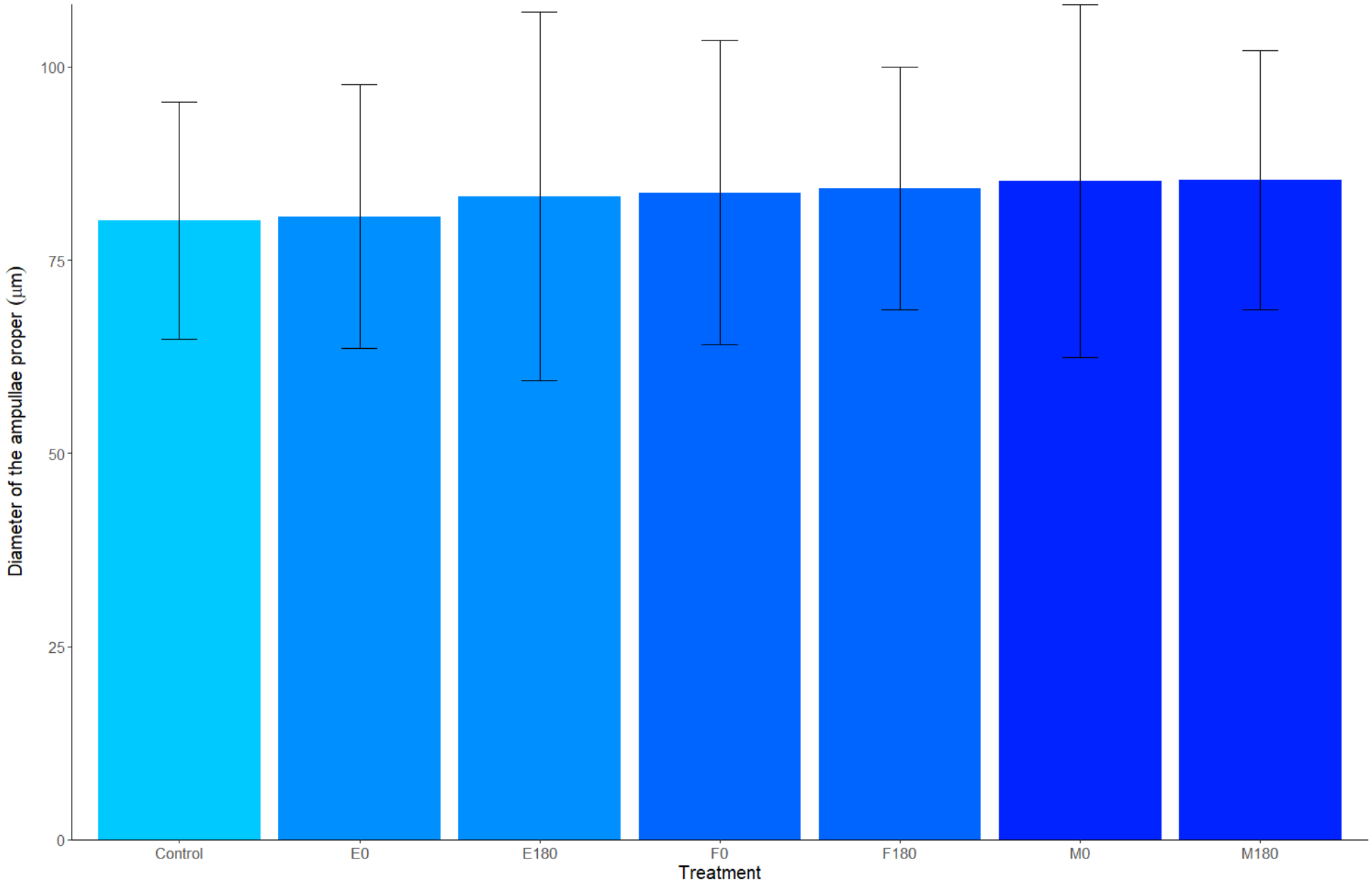

Figure 6.5. Bar graph comparing the mean standard deviation of the diameter of the ampullae proper across treatments.

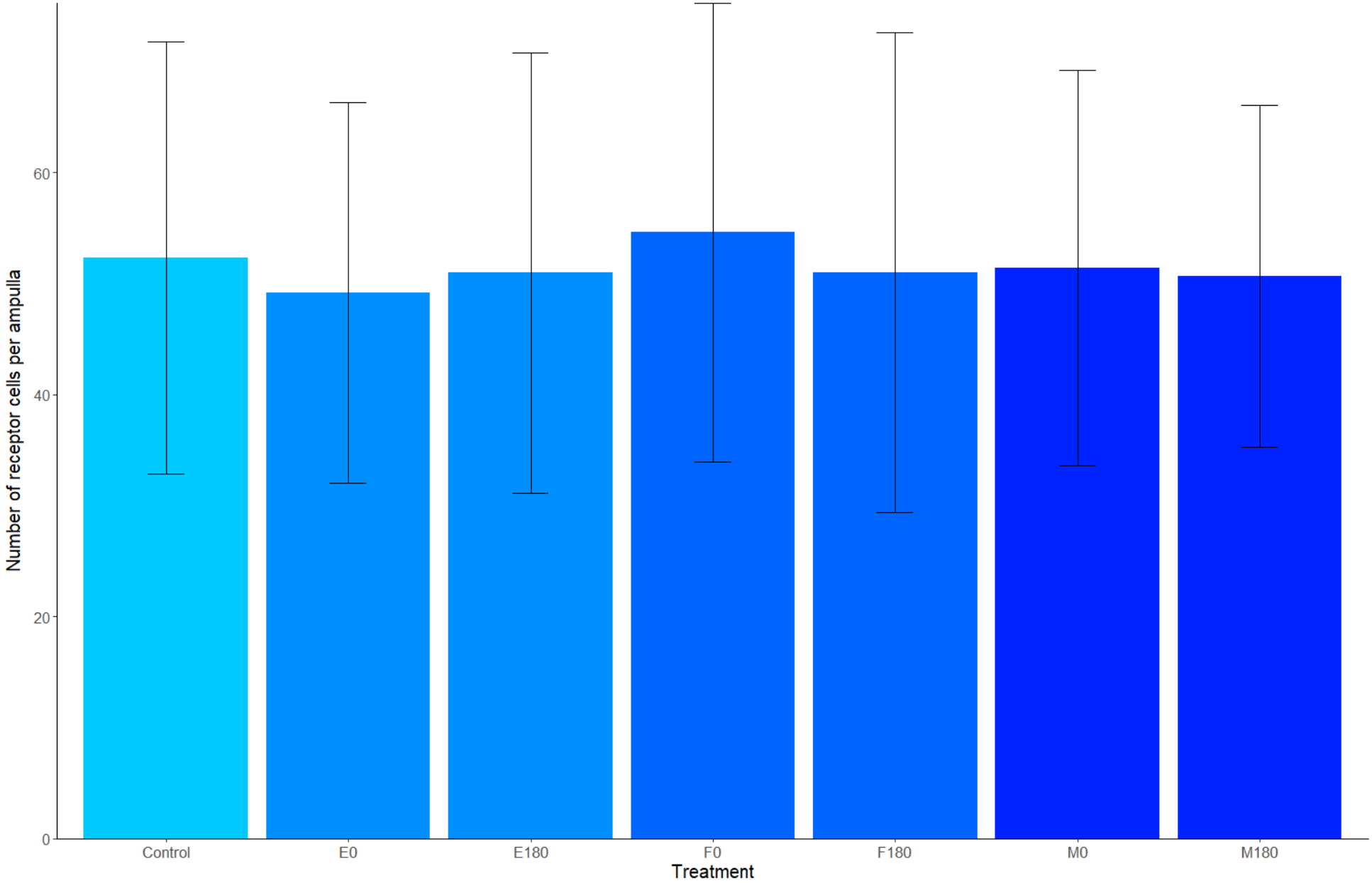

Figure 6.6. Bar graph comparing the mean standard deviation of the number of receptor cells per ampullae across treatments.

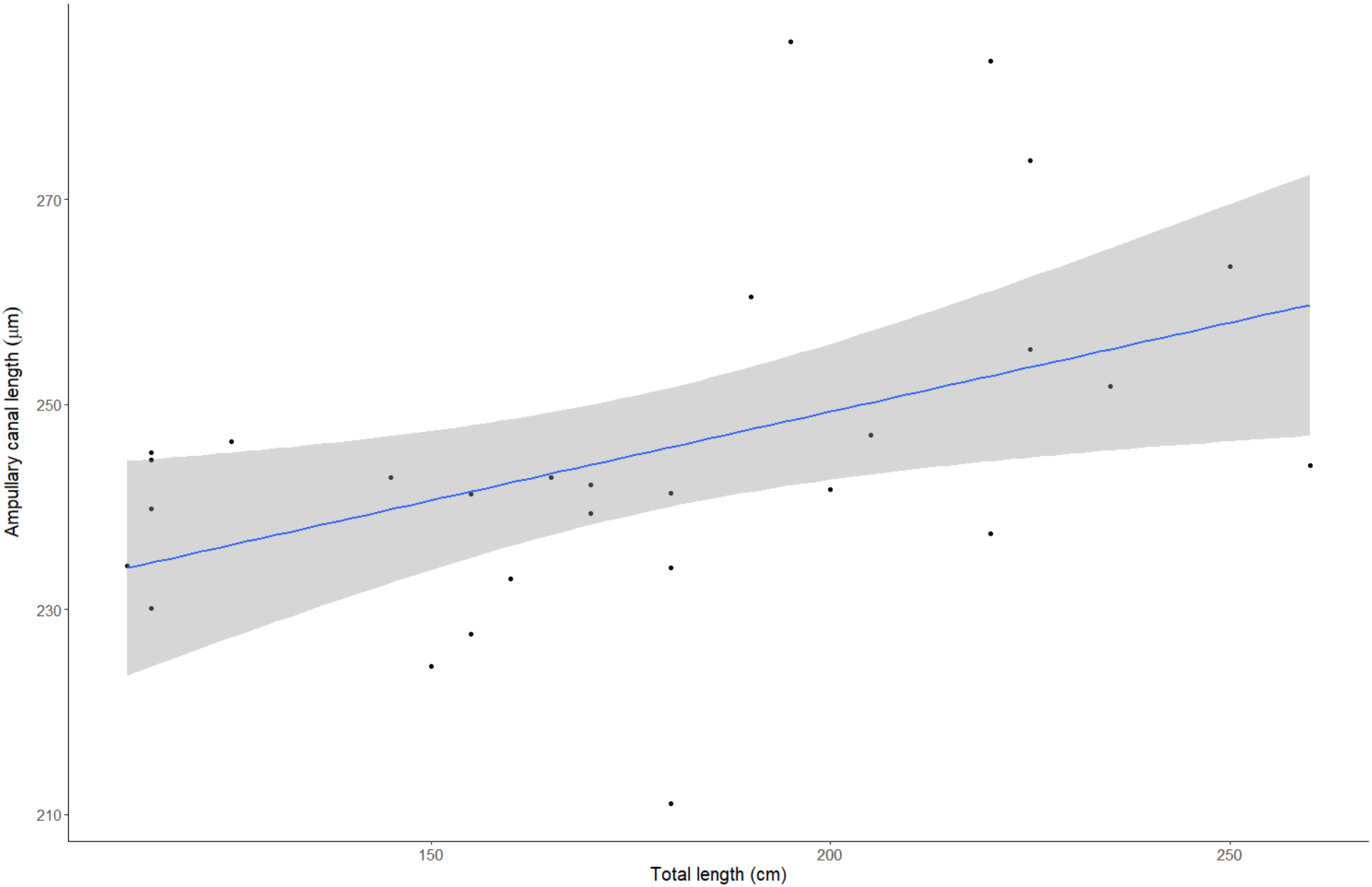

Figure 6.7A. Regression plot exposing the positive correlation between the total length of a catfish (in cm) and the length of its ampullary canals (in µm).

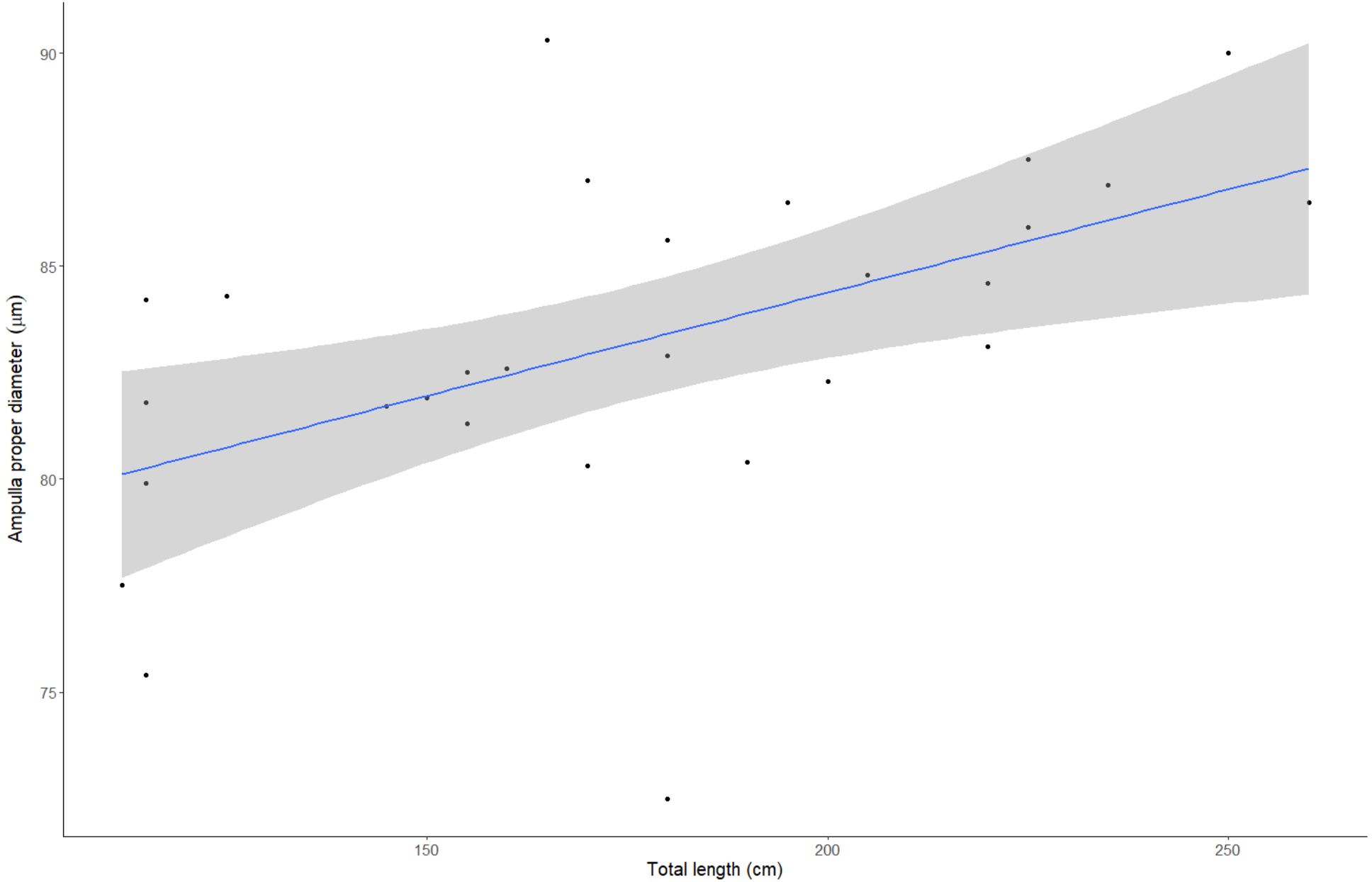

Figure 6.7B. Regression plot exposing the positive correlation between the total length of a catfish (in cm) and the diameter of its ampullae proper (in µm).

Discussion

The apparent lack of phenotypic plasticity in the morphology of the teleost ampullary organs provided by the results of this study was unexpected. The unchanged morphology, excluding the small scaling relationships for canal length and ampulla proper diameter, raises questions about what factors can affect the morphology of these sensory organs.

Differences were expected to be present between individuals from different treatments at the end of the experiment based on previous research on the morphology of the teleost ampullary organs of catfish from different salinities and the supposed propensity of this species to migrate (Herrick, 1901; Friedrish-Freksa 1930; Wachtel & Szamier, 1969; Jørgensen, 1992; Whitehead *et al*., 1999; 2000; 2015; Gauthier *et al*., 2015). For example, while macro-ampullae were never observed in marine *N. graeffei*, wild specimens from Moreton Bay did exhibit significantly longer ampullary canals, and more receptor cells per ampullae than their freshwater and estuarine conspecifics (Gauthier *et al*., 2015). Micro-ampullae were also observed in some *N. graeffei* individuals residing in fully freshwater areas (Whitehead *et al*., 2000). Neither of these forms of teleost ampullary organs were found in the specimens of this current study, and all ampullary organs were of the mini-ampullae type, with no significant morphological variation between them. However, the presence of both macro- and micro-ampullae in the estuarine *P. argyropleuron* suggests that salinity may not be the only factor affecting the morphology of a species' ampullary organs.

The movement ecology of *N. graeffei* in eastern Australia is little known. While studies on this species in the Clarence River in New South Wales found no differences in seasonal abundance, the author suggested that this species may undergo anadromous migrations in Queensland based on temporal variations in fish assemblages (Rimmer, 1985). However, more recent studies indicate that the movements of *N. graeffei* are spread over too wide a time-scale to be related to spawning events (Stuart & Berghuis, 2002; Stuart *et al*., 2007; Oughton, 2014). In addition to these reported movements, some freshwater populations of *N. graeffei* are land-locked, such as the one found in Lake Wivenhoe, which was the subject of a previous study of the electrosensory system of this species (Whitehead *et al*., 2000). There is a possibility that there was some misidentification of this species in previous studies as Ariidae catfish in south-east Queensland are generally identified through tooth morphology (Blaber *et al.*, 1994), and the distribution of this species over such a large area and different environments suggest that there could possibly be cryptic species. However,

to positively identify whether the different populations of *N. graeffei* in South East Queensland are effectively cryptic species, with their own form of ampullary organs, a proper genetic study should be undertaken. Unfortunately, no fin clips were collected during this or previous studies on this species.

The apparent absence of phenotypic plasticity, but presence of different forms of ampullary organs in wild caught *N. graeffei*, may indicate that the electrosensory system's morphology in silurids may only be influenced by salinity during early development, rather than changes during an individual's lifestyle. In the channel catfish, *Ictalurus nebulosus*, the development of the lateral line and, subsequently, of the electrosensory system occurs post-hatching, at around stage 43 of larval development (Northcutt, 2003). While there is no information about the ontogeny of these sensory systems in ariid catfish, we can expect them to develop at a similar stage. A follow up experiment involving raising catfish larvae immediately after hatching in different environmental conditions could shed light about whether salinity can affect the morphology of the electrosensory system at all, or whether it is restricted to inheritability.

While the area of the Brisbane River where the juvenile catfish were captured for this experiment is mainly freshwater, the river is still affected by the tide, and a saltwater wedge may reach the collection site during high tide, effectively exposing resident catfish to daily fluctuations in salinity (Yu *et al*., 2014). All the ampullary organs observed in this study closely resembled the mini-ampullae described in the freshwater and estuarine specimens of this species that were sampled in a different part of the Brisbane River that may have also been subject to daily fluctuations in salinity (Gauthier *et al*., 2015). While the length of the ampullary canals and width of the ampullae proper in the current study closely resemble those described for the freshwater specimens, the number of receptor cells per ampulla is very similar to that observed previously in estuarine individuals (Gauthier *et al*., 2015). Given the lack of morphological variation these mini-ampullae presumably work over a range of environmental salinities, that allows for a functional electroreceptive ability throughout the tidal cycle. The ampullary system may perform with optimal sensitivity only at a particular salinity, but of sufficient, albeit suboptimal sensitivity over other salinities that might be encountered in this euryhaline species.

The observation of budding ampullae confirm that new ampullary organs are still being formed by the specimens throughout the entire experiment. The morphology of these newly

formed ampullae is similar to those of already present electrosensory organs and does not appear to be affected by the new environmental conditions the fish live in. The variations observed in the measured characteristics of the ampullary organs for each fish may be a consequence of budding. The budding process observed here is identical to the one described in Gauthier *et al*. (2015) where ampullae grow larger, before dividing in two and creating a new sensory organ of a smaller than average size.

The regression analyses indicate that the body size may influence certain dimensions of their ampullary organs, with a positive correlation between L_T and the length of the ampullary canals and the diameter of ampullae proper. However, previous studies have suggested that longer ampullary canals are observed in individuals that originate from more saline conditions, as this creates a sufficient potential difference to detect the surrounding weak electric fields, and the size of the animal should not impact how long the canal has to be to detect that potential difference (Kalmijn, 1974). Larger ampullae proper typically have more receptor cells and are thought to be more sensitive than their smaller counterparts (Raschi, 1986). However, in this case, there is no significant increase in numbers of receptor cells per ampulla. The largest animal used in this study was only 26 cm, while the species grows to at least 60 cm L_T (Grant, 2008). Studying the ampullary organs of more and larger animals could help improve our understanding of any relationship between fish size and morphological features of their ampullary organs. Ideally, behavioural and physiological evaluation of teleost ampullary organ function at different salinities would accompany a scaling study.

Acknowledgments

I would like to thank the staff of the Moreton Bay Research Station for their help in housing and daily care of the fish, this experiment would not have been possible without them. I would also like to thank Takuhiro Yamada, Rodrigo Zorrilla, and Daniel Browne for their help in acquiring the juvenile catfish for the experiment.

Chapter VIII

Discussion

This Chapter is presented in several parts. First comes a synthesis of my studies on the ampullae of Lorenzini of sharks and rays. Second is a short speculative discussion of the experiment to test salinity-driven phenotypic plasticity in the ampullary organs of juvenile catfish. I then provide a brief comparison to other sensory systems, and ideas for future research.

I) Variation in the distribution and morphology of the electrosensory system of elasmobranchs

This thesis aims to further our understanding of the influence of habitat, lifestyle, and diet on the distribution, gross morphology, and ultrastructure of the elasmobranch electrosensory system. The distribution of the ampullary pores appears to be the main characteristic affected by these factors, whereas subtle differences in the gross morphology and ultrastructure of their ampullae of Lorenzini are most likely a consequence of other factors, such as phylogeny and size.

Variations in the distribution and counts of ampullary pores

Benthic rays generally have a very similar distribution of their ampullary pores among species, with a greater density of pores on the ventral surface than on the dorsal surface, especially around the mouth and the snout. These pores extend to parts of their pectoral fins and around the visceral cavity, and number around 1000 in the species investigated in this thesis. This pattern is consistent with previous descriptions of the distribution of ampullary pores in benthic rays (Jordan, 2008; Kempster *et al*., 2012; Camilieri-Asch *et al*., 2013). The bentho-pelagic eagle ray, *Aetobatus ocellatus*, has a similar number of ampullary pores, but these are distributed in a markedly different pattern. While there is still a much greater concentration of pores on their ventral surface, very few occur on the body, and none on the pectoral fins. Most of their ampullary pores are concentrated around the mouth and on the snout, more so than in benthic rays, a pattern also described in the bat ray *Myliobatis californica*. However, the complete absence of ampullary pores on the pectoral fins of *A. ocellatus* differs from observations in *M. californica* where some ampullary pores occur on the fins (Jordan, 2008). The continuous, large amplitude of an eagle ray's oscillatory swimming movement compared to the undulations of a benthic ray could explain the difference in distribution of the ampullary pores between these lifestyles, but the variations

in pore distribution between the two species of eagle rays challenges that explanation (Rosenberg, 2001). These predominantly ventral distributions of ampullary pores, with a concentration of ampullae around the feeding apparatus, are consistent with the biology of these species. Reliance on electroreception to detect prey during foraging is high, as prey may be buried in the substrate, but even if exposed, due to the ventral mouth and dorsally-located eyes, the rays are unable to see their prey at the time of ingestion.

The situation in selachimorphs is different, with the ampullary pores being restricted to the head, and none occurring on the body. The relatively small, demersal longtail carpet sharks, *Hemiscyllium ocellatum* and *Chiloscyllium punctatum* (family Hemiscyllidae) that inhabit similar environments and feed on similar prey, have the lowest mean number of ampullary pores encountered in this study (~430 and ~580, respectively). These pores are distributed in no discernible pattern around the head, but with a heavier concentration around the tip of the snout. Conversely, the ampullary pores of bentho-pelagic and pelagic sharks form distinct patterns around the head. In those species, the patterns are remarkably similar among congeners, despite some differences in their lifestyles and the range of environments in which they may be found. Overall, the distribution of ampullary pores appears to be more influenced by the biology of the fish, especially the dominance of other senses during predation, such as vision in the highly visual predator *Isurus oxyrinchus*. This species possesses fewer ampullary pores than the other pelagic species examined throughout this thesis (~830 vs ~1400-2000 for all Carcharhinidae and ~870 for the bentho-pelagic *Hemigaleus australiensis*), but still appear to rely on electroreception during foraging. *Isurus oxyrinchus* exhibits a peculiar “V” shaped pattern of ampullary pores on the dorsal surface of its head that is hypothesized to be used for prey detection immediately before striking the prey from below. This peculiar pattern has not been observed in any other species to date. *Galeocerdo cuvier*, on the other hand, has a much heavier concentration of ampullary pores on its ventral surface. Compared to *I. oxyrinchus*, *G. cuvier* is a slower swimmer, with a much more diverse diet that includes benthic prey and thus would benefit more from a higher resolution to electric fields situated below its head. The other species examined here tend to have a more even ventral to dorsal distribution, with more numerous ampullary pores, which appears to reflect their broader foraging repertoire. Contrary to previous studies, intraspecific variations were observed in the number of ampullary pores (Kempster *et al*., 2012). The one specimen of *Galeocerdo cuvier* examined had a much higher number of ampullary pores than was reported in previous studies, but may also have been a much larger specimen (Raschi, 1986; Cornett, 1986). Additionally, near-term embryos of

Carcharhinus falciformis had only half as many ampullary pores as their mother, indicating that this number is not fixed ontogenetically. However, Kempster *et al.* (2012) provided a robust examination of the number of ampullary pores in several specimens of four species of elasmobranchs, *Raja clavata*, *Mustelus asterias*, *Scyliorhinus stellaris*, and *Scyliorhinus canicular*, and found no evidence of intraspecific variations. Possibly, the number of ampullary pores may plateau during development, at a size that would differ interspecifically. The four species examined in the study by Kempster *et al*. (2012) are noticeably smaller than both *C. falciformis* and *G. cuvier*, which would likely impact the size at which that number of pores plateaus and could explain the presence of intraspecific variations in my examinations.

In most of the elasmobranchs I examined, the anterior ampullary pores were generally much smaller and more numerous than the pores located posterior to the eye socket. This pattern is consistent with the theory that the ampullary organs originating from different pore locations perform distinct functions (Tricas & New, 1998). The smaller, more numerous pores on the snout are typically associated with ampullary canals that run perpendicular to the skin and lead to ampullae used for the detection of prey (Tricas & New, 1998). On the other hand, canals originating from the posterior pores run parallel to the epidermis and are thought to be associated with the detection of uniform electric fields, such as those generated in relation to the Earth's geomagnetic fields (Tricas & New, 1998). The exception to this rule was the lack of size difference between the anterior and posterior pores in the two demersal sharks, *H. ocellatum* and *C. punctatum*, despite preserving a higher concentration of pores on the snout than posterior to the eyes. Neither of these two species is known to be migratory, potentially reducing the necessity of detecting uniform electric fields.

Variations in the shape of the ampullary canals

The quasi-sinusoidal shape of the ampullary canals initially encountered in benthic dasyatids was initially quite puzzling. These peculiar ampullary canals run parallel to the epidermis, and are located on both the dorsal and ventral surface of *Aetobatus ocellatus*, suggesting that their function is unlikely to be related to feeding. The quasi-sinusoidal shape suggests a sort of electrical filter, but further work is required to determine of what type. The presence of these canals in *H. ocellatum* indicates that this feature is not restricted to batoids; however, its absence in *C. punctatum* means that it is not characteristic of the family. These

quasi-sinusoidal ampullary canals were alluded to in a previous study by Chu & Wen (1979) but had not been mentioned in any other published work since. The individuals I examined are unlikely to be the only ones with those peculiar canals and identifying the range of species in which they occur would assist in identifying their potential function.

Interestingly, despite the differences in its shape, the ampullary canal wall is very similar in both sharks and rays, being only two cells thick and adjoined by tight junctions with underlying desmosomes. This structure is consistent among all the species I examined, but also all elasmobranchs studied previously (Waltmann, 1966; Whitehead, 2002b; Jørgensen, 2005, Whitehead *et al*., 2015a).

Gross morphology of the ampullae proper

The two types of ampullae proper identified in the elasmobranchs examined in this study are the alveolar types, present in all batoids, and the lobular types observed in all selachimorphs. While the lobular type of ampullary organs is quite widespread, the alveolar type appears to be less frequent (Jørgensen, 2005). I identified these alveolar ampullae through confocal microscopy, which allowed for a clear view of the duct connecting each sensory chamber to the main canal, a technique that has not been used for this purpose in any other published study. There may have been some misidentification, or lack of identification, in previous work, that could impact the frequency of occurrence of this type of ampullary organ. The specimens of *Hemitrygon fluviorum* I examined had a W_D of about 60 cm, with ampullae typically exceeding 700 µm in average diameter. On the other hand, the smaller coastal species of sharks used in this study, *Carcharhinus cautus*, *C. limbatus*, *C. tilstoni*, and *Hemigaleus australiensis* were about 80 cm L_T and their lobular ampullae were typically under 700 µm in average diameter. Larger ampullae typically possess more receptor cells, and thus could be more sensitive to weak electric fields (Raschi, 1986). However, there appears to be little variations in the minimum electrosensory response threshold between sharks and rays (Kajiura & Holland, 2002; Kajiura, 2003; Jordan *et al*., 2009). Any possible differences in sensitivity between the two types of ampullae, if present, do not appear to relate to prey selection, as the diet of batoids consists predominantly of buried prey (Pardo *et al*., 2015). Both *H. ocellatum* and *C. punctatum* also feed largely on buried prey (Heupel & Bennett, 1998), and these two species possess lobular ampullae, with a size consistent with the ampullary organs observed in other selachimorphs.

In both alveolar and lobular ampullae, the primary difference between species of each superorder was the number of sensory chambers per ampulla. This quantity is not a fixed value, and some variations can be observed among conspecifics, there were 5-6 chambers per ampulla in the smaller species of both sharks and rays, while there were up to 8 chambers for the larger species. This increase in quantity of sensory chambers per ampullae in usually correlated with an increase in size of the ampullae proper as well. The ampullae proper of the euryhaline *H. fluviorum* also had more sensory chambers than the marine *M. toshi* and *N. trigonoides*. Contrary to what was initially hypothesized, this difference is unlikely to be a consequence of the size difference between specimens, the embryos of *Carcharhinus falciformis* both possess ampullae with 6-8 sensory chambers, the same range that was found in the adult *C. falciformis*.

Adult *C. falciformis* also exhibit the largest ampullae proper recorded during this thesis, despite not being the largest specimen examined (212 cm L_T *vs* 348 cm L_T for *Galeocerdo cuvier*). Not only does this raise the question as to why an oceanic, pelagic species would require such sensitive ampullae, it also indicates that ampullae of the same type not only scale with the size of the animal, but also that their gross morphology is species dependent. The electric fields generated by teleosts vary interspecifically but there appears to be no relationship between the mass and length of an animal and its electric potential (Bedore & Kajiura, 2013). Investigating the bioelectric fields produced by the preferred prey of *C. falciformis* could provide an insight into why they have such large ampullae proper.

Ultrastructure of the sensory epithelium

The most salient difference in the structure of the sensory epithelium occurs between batoids and selachimorphs. Apically nucleated supportive cells protruding heavily into the lumen were present in all the rays examined but not in any of the sharks. This was interesting but once again does not appear to be linked to a particular lifestyle, diet, or habitat. The function for this peculiar morphology of the supportive cells remains obscure.

The receptor cells of most species of both batoids and selacimorphs are similar in shape and structure to previous descriptions, with generally rounded, pear-shaped receptor cells with a central round nucleus, a single kinocilium extending from the apex of the cell and into the ampullary lumen, and a neural terminal at the base of the cell. However, while the sensory epithelium of both *H. ocellatum* and *C. punctatum* seems to be of similar

composition to other sharks, it appears to be somewhat flattened when compared to other elasmobranchs. The functional role, if any, of this peculiar morphology of the sensory epithelium observed in these two species is unknown.

Diet

Whether the preferred type of prey of a species could affect the ultrastructure of their ampullary organs was one of the main factors investigated throughout this thesis. This aspect was primarily investigated in the three sympatric benthic rays examined in Chapter II, with documented differences in diet (Pardo *et al*., 2015). There were no variations between the ultrastructure of the ampullae of these three species that could reasonably be attributed to their differences in diet. This aspect was also confirmed in sharks; most of the Carcharhinidae investigated generally possess a preference for teleosts (Stevens, 1984), as opposed to the clear preference for cephalopods in *Hemigaleus australiensis* (Taylor *et al*., 2008), which exhibited ampullae of Lorenzini that are morphologically indistinguishable from those of other sharks.

Lifestyle & habitat

Coastal elasmobranchs live in an electrically noisier environment than oceanic species and would likely benefit from adaptations that act to filter out extraneous electrical noise (Kalmijn, 1974); while benthic species feeding on buried prey tend to be more reliant on electroreception and may be advantaged by larger, more sensitive ampullae to accurately pinpoint the position of their prey. However, none of my findings indicate that such factors influence either the morphology or the ultrastructure of the ampullae of Lorenzini in these elasmobranchs.

Conclusion

This study confirms that the distribution of ampullary pores in elasmobranch is affected by the environment and lifestyle of a species. However, the few observed variations in the ultrastructure of the ampullae of Lorenzini between the different species of chondrichthyans examined in this thesis are unlikely to be a consequence of their differences in diet, lifestyle, or environment.

II) Lack of phenotypic plasticity in the teleost ampullary organs of *Neoarius graeffei*

The second aspect of this thesis was to investigate whether the teleost ampullary organs of juvenile *Neoarius graeffei* raised in different salinities had the ability to undergo phenotypic plasticity. The teleost ampullary organs of this species were previously observed to possess different morphologies in habitats that differed in salinity from which wild specimens were captured (Gauthier *et al*., 2015). However, there was no concrete evidence that the electrosensory system of *N. graeffei* could adapt to new environmental conditions when raised at different salinities in a laboratory setting.

The absence of detectable morphological variations, at least at the level of this experiment, in the electrosensory system of *N. graeffei* specimens raised under different environmental conditions was unexpected. The presence of budding ampullae in individuals throughout the duration of the experiment indicates that new ampullae were being formed, but not of the morphology that was expected for the conductivity of the environment in which they were being reared. These results indicate that the ampullary organs of this species of catfish are unlikely to adapt to their new environmental conditions as they migrate through different environments. This could potentially mean that the mini-ampullae observed in this species are able to work for both marine and freshwater environments, thus not requiring adaptations during their migrations. While this intermediate form of ampullary organs may not work optimally in either environment, the costs of phenotypic plasticity may be too high for too small of a benefit (DeWitt *et al*., 1998; Murren *et al*., 2015). This explanation also fits well with the environmental conditions encountered in the Brisbane River, where daily tidal fluctuations occur, bringing a layer of saltwater up into freshwater areas of the river (Yu *et al*., 2014). Another avenue to consider is whether the environmental conditions during ontogeny could influence the morphology of their teleost ampullary organs. In another species of catfish, *Ictalurus nebulosus*, the electrosensory system appears from stage 43 of development (Northcutt, 2003); while *N. graeffei* may not be able to adapt to new environmental conditions during its lifetime, they may have influenced its electrosensory system during development.

III) Comparison with other sensory systems

Interestingly, the gross morphology and ultrastructure of electroreceptive ampullary organs appear to be remarkably well conserved interspecifically when compared to other sensory organs. In the introduction, I provided a brief description of a select few sensory systems in fishes, including how their respective sensory organs vary in structure in accordance with variations in their behaviour or environmental conditions. For example, the visual system may undergo daily, or seasonal structural changes to accommodate variations in light conditions, with a similar phenomenon observed in the olfactory system with the presence of a higher concentration of crypt cells during the mating seasons (Loew & Dartnall, 1976; Burnside *et al*., 1983; Hamdani *et al*., 2008). There are no comparable variations occurring in the structure of the ampullae of Lorenzini of elasmobranchs. While the structural differences in the supportive cells of batoids appear rather peculiar, their functional role, if any, remains obscure. The variations in the shape of the ampullary canals are reminiscent of the different canal morphologies of the mechano-sensory lateral line, but their functions remain uncertain.

The occurrence of so few structural variations in the electrosensory system of species inhabiting different habitats, or with different behaviours, indicate that the structure of the electrosensory system may be considered optimal under a wide range of different conditions.

IV) Future directions

Elasmobranchs

Unfortunately, I had no access to any deep-water species of elasmobranchs during this thesis. Deep-dwelling species are thought to utilise their electrosensory system more than shallow water elasmobranchs to compensate for the lack of light, and deep-water skates were shown to possess more sensory chambers than shallow water species (Raschi, 1986). Any deep-water species, including chimaeras, would have been very interesting to examine and to compare with both coastal and pelagic species. A comparison between two closely related skates, the deep-dwelling New-Zealand rough skate, *Zearaja nasuta*, and the maugean skate, *Zearaja maugeana*, that occurs only in shallow, tannin-rich waters, could reveal whether these environmental conditions can affect the structure of their electrosensory system.

While the function, if any, of the apically nucleated supportive cells in batoids would be quite difficult to test, the occurrence of quasi-sinusoidal canals in *H. ocellatum* but not in *C. punctatum* offers an interesting avenue of research. These two species are quite common, hardy species that can easily be kept in aquaria, are relatively closely related, and possess a similar foraging strategy. They would be ideal to run a comparative behavioural experiment and investigate any variations in their responses, or sensitivity to electric fields of different strengths. Electrical engineers were consulted and suggested that this peculiar shape appears to be a form of electrical filter. Investigating the structure, exact shape, dielectric properties and dimensions of the ampullary canal would allow creation of a model of the ampullary organ and obtain a more accurate idea of the function.

A comparison of the chemical composition of the mucopolysaccharide gel inside the ampullary canal may also be helpful. This mucopolysaccharide was the main source of problems during the processing steps of the ampullae for both SEM and TEM work and caused many delays. The gel of the larger pelagic sharks reacted quite differently to the processing compared to that of the smaller species or rays; either hardening, which prevented sectioning, or completely preventing EPON resin infiltration, leading to poor quality ultramicrotome sections.

Finally, a behavioural study comparing the sensitivity and resolution of the ampullae of Lorenzini between juvenile and adult specimens of the same species would be extremely beneficial in identifying how the variations observed in the gross morphology of the ampullary organs between specimens of different sizes could affect them. The embryonic *Carcharhinus falciformis* exhibit half the number of ampullary pores than the adult, that are twice as densely packed, but much smaller in diameter. The associated ampullary organs have a similar number of sensory chambers and ultrastructure, but, in the embryos, are about a third of the size of those of the adult. These ontogenetic variations offer an interesting situation to test how the sensitivity of the electrosensory system of a species may change with growth, and whether the more numerous, but less densely packed ampullary pores on the snout of an animal offer the same resolution in adults as it does in juveniles.

Siluriforms

The presence of different forms of ampullary organs in wild *Neoarius graeffei* despite the apparent lack of phenotypic plasticity in the morphology of their electrosensory system raises many questions about what factors affect the shape of their ampullary organs, and at what time during development these factors are influential. The animals used in the plasticity experiment were juveniles but already had a fully formed and functional electrosensory system. To be able to identify whether the environmental conditions at the time of development of the ampullary organs can affect the shape of the electrosensory system, a different version of the experimental set up used in this study could be performed. Instead of collecting juveniles from one environment, breeding adult specimens from different environments (freshwater, estuarine, marine) could be collected, and acclimated to the same environmental condition used in the phenotypic plasticity experiment. Keeping the adults (and their future offspring) separated as to not mix individuals that originated from different environments, this set up would result in nine treatment tanks, three for each salinity. Comparing the gross morphology of the electrosensory system of the resulting juvenile fish to specimens from every other treatment and to their parents would give a much better indication of whether the morphological variations observed in wild specimens that originate from different environments are a consequence of the environmental conditions at the time of the development of the electrosensory system, or is inherited by their progenitor. Another important aspect to test would be the sensitivity and effectiveness of the mini-ampullae observed in every specimens of *N. graeffei* examined in this thesis. These mini-ampullae are hypothesized to be able to function in different environments of varying

salinities, which could explain the lack of phenotypic plasticity as individuals migrate to different areas. Testing the behavioural responses of *N. graeffei* to a similar electrical stimulus but in environments of different salinities could reveal whether this type of ampullary organ can function in all of them. Should the results be positive, a secondary experiment could be run on the sensitivity of these ampullary organs in different environments to identify whether they function more efficiently in certain conditions or not.

V) Conclusion

Throughout this thesis, I confirmed that the distribution of the ampullary pores in elasmobranchs could be affected by their environment and lifestyle, and, just like the gross morphology of the ampullae proper, could be ontogenetically variable. I discovered previously undocumented structural features of the ampullae proper of rays and benthic sharks, but found no evidence that these discoveries were a consequence of an animal's lifestyle, environment, or diet. While these results highlight the effectiveness of the cellular structure of the ampullae of Lorenzini, they also raise questions about what could have induced those variations observed in certain species and emphasize the importance of future research in field to elucidate those questions.

The lack of observable phenotypic plasticity in teleost ampullary organs in a euryhaline catfish challenges the hypothesis that 'environmental salinity may influence morphology'. These results open up new avenues of research in order to better understand the effects that surrounding environmental conditions can have on the shape and sensitivity of a species' electrosensory system.

Bibliography

Aadland, C.R. (1992). Anatomical observation and description of the ampullae of Lorenzini in the shortfin mako shark *Isurus oxyrinchus*. MSc thesis, Bucknell University, 51 pp.

Albert, J. S., and Crampton, W.G.R. (2005). Electroreception and electrogenesis. In*: The Physiology of Fishes* 3rd Edition (Evans, D.H., Claiborne, J.B., eds.), pp. 431-472. Boca Raton: Taylor & Francis.

Andres, K.H., and von Düring, M. (1988). Comparative anatomy of vertebrate electroreceptors. *Progress in Brain Research* **74**, 113-131.

Andres, K.H., von Düring, M., Iggo, A., Proske, U. (1991). The anatomy and fine structure of the echidna *Tachyglossus aculeatus* snout with respect to its different trigeminal sensory receptors including the electroreceptors. *Anatomy and Embryology* **184,** 371-393.

Bastian, J. (1986). Electrolocation: behavior, anatomy, and physiology. In *Electroreception* (Bullock, T.H., Heiligenberg, W., eds.), pp. 577-612. Chichester, New York, Brisbane, Toronto, Singapore: John Wiley & Sons.

Bauer, R., Denizot, J.P. (1972). Sur la presence et la repartition des organs ampullaires chez *Plotosus anguillaris*. *Archives d'Anatomie Microscopique* **61,** 85-90.

Bedore, C.N., Kajiura, S.M. (2013). Bioelectric Fields of Marine Organisms: Voltage and Frequency Contributions to Detectability by Electroreceptive Predators. *Physiological and Biochemical Zoology* **86**, 298-311.

Blaber, S.J.M., Brewer D.T., Salini, J.P. (1994). Diet and dentition in tropical ariid catfishes from Australia. *Environmental Biology of Fishes* **40**, 159-174.

Bleckmann, H., Hofmann, M.H. (1999). Special senses. In *Sharks*, *Skates and Rays: The Biology of Elasmobranch Fishes* (Hamlett, W.C., ed.), pp. 300-328. Baltimore: Johns Hopkins University Press.

Bleckmman, H., and Zelick, R. (2009). Lateral line system of fish. *Integrative Zoology* **4**, 13-25.

Blonder, B.I., and Alevizon, W.S. (1988). Prey discrimination and electroreception in the stingray *Dasyatis sabina*. *Copeia* **1988**, 33-36.

Bodznick, D., Montgomery, J., Tricas, T.C. (2003). Electroreception: extracting behaviorally important signals from noise. In *Sensory Processing in Aquatic Environments* (Collin, S.P., Marshall, N.J., eds.), pp. 389-403. New York, Berlin, Heidelberg, Hong Kong, London, Milan, Paris, Tokyo: Springer.

Bodznick, D., Montgomery, J. (2005). The physiology of low-frequency electrosensory systems. In *Electroreception* (Bullock, T.H., Hopkins, C.D., Popper, A.N., Fay, R.R., eds.), pp. 132-153. New York, Berlin, Heidelberg, Hong Kong, London, Milan, Paris, Tokyo: Springer.

Bonfil, R. (2008). The biology and ecology of the silky shark, *Carcharhinus falciformis*. In *Sharks of the Open Ocean: Biology*, *Fisheries and Conservation* (Camhi, M., Pikitch, E. K., Babcock, E. A., eds.), pp. 114-127. Blackwell Science.

Bretschneider, F., Peters, R.C. (1992). Transduction and transmission in ampullary electroreceptors of catfish. *Comparative Biochemistry and Physiology* **103,** 245-252.

Brown, B.R., Hughes, M.E., Russo, C. (2005). Infrastructure in the electric sense: Admittance data from shark hydrogels. *Journal of Comparative Physiology A* **191**, 115–123.

Bullock, T.H. (1973). Seeing the world through a new sense: electroreception in fish. *American Scientist* **61**, 316-325.

Bullock, T.H. (1982). Electroreception. *Annual Review of Neuroscience* **5**, 121-170.

Burnside, B., Adler, A., O'Connor, P. (1983). Retinomotor pigment migration in the teleost retinal pigment epithelium. 1. Roles for actin and microtubules in pigment granule transport and cone movement. *Investigative Ophthalmology & Visual Science* **24**, 1-15.

Camilieri-Asch, V., Kempster, R.M., Collin, S.P., Johnstone, R.W., Theiss, S.M. (2013). A comparison of the electrosensory morphology of a euryhaline and a marine stingray. *Zoology* **116**, 270-276.

Chu, Y.T., and Wen, M.C. (1979). *Monograph of Fishes of China (2): A Study of the Lateral Line Canals System and that of Lorenzini Ampullae and Tubules of Elasmobranchiate Fishes of China*. 204p. Shanghai: Science and Technology Press.

Collin, S.P., and Whitehead, D.L. (2004). The functional roles of electroreception in non-electric fishes. *Animal Biology* **54**, 1-25.

Collin, S.P., Kempster, R.M., Yopak, K.E. (2015). How elasmobranchs sense their environment. In *Physiology of elasmobranch fishes: structure and interaction with environment* (Shadwick, R.E., Farrell, A.P., Brauner, C.J., eds.), pp. 19-99. New York: Elsevier.

Coombs, S., Janssen, J., Webb, J.F. (1988). Diversity of lateral line systems: evolutionary and functional considerations. In *Sensory biology of aquatic animals* (Atema, J., Fay, R.R., Popper, A.N., Tavolga, W.N., eds.), pp. 553-593. New-York, Berlin, Heidelberg, London, Paris, Tokyo: Springer-Verlag.

Coombs, S., and Montgomery, J.C. (1999). The enigmatic lateral line system. In *Comparative hearing: fish and amphibians* (Fay, R.R., and Popper, A.N., eds.), pp. 319-362. New-York: Springer.

Coombs, S., and Braun, C.B. (2003). Information processing by the lateral line system. In *Sensory Processing in Aquatic Environments* (Collin, S.P., Marshall, N.J., eds.), pp. 122-138. New York, Berlin, Heidelberg, Hong Kong, London, Milan, Paris, Tokyo: Springer.

Cornett, A. (2006) Ecomorphology of shark electroreceptors. MS thesis, Florida Atlantic University, Boca Raton, FL. 111p.

Corwin, J.T. (1981). Morphology of the macula neglecta in sharks of the genus *Carcharhinus*. *Journal of Morphology* **152**, 341-362.

Crooks, N., and Waring, C.P. (2013). A study into the sexual dimorphisms of the ampullae of Lorenzini in the lesser-spotted catshark, *Scyliorhinus canicula* (Linnaeus, 1758). *Environmental Biology of Fishes* **96,** 585-590.

Czech-Damal, N.U., Liebschner, A., Miersch, L., Klauer, G., Hanke, F.D., Marshall, C., Dehnhardt, G., Hanke, W. (2012). Electroreception in the Guiana dolphin (*Sotalia guianensis*). *Proceedings of the Royal Society of London B* **279**, 663-668.

Daddow, L.Y.M. (1986). An abbreviated method of the double lead stain technique. *Journal of Submicroscopic Cytology* **18**, 221-224.

Denton, E.J., and Gray, J.A.B. (1988). Mechanical factors in the excitation of the lateral line of fishes. In *Sensory biology of aquatic animals* (Atema, J., Fay, R.R., Popper, A.N., Tavolga, W.N., eds.), pp. 595-617. New-York, Berlin, Heidelberg, London, Paris, Tokyo: Springer-Verlag.

Denton, E.J., and Gray, J.A.B. (1989). Some observations on the forces acting on neuromasts in fish lateral line canals. In *Neurobiology and evolution of the lateral line system* (Coombs, S., Gomer, P., Munz, H., eds.), pp. 229-246. New-York: Springer-Verlag.

DeWitt, T.J., Sih, A., Wilson, D.S. (1998). Costs and limits of phenotypic plasticity. *Trends in Ecology & Evolution* **13**, 77-81.

Dijkgraaf, S., and Kalmijn, A.J. (1962). Nerhaltensversuche zur function der lorenzinischen ampyllen. *Naturwissenschaften* **49**, 400.

Dijkgraaf, S. (1963). The functioning and significance of the lateral line organs. *Biological reviews* **38**, 51-106.

Dijkgraaf, S. (1964). Electroreception and the ampullae of Lorenzini in elasmobranchs. *Nature* **201,** 523.

Doyle, J. (1967). The ‘Lorenzan sulphates’. *Biochemical Journal* **103**, 325-330.

Dye, J.C., and Meyer, J.H. (1986). Central control of the electric organ discharge in weakly electric fish. In *Electroreception* (Bullock, T.H., Heiligenberg, W., eds.), pp. 71-102. Chichester, New York, Brisbane, Toronto, Singapore: John Wiley & Sons.

Egeberg, C.A., Kempster, R.M., Theiss, S.M., Hart, N.S., Collin, S.P. (2014). The distribution and abundance of electrosensory pores in two benthic sharks: a comparison of the wobbegong shark, *Orectolobus maculatus*, and the angel shark, *Squatina australis*. *Marine and Freshwater Research* **65,** 1003-1008.

Evangelista, C., Mills, M., Siebeck, U. E., Collin, S. P. (2010). A comparison of the external morphology of the membranous inner ear in elasmobranchs. *Journal of Morphology* **271**, 483-495.

Evans, B.I. (2004). A fish's eye view of habitat change. In *The senses of fish: adaptations for the reception of natural stimuli* (von der Emde, G., Mogdans, J., Kapoor, B.G., eds.), pp. 1-30. Springer Netherlands: Springer Science & Business Media.

Evans, B.I., and Fernald, R.D. (1990). Metamorphosis and fish vision. *Journal of Neurobiology* **21**, 1037-1052.

Fay, R.R., and Popper, A.N. (1975). Modes of stimulation of the teleost ear. *Journal of Experimental Biology* **62**, 379-387

Ferrando, S., Bottaro, M., Gallus, L., Giosi, L., Vacchi, M., Tagliafierro, G. (2006). Observations of crypt neuron-like cells in the olfactory epithelium of a cartilaginous fish. *Neuroscience Letters* **403**, 280-282.

Filer, J.L., Booker, C.G., Sims, D.W. (2008). Effects of environment on electric field detection by small spotted catshark *Scyliorhinus canicula*. *Journal of Fish Biology* **72**, 1450-1462.

Fishelson, L., and Baranes, A. (1998). Distribution, morphology, and cytology of ampullae of Lorenzini in the Oman shark, *Iago omanensis* (Triakidae), from the Gulf of Aqaba, Red Sea. *The Anatomical Record* **251**, 417-430.

Friedrich-Freksa, V.H. (1930). Lorenzini*sch*e ampullen be idem siluroiden *Plotosus anguillaris* bloch*. Zoologischer Anzeiger* **87,**49-66.

Gardiner, J.M., Atema, J., Hueter, R.E., Motta, P.J. (2014). Multisensory integration and behavioural plasticity in sharks from different ecological niches. *Plos One* **9**, e93036.

Gauthier, A.R.G., Whitehead, D.L., Bennett, M.B., Tibbetts, I.R. (2015). Morphology of the teleost ampullary organs in marine salmontail catfish *Neoarius graeffei* (Pisces: Ariidae) with comparative analysis to freshwater and estuarine conspecifics. *Journal of Morphology* **276**, 1047-1054.

Gauthier, A.R.G., Whitehead, D.L., Tibbetts, I.R., Cribb, B.W., Bennett, M.B. (2018). Morphological comparison of the ampullae of Lorenzini of three sympatric benthic rays. *Journal of Fish Biology* **92**, 504-514.

Grant, E. (2008). Grant's Guide to Fishes. 880p. Brisbane: EM Grant Pty Limited.

Gregory, J.E., Iggo, A., McIntyre, A.K., Proske, U. (1988). Receptors in the bill of the platypus. *The Journal of Physiology* **400**,349-366.

Gruber, S. H., Gulley, R. L. and Brandon, J. (1975). Duplex retina in seven elasmobranch species. *Bulletin of Marine Science* **25**, 353-358.

Gruber, S.H., and Cohen, J.L. (1985). Visual system of the white shark, *Carcharhodon Carcharias*, with emphasis on retinal structure. *Memoirs of the California Academy of Science* **9**, 61-72.

Hamdani, E.H., Lastein, S., Gregersen, F., Døving, K.B. (2008). Seasonal variations in olfactory sensory neurons – fish sensitivity to sex pheromones explained? *Chemical Senses* **33**, 119-123.

Hansen, A., Eller, P., Finger, T.E., Zeiske, E. (1997). The crypt cell: a microvillous ciliated olfactory receptor cell in teleost fishes. *Chemical Senses* **22**, 694-695.

Hart, N. S., Lisney, T. J., Marshall, N. J., Collin, S. P. (2004). Multiple cone visual pigments and the potential for trichromatic colour vision in two species of elasmobranch. *Journal of Experimental Biology* **207**, 4587-4594.

Herrick, C.J. (1901). The cranial nerves and cutaneous sense organs of the North American Siluroid fishes. *Journal of Comparative Neurology* **11**, 177-254.

Heupel, M.R., and Bennett, M.B. (1998). Observations on the diet and feeding habits of the epaulette shark, *Hemiscyllium ocellatum* (Bonnaterre), on Heron Island Reef, Great Barrier Reef. *Australian Marine and Freshwater Research* **49**, 753-756.

Hopkins, CdD. (2014). Electroreception. In Encyclopedia Britannica: http://www.britannica.com/science/electroreception.

Howland, H. C., and Masci, J. (1973). The phylogenetic allometry of the semicircular canals of small fishes. *Zeitschrift für Morphologie und Ökologie der Tiere* **75**, 283-296.

Hueter, R.E., Mann, D.A., Maruska, K.P., Sisneros, J.A., Demski, L.S. (2004). Sensory biology of elasmobranchs. In *Biology of sharks and their relative* (Carrier, J.C., Musick, J.A., Heithaus, M.R., eds.), pp. 325-368. CRC Press: Boca Raton.

Jacobsen, I.P., and Bennett, M.B. (2010). Age and growth of *Neotrygon picta*, *Neotrygon annotata* and *Neotrygon kuhlii* from north-east Australia, with notes on their reproductive biology. *Journal of Fish Biology* **77**, 2405-2422.

Jacobsen, I.P., and Bennett, M.B. (2012). Feeding ecology and dietary comparison among three sympatric *Neotrygon* (Myliobatoidei: Dasyatidae) species. *Journal of Fish Biology* **80**, 1580-1594.

Janssen, J., Coombs, S., Hoekstra, D., Platt, C. (1987). Anatomy and differential growth of the lateral line system of the mottled sculpin, *Cotus bairdi* (Scorpaeniformes: Cottidae). *Brain, Behavior and Evolution* **30**, 210-229.

Janssen, J. (2004). Lateral line sensory ecology. In *The senses of fish: adaptations for the reception of natural stimuli* (von der Emde, G., Mogdans, J., Kapoor, B.G., eds.), pp. 231-264. Springer Netherlands: Springer Science & Business Media.

Jones, G. M., and Spells, K. E. (1963). A theoretical and comparative study of the functional dependence of the semicircular canal upon its physical dimensions. *Proceedings of the Royal Society of London B* **157**, 403-419.

Jordan, L.K. (2008). Comparative morphology of stingray lateral line canal and electrosensory systems. *Journal of Morphology* **269**, 1325-1339.

Jordan, L.K., Kajiura, S.M., Gordon, M.S. (2009). Functional consequences of structural differences in stingray sensory systems. Part II: electrosensory system. *Journal of Experimental Biology* **212,** 3044-3050.

Jordan, L.K., Mandelman, J.W., Kajiura, S.M. (2011). Behavioral responses to weak electric fields and a lanthanide metal in two shark species. *Journal of Experimental Marine Biology and Ecology* **409**, 345–350.

Jørgensen, J.M. (1992). The electrosensory cells of the ampullary organ of the transparent catfish (*Kryptopterus bicirrhus*). *Acta Zoologica* **73**, 79-83.

Jørgensen, J.M. (2005). Morphology of electroreceptive sensory organs. In *Electroreception* (Bullock, T.H., Hopkins, C.D., Popper, A.N., Fay, R.R., eds.), pp. 47-67. New York, Berlin, Heidelberg, Hong Kong, London, Milan, Paris, Tokyo: Springer.

Josberger, E.E., Hassanzadeh, P., Deng, Y., Sohn, J., Rego, M.J., Amemiya, C.T., Rolandi, M. (2016). Proton conductivity in ampullae of Lorenzini jelly. *Sciences Advances* **13**, e1600112.

Kajiura, S.M., and Holland, K.N. (2002). Electroreception in juvenile scalloped hammerhead and sandbar sharks. *Journal of Experimental Biology* **205**, 3609-3621.

Kajiura, S.M. (2003). Electroreception in neonatal bonnethead sharks, *Sphyrna tiburo*. *Marine Biology* **143,** 603-611.

Kalmijn, A.J. (1966). Electro-perception in sharks and rays. *Nature* ***212***, *1232-1233.*

Kalmijn, A.J. (1971). The electric sense of sharks and rays. *Journal of Experimental Biology* **55**, 371-383.

Kalmijn, A.J. (1972). Bioelectric fields in sea water and the function of the ampullae of Lorenzini in elasmobranch fishes. *SIO Reference*, *Scripps Institution of Oceanography*, *UC San Diego.*

Kalmijn, A.J. (1973). Electro-orientation in sharks and rays: theory and experimental evidence. Oceanography SIo, editor. United States. Office of Naval Research: National Technical Information Service, US Dept. of Commerce.

Kalmijn, A.J. (1974). The detection of electric fields from inanimate and animate sources other than electric organs. In *Handbook of Sensory Physiology* (Fessard, A., ed.), pp. 147-200. Berlin: Springer-Verlag Berlin.

Kalmijn, A.J. (1978). Electric and magnetic sensory world of sharks, skates, and rays. In *Sensory Biology of Sharks*, *Skates*, *and Rays* (Hodgson, E.S., Mathewson, R.F., eds.), pp. 507-528. Arlington: Naval Research Department.

Kalmijn, A.J. (1982). Electric and magnetic field detection in elasmobranch fishes. *Science* **218**, 916-918.

Kalmijn, A.J. (1988). Detection of weak electric fields. In *Sensory biology of aquatic animals* (Atema, J., Fay, R.R., Popper, A.N., Tavolga, W.N., eds.), pp. 150-186. New-York, Berlin, Heidelberg, London, Paris, Tokyo: Springer-Verlag.

Kalmijn, A.J. (1989). Functional evolution of lateral line and inner ear sensory systems. In *The mechanosensory lateral line: neurobiology and evolution* (Coombs, S., Görner, P., Münz, H., eds.), pp. 187-215. New-York: Springer-Verlag.

Kalmijn, A.J. (1997). Electric and near-field acoustic detection, a comparative study. *Acta Physiologica Scandinavia Stockholm* **638**, 25-38.

Kasumyan, A. (2003). The lateral line in fish: structure, function, and role in behavior. *Journal of Ichthyology* **43**, 175-213.

Kempster, R.M., and Collin, S.P. (2011a). Electrosensory pore distribution and feeding in the megamouth shark *Megachasma pelagios* (Lamniformes: Megachasmidae). *Aquatic Biology* **11**, 225-228.

Kempster, R.M., and Collin, S.P. (2011a). Electrosensory pore distribution and feeding in the basking shark *Cetorhinus maximus* (Lamniformes: Cetorhinidae). *Aquatic Biology* **12**, 33-36.

Kempster, R.M., McCarthy, I.D., Collin, S.P. (2012). Phylogenetic and ecological factors influencing the number and distribution of electroreceptors in elasmobranchs. *Journal of Fish Biology* **80**, 2055-2088.

Kempster, R.M., Hart, N.S., Collin, S.P. (2013). Survival of the stillest: predator avoidance in shark embryos. *PLoS One* **8,** e52551.

Kempster, R.M., Egeberg, C.A., Hart, N.S., Ryan, L., Chapuis, L., Kerr, C.C., Schmidt, C., Huveneers, C., Gennari, E., Yopak, K.E., Meeuwig, J.J., Collin, S.P. (2016). How close is too close? The effect of a non-lethal electric shark deterrent on white shark behaviour. *PLoS One* **11(7)**, e0157717.

Kramer, B. (1996). *Electroreception and communication in fishes*. 119p. Stuttgart, Jena, Lübeck, Ulm: Gustav Fisher.

Ladich, F., and Schulz-Mirbach, T. 2016. Diversity in fish auditory systems: One of the riddles of sensory biology. *Frontiers in Ecology and Evolution* **4**, 28.

Last, P.R., Stevens, J.D. (2009). *Sharks and rays of Australia*. 656p. Collingwood: CSIRO Publishing.

Last, P.R., Naylor, G.J.P., Manjaji-Matsumoto, B.M. (2016b). A revised classification of the family Dasyatidae (Chondrichthyes: Myliobatiformes) based on new morphological and molecular insights. *Zootaxa* **4139(3)**, 345-368.

Last, P. R., White, W. T., Séret, B. (2016a). Taxonomic status of maskrays of the *Neotrygon kuhlii* species complex (Myliobatoidei: Dasyatidae) with the description of three new species from the Indo-West Pacific. *Zootaxa* **4083**, 533-561.

Lekander, B. (1949). The sensory line system and the canal bones in the head of some Ostariophysi. *Acta Zoologica* **30**, 1-131.

Lissmann, H.W. (1958). On the function and evolution of electric organs in fish. *Journal of Experimental Biology* **35**, 156-191.

Lissmann, H.W., and Machin, K.E. (1963). Electric receptors in a non-electric fish (*Clarias*). *Nature* **199**, 88-89.

Loew, E., and Dartnall, H.J.A. (1976). Vitamin A1/A2-based pigment mixtures in cones of the rudd. *Vision Research* **16**, 891-896.

Lu, J., and Fishman, H.M. (1994). Interaction of apical and basal membrane ion channels underlies electroreception in ampullary epithelia of skates. *Biophysical Journal* **67**,1525-1533.

Manger, P.R., Pettigrew, J.D. (1996). Ultrastructure, number, distribution and innervation of electroreceptors and mechanoreceptors in the bill skin of the platypus, *Ornithorhynchus anatinus*. *Brain*, *Behavior and Evolution* **48**, 27-54.

Marcotte, M.M., and Lowe, C.G. (2008). Behavioral responses of two species of sharks to pulsed, direct current electrical fields: Testing a potential shark deterrent. *Marine Technology Society Journal* **42**, 53-61.

Marshall, J.N., and Vorobyev, M. (2003). The design of color signals and color vision in fishes. In *Sensory Processing in Aquatic Environments* (Collin, S.P., Marshall, N.J., eds.), pp. 194-202. New York, Berlin, Heidelberg, Hong Kong, London, Milan, Paris, Tokyo: Springer.

McGowan, D. W., and Kajiura, S. M. (2009). Electroreception in the euryhaline stingray, *Dasyatis sabina*. *Journal of Experimental Biology* **212**, 1544-1552.

Montgomery, J.C. (1991). “Seeing” with nonvisual senses: mechano- and electrosensory systems of fish. *Physiology* **6**, 73-77.

Montgomery, J., and Skipworth, E. (1997). Detection of weak water jets by the short-tailed stingray *Dasyatis brevicaudata* (Pisces: Dasyatidae). *Copeia* **1997**, 881–883.

Montgomery, J.C., Baker, C.F., Carton A.G. (1997). The lateral line can mediate rheotaxis in fish. *Nature* **389**, 960-963.

Montgomery, J.C., Bodznick, D., Yopak, K.E. (2012). The cerebellum and cerebellum-like structures of cartilaginous fishes. *Brain*, *Behavior and Evolution* **80**, 152-165.

Mullinger, A.M. (1964). The fine structure of ampullary electric receptors in *Amiurus*. *Proceedings of the Royal Society of London B* **160**, 345-359.

Münz, H., and Claas, B. (1983). The functional organization of neuromasts in the lateral-line system of a Cichlid fish: advances in vertebrate neuroethology. In *NATO Advanced Science Institutes Series*, *vol. 56*. New York, NY: Springer.

Murray, R.W. (1957). Evidence for a mechanoreceptive function of the ampullae of Lorenzini. *Nature* **179**, 106-107.

Murray, R.W. (1960). The response of the ampullae of Lorenzini of elasmobranchs to mechanical stimulation. *Journal of Experimental Biology* **37**, 417-424.

Murray, R.W. (1974). The ampullae of Lorenzini. In *Handbook of Sensory Physiology* (Fessard, A., ed.), pp. 125-146. Berlin: Springer-Verlag Berlin.

Murren, C.J., Auld, J.R., Callahan, H., Ghalambor, C.K., Handelsman, C.A., Heskel, M.A., Kingslover, J.G., Maclean, H.J., Masel, J., Maughan, H., Pfennig, D.W., Relyea, R.A., Seiter,

S., Snell-Rood, E., Steiner, U.K., Schlichting, C.D. (2015). Constraints on the evolution of phenotypic plasticity: limits and costs of phenotype and plasticity. *Heredity* **115**, 293-301.

New, J.G. (1997). The evolution of vertebrate electrosensory systems. *Brain*, *Behavior and Evolution* **50**, 244-252.

Norris, H.W. (1929). The distribution and innervation of the ampullae of Lorenzini of the dogfish, *Squalus acanthias*. Some comparisons with conditions in other plagiostomes and corrections of prevalent errors. Journal of Comparative Neurology **47**, 449-465.

Northcutt, R.G. (2003). Development of the lateral line system in the channel catfish. In *The Big Fish Bang. Proceedings of the 26th Annual Larval Fish Conference* (Browman, H.I., Skiftesvik, A.B., eds.), pp. 137-159. Bergen, Norway: Institute of Marine Research.

Obara, S. (1976). Mechanism of electroreception in ampullae of Lorenzini of the marine catfish *Plotosus*. In *Electrobiology of Nerve*, *Synapse and Muscle* (Reuben, J.P., Purpura, D.P., Bennett, M.V.L., Kandel, E.R., eds.), pp. 129-147. New York: Raven Press.

Obara, S., Sugawara, Y. (1984). Electroreceptor mechanisms in teleost and non-teleost fishes. In *Comparative Physiology of Sensory Systems* (Bolis, L., Keynes, R.D., Maddrell, S.H.P., eds.), pp. 509-523. New York: Cambridge University Press.

Oughton, S. (2014). Movements of forktail catfish in the Daly River, Northern Territory, as determined by otolith chemistry analysis [dissertation]. Darwin (Australia): Charles Darwin University. 64p.

Pardo, S.A., Burgess, K.B., Teixeira, D., Bennett, M.B. (2015). Local-scale resource partitioning by stingrays on an intertidal flat. *Marine Ecology Progress Series* **533**, 205-218.

Parker, G.H., and van Heusen, A.P. (1917). The responses of the catfish, *Amirus nebulosus*, to metallic and non-metallic rods. *American Journal of Physiology* **44**, 405-420.

Peach, M.B., and Marshall, N.J. (2000). The pit organs of elasmobranchs: a review. *Philosophical Transactions of the Royal Society of London B* **355**, 1131-1134.

Pierce, S.J., Pardo, S.A., Bennett, M.B. (2009). Reproduction of the blue-spotted maskray *Neotrygon kuhlii* (Myliobatoidei: Dasyatidae) in south-east Queensland, Australia. *Journal of Fish Biology* **74**, 1291-1308.

Platt, C., Popper, A.N. (1981). Fine structure and function of the ear. In *Hearing and sound communication in fishes* (Tavolga, W.N., Popper, A.N., Fay, R.R., eds.), pp.3-38. New York: Springer-Verlag.

Popper, A.N. (2002). Structure-function relationships in the ears of fishes. *Bioacoustics* **12**, 114-118.

Popper, A.N., Fay, R.R., Platt, C., Sand, O. (2003). Sound detection mechanisms and capabilities of teleost fishes. In *Sensory Processing in Aquatic Environments* (Collin, S.P., Marshall, N.J., eds.), pp. 3-38. New York, Berlin, Heidelberg, Hong Kong, London, Milan, Paris, Tokyo: Springer.

Puzdrowski, R.L. (1989). Peripheral distribution and central projections of the lateal-line nerves in gold-fish, *Carassus auratus*. *Brain*, *Behavior and Evolution* **34**, 110-131.

Raschi, W. (1986). A morphological analysis of the ampullae of Lorenzini in selected skates (Pisces, Rajoidei). *Journal of Morphology* **189**, 225-248.

Raschi, W., and Tabit, C. (1992). Functional aspects of placoid scales: a review and update. *Australian Journal of Marine and Freshwater Research* **43**, 123-147.

Raschi, W.G., Aadland, C., Keithar, E.D. (2001). A morphological and functional analysis of the ampullae of Lorenzini in selected galeoids sharks. In *Sensory biology of jawed fishes: new insights* (Kapoor, B.G. & Hara, T.J., eds.), pp. 297-316. Enfield: Science Publishers, Inc.

Raschi, W., and Gerry, S.P. (2003). Adaptations in the elasmobranch electroreceptive system. In *Fish Adaptations* (Val, A.L., Kapoor, B.G., eds.), pp. 233-258. Enfield NH: Scientific Publishers.

Reif, W.E. (1978). Types of morphogenesis of the dermal skeleton in fossil sharks. *Paläontologische Zeitschrift* **52**, 110-128.

Rimmer, M.A. (1985). Reproductive cycle of the fork-tailed catfish *Arius graeffei* Kner&Steindachner (Pisces: Ariidae) from the Clarence River, New South Wales*. Australian Journal of Marine and Freshwater Research* **36**, 23-32.

Rivera-Vicente, A.C., Sewell, J., Tricas, T. C. (2011). Electrosensitive spatial vectors in elasmobranch fishes: implications for source localization. *PLoS ONE* **6**, e16008.

Rosenberg, L.J. (2001). Pectoral fin locomotion in batoid fishes: undulation versus oscillation. *Journal of Experimental Biology* **204**, 379-394.

Sand, A. (1938). The function of the ampullae of Lorenzini, with some observations on the effect of temperature on sensory rhythms. *Proceedings of the Royal Society of London B* **125**, 524-553.

Schäfer. B.T., Malavasi, C.E., Favaron, P.O., Ambrosio, C.E., Miglino, M.A., De Amorinm, A.F., Rici, R.E.G. (2012). Morphological observations of ampullae of Lorenzini in Squatina Guggenheim and S. occulta (Chondrichthyes, Elasmobranchii, Squatinidae). *Microscopy Research & Technique* **75**, 1213-1217.

Scheich, H., Langner, G., Tidemann, C., Coles, R.B., Guppy, A. (1986). Electroreception and electrolocation in platypus. *Nature* **319**, 401-402.

Schluessel, V., Bennett, M.B., Bleckmann, H., Blomberg, S., Collin, S.P. (2008). Morphometric and ultrastructural comparison of the olfactory system in elasmobranchs: the significance of structure–function relationships based on phylogeny and ecology. *Journal of Morphology* **269**, 1365-1386.

Schluessel, V., Bennett, M. B., Bleckmann, H., Collin, S. P. (2010). The role of olfaction throughout juvenile development: functional adaptations in elasmobranchs. *Journal of Morphology* **271**, 451-461.

Sillman, A.J., and Dahlin, D.A. (2004). The photoreceptors and visual pigments of sharks and sturgeons. In *The senses of fish: adaptations for the reception of natural stimuli* (von der

Emde, G., Mogdans, J., Kapoor, B.G., eds.), pp. 31-54. Springer Netherlands: Springer Science & Business Media.

Sisneros, J.A., Tricas, T.C., Luer, C.A. (1998). Response properties and biological function of the skate electrosensory system during ontogeny. *Journal of Comparative Physiology A* **183**, 87-99.

Stevens, J.D. (1984). Biological observations on sharks caught by sport fishermen off New South Wales. *Australian Journal of Marine and Freshwater Research* **35**, 573-590.

Stuart, I.G., and Berghuis, A.P. (2002). Upstream passage of fish through a vertical-slot fishway in an Australian subtropical river. *Fisheries Management and Ecology* **9**, 111-122.

Stuart, I.G., Berghuis, A.P., Long, P.E., Mallen-Cooper, M. (2007). Do fish locks have potential in tropical rivers? *River Research and Applications* **23**, 269-286.

Szabo, T., Enger, P.S., Kalmijn, A.J., Bullock, T.H. (1972). Microampullary organs and a submandibular sense organ in freshwater ray, *Potamotrygon*. *Journal of Comparative Physiology* **79**, 15-27.

Taylor, S.M., and Bennett, M.B. (2008). Cephalopod dietary specialization and ontogenetic partitioning of the Australian weasel shark *Hemigaleus australiensis* White, Last & Compagno. *Journal of Fish Biology* **72**, 917-936.

Theiss, S. M., Lisney, T. J., Collin, S. P., Hart, N. S. (2007). Colour vision and visual ecology of the blue-spotted maskray, *Dasyatis kuhlii* Muller & Henle, 1814. *Journal of Comparative Physiology A* **193**, 67-79.

Theiss, S., Collin, S., Hart, N. (2011). Morphology and distribution of the ampullary electroreceptors in wobbegong sharks: implications for feeding behaviour. *Marine Biology* **158**, 723-735.

Thommesen, G. (1983). Morphology distribution and specificity of olfactory receptor cells in salmonid fishes. *Acta Physiologica Scandinavica* **117**, 241-250.

Thomson, K.S. (1977). On the individual history of cosmine and a possible electroreceptive function of the pore-canal system in fossil fishes. In *Problems in Vertebrate Evolution* (Andrews, S.M., Miles, R.S., Walker, A.D., eds.), pp. 247-270. London, Academic Press.

Tricas, T.C., Michael, S.W., Sisneros, J.A. (1995). Electrosensory optimization to conspecific phasic signals for mating. *Neuroscience Letters* **202,** 129-132.

Tricas, T.C., and New, J.G. (1998). Sensitivity and response dynamics of electrosensory primary afferent neurons to near threshold fields in the round stingray. *Journal of Comparative Physiology A* **182**, 89-101.

Tricas, T.C. (2001). The neuroeology of the elasmobranch electrosensory world: why peripheral morphology shapes behaviour. *Environmental Biology of Fishes* **60**, 77-92.

Van-Eyk, S. M., Siebeck, U. E., Champ, C. M., Marshall, J., Hart, N. S. (2011). Behavioral evidence for color vision in an elasmobranch. *Journal of Experimental Biology* **214**, 4186-4192.

Van Netten, S.M., and Kroese, A.B.A. (1989). Dynamic behaviour and micromechanical properties of the cupula. In *The mechanosensory lateral line: neurobiology and evolution* (Coombs, S., Görner, P., Münz, H., eds.), pp. 247-264. New-York: Springer-Verlag.

Von der Emde, G., Bell, C.C. (2003). Active electrolocation and its neural processing in mormyrid electric fishes. In *Sensory Processing in Aquatic Environments* (Collin, S.P., Marshall, N.J., eds.), pp. 92-107. New York, Berlin, Heidelberg, Hong Kong, London, Milan, Paris, Tokyo: Springer.

von der Emde, G. (2006). Non-visual environmental imaging and object detection through active electrolocation in weakly electric fish. *Journal of Comparative Physiology A* **192**, 601-612.

Vasconcelos, R.O., Alderks, P.W., Sisneros, J.A. (2016). Development of structure and sensitivity of the fish inner ear. In *Fish hearing and bioacoustics* (Sisneros, J.A., ed.), pp. 291-318. New, York, Dordrecht, London: Springer.

Vulo, R., and Guinot, G. (2015). Denticle-embedded ampullary organs in a Cretaceous shark provide unique insight into the evolution of elasmobranch electroreceptors. *The Science of Nature* **102**, 65.

Wachtel, A.W., and Szamier, R.B. (1969). Special cutaneous receptor organs of fish. *Journal of Morphology* **128**, 291-308.

Wagner, H., Fröhlich, E., Negishi, K., Collin, S.P. (1998). The eyes of deep-sea fish II. Functional morphology of the retina. *Progress in retinal and eye research* **17**, 637-685.

Waltmann, B. (1966). Electrical properties and fine structure of the ampullary canals of Lorenzini. *Acta Physiology Scandinavia* **66**, 1-60.

Warrant, E.J., Collin, S.P., Locket, N.A. (2003). Eye design and vision in deep-sea fishes. In *Sensory Processing in Aquatic Environments* (Collin, S.P., Marshall, N.J., eds.), pp. 303-322. New York, Berlin, Heidelberg, Hong Kong, London, Milan, Paris, Tokyo: Springer.

White, W.T., Platell, M.E., Potter, I.C. (2004). Comparisons between the diets of four abundant species of elasmobranchs in a subtropical embayment: implications for resource partitioning. *Marine Biology* **144**, 439-448.

White, W.T., Last, P.R., Naylor, G.J.P., Jensen, K., Caira, J.N. (2010). Clarification of *Aetobatus ocellatus* (Kuhl, 1823) as a valid species, and a comparison with *Aetobatus narinari* (Euphrasen, 1790) (Rajiformes: Myliobatidae). *CSIRO Marine and Atmospheric Research Paper* **32**, 146.

Whitehead, D. L., Tibbetts, I.R., Daddow, L.Y.M. (1999). Distribution and morphology of the ampullary organs of the salmontail catfish, *Arius graeffei*. *Journal of Morphology* **239**¸97-105.

Whitehead, D.L., Tibbetts, I.R., Daddow, L.Y.M. (2000). Ampullary organ morphology of freshwater Salmontail catfish, *Arius graeffei*. *Journal of Morphology* **246**, 142-149.

Whitehead, D.L. (2002a). Variations in ampullary organ morphology and electroreception due to environmental characteristics in members of Siluriformes and Charcharhinidae [dissertation]. Brisbane (Australia): The University of Queensland. 126p.

Whitehead, D.W. (2002b). Ampullary organs and electroreception in freshwater *Carcharhinus leucas*. *Journal of Physiology Paris* **96**, 391-395.

Whitehead, D.L., Tibbetts, I.R., Daddow, L.Y.M. (2003). Microampullary organs of a freshwater eel-tailed catfish, *Plotosus (tandanus) tandanus*. *Journal of Morphology* **255**, 253-260.

Whitehead, D.L., Gauthier, A.R.G., Mu, E.W.H., Bennett, M.B., Tibbetts, I.R. (2015a). Morphology of the ampullae of Lorenzini in juvenile freshwater *Carcharhinus leucas. Journal of Morphology* **276**, 481-493.

Whitehead, D.L., Gauthier, A.R.G., Cameron, R.M.E., Perutz, M., Tibbetts, I.R. (2015b). Ultrastructure of the ampullary organs of *Plicofollis argyropleuron* (Siluriformes: Ariidae). *Journal of Morphology* **276**, 1405-1411.

Winther-Janson, M., Wueringer, B.E., Seymour, B.E. (2012). Electroreceptive and mechanoreceptive anatomical specialisations in the epaulette shark (*Hemiscyllium ocellatum*). *PLoS One* **7**, e49857.

Wueringer, B., and Tibbetts, I.R. (2008). Comparison of the lateral line and ampullary systems of two species of shovelnose ray. *Reviews in Fish Biology and Fisheries* **18**, 47-64.

Wueringer, B.E., Tibbetts, I.R., Whitehead, D.L. (2009). Ultrastructure of the ampullae of Lorenzini of *Aptychotrema rostrata* (Rhinobatidae). *Zoomorphology* **128**, 45-52.

Wueringer, B. E., Squire Jnr, L., Kajiura, S. M., Tibbetts, I. R., Hart, N. S., Collin, S. P. (2012). Electric field detection in sawfish and shovelnose rays. *PLoS One* **7**, e41605.

Yan, H.Y. (2004). The role of gas-holding structures in fish hearing: an acoustically evoked potentials approach. In *The senses of fish: adaptations for the reception of natural stimuli* (von der Emde, G., Mogdans, J., Kapoor, B.G., eds.), pp. 189-209. Springer Netherlands: Springer Science & Business Media.

Yopak, K.E., and Lisney, T.J. (2012). Allometric scaling of the optic tectum in cartilaginous fishes. *Brain Behavior and Evolution* **80**, 108-126.

Yopak, K.E., Lisney, T.J., Collin, S.P. (2015). Not all sharks are ‘‘swimming noses’’: variation in olfactory bulb size in cartilaginous fishes. *Brain Structure and Function* **220**, 1127-1143.

Yu, Y., Zhang, H., Lemckert, C.J. (2014). Salinity and turbidity in the Brisbane River estuary, Australia. *Journal of Hydrology* **519**, 3338-3352.

Zakon, H.H. (1986). The electroreceptive periphery. In *Electroreception* (Bullock, T.H., Heiligenberg, W., eds.), pp.103-156. Chichester, New York, Brisbane, Toronto, Singapore: Wiley.

Zupanc, G.K.H., and Bullock, T.H. (2005). From electrogenesis to electroreception: An Overview. In *Electroreception* (Bullock, T.H., Hopkins, C.D., Popper, A.N., Fay, R.R., eds.), 467p. New York, Berlin, Heidelberg, Hong Kong, London, Milan, Paris, Tokyo: Springer.

Appendix

THE UNIVERSITY OF QUEENSLAND
AUSTRALIA

UQ Research and Innovation
Director, Research Management Office
Nicole Thompson

Animal Ethics Approval Certificate

18-Apr-2016

Please check all details below and inform the Animal Welfare Unit within 10 working days if anything is incorrect.

Activity Details

Chief Investigator:	Professor Mike Bennett
Title:	Morphology and ultrastructure of ampullary organs in catfish, sharks and rays
AEC Approval Number:	SBMS/406/14
Previous AEC Number:	
Approval Duration:	22-Apr-2015 to 22-Apr-2018
Funding Body:	
Group:	Native and exotic wildlife and marine animals
Other Staff/Students:	Ian Tibbetts, Arnault Gauthier, Darryl Whitehead
Location(s):	St Lucia Bldg 69 - Centre for Marine Studies Moreton Bay Research Centre Other Queensland Location

Summary

Subspecies	Strain	Class	Gender	Source	Approved	Remaining
Fish		Juvenile / Weaners / Pouch animal	Unknown	Natural Habitat	175	175
Fish		Adults	Unknown	Natural Habitat	550	550

Permits

Marine Parks Permits QS2015/CVL1400	01-Aug-2015 to 31-Jul-2018
General Fisheries Permit 165491	10-Sep-2013 to 10-Sep-2018
General Fisheries Permit 144801	21-Jan-2011 to 21-Jan-2016

Provisos

Approval Details

Description	Amount	Balance
Fish (Unknown, Adults, Natural Habitat)		
22 Apr 2015 Initial approval	550	550
Fish (Unknown, Juvenile / Weaners / Pouch animal, Natural Habitat)		
22 Apr 2015 Initial approval	175	175

Animal Welfare Unit
UQ Research and Innovation
The University of Queensland

Cumbrae-Stewart Building
Research Road
Brisbane Qld 4072 Australia

+61 7 336 52925 (Enquiries)
+61 7 334 68710 (Enquiries)
+61 7 336 52713 (Coordinator)

animalwelfare@research.uq.edu.au
uq.edu.au/research

Supplementary Figure – Chapter IV

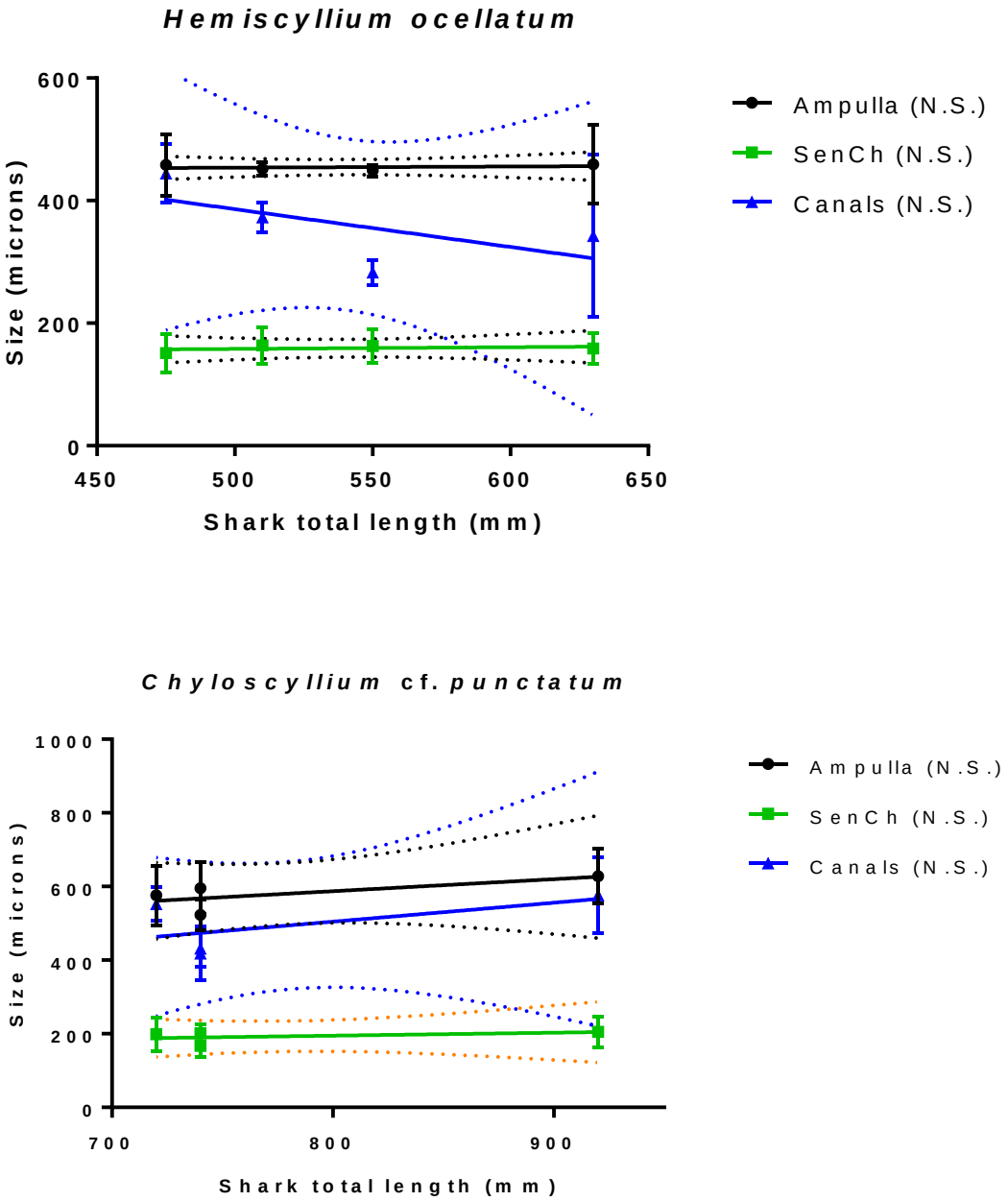

Figure S1. Regression plots based on the mean values of each measured characteristics of the ampullary organs for both species, with a 95% confidence interval.